University of Alberta

Photodecarboxylation of Amino Acids and the Synthesis of DAP Analogs to be Tested Against Enzymes Involved in Plant Lysine Biosynthesis

by

Mitchel D. Flegel 

A thesis submitted to the Faculty of Graduate Studies and Research in partial fulfillment of the requirements for the degree of

Master of Science

Department of Chemistry

Edmonton, Alberta

Spring 2007

Reproduced with permission of the copyright owner. Further reproduction prohibited without permission.

Library and Archives Canada

Published Heritage Branch

395 Wellington Street
Ottawa ON K1A 0N4
Canada

Bibliothèque et Archives Canada

Direction du Patrimoine de l'édition

395, rue Wellington
Ottawa ON K1A 0N4
Canada

Your file Votre référence
ISBN: 978-0-494-29957-9
Our file Notre référence
ISBN: 978-0-494-29957-9

NOTICE:
The author has granted a non-exclusive license allowing Library and Archives Canada to reproduce, publish, archive, preserve, conserve, communicate to the public by telecommunication or on the Internet, loan, distribute and sell theses worldwide, for commercial or non-commercial purposes, in microform, paper, electronic and/or any other formats.

The author retains copyright ownership and moral rights in this thesis. Neither the thesis nor substantial extracts from it may be printed or otherwise reproduced without the author's permission.

AVIS:
L'auteur a accordé une licence non exclusive permettant à la Bibliothèque et Archives Canada de reproduire, publier, archiver, sauvegarder, conserver, transmettre au public par télécommunication ou par l'Internet, prêter, distribuer et vendre des thèses partout dans le monde, à des fins commerciales ou autres, sur support microforme, papier, électronique et/ou autres formats.

L'auteur conserve la propriété du droit d'auteur et des droits moraux qui protège cette thèse. Ni la thèse ni des extraits substantiels de celle-ci ne doivent être imprimés ou autrement reproduits sans son autorisation.

In compliance with the Canadian Privacy Act some supporting forms may have been removed from this thesis.

While these forms may be included in the document page count, their removal does not represent any loss of content from the thesis.

Conformément à la loi canadienne sur la protection de la vie privée, quelques formulaires secondaires ont été enlevés de cette thèse.

Bien que ces formulaires aient inclus dans la pagination, il n'y aura aucun contenu manquant.

Canada

Reproduced with permission of the copyright owner. Further reproduction prohibited without permission.

Dedicated to my grandfather

Reproduced with permission of the copyright owner. Further reproduction prohibited without permission.

ABSTRACT

This thesis consists of two related projects. The first project presented describes the photoinduced decarboxylation of amino acids to yield amines. The decarboxylation of (*S*)-2-(*N*-benzyloxycarbonylamino)-3-phenylpropanoic acid (**29**) using 1,10-phenanthroline (**30**) as the aza aromatic compound was investigated. Differentially substituted 1,10-phenanthrolines and acridines with varying electron donating and withdrawing capabilities were prepared and tested. The stereochemistry of the decarboxylation was investigated with 2-(*tert*-butoxycarbonylamino)-3-phenylpropanoic acid d_5,α, β, β-d_8 (**52**).

In the second project, three 2,6-diaminopimelic acid (DAP) isomers (**1-3**) were synthesized using diacyl peroxide methodology to investigate the substrate recognition of diaminopimelate epimerase and LL-diaminopimelate aminotransferase from *Arabidopsis thaliana*. A potential transition state analog, (±)-1-aminocyclohexane-1,3-dicarboxylic acid (**89**), was also prepared by a Bucherer-Berg reaction and tested against LL-diaminopimelate aminotransferase for inhibition.

Analysis of the DAP content in *Arabidopsis thaliana* and *Brassica napus* was successfully determined by chiral GC-MS. These results were confirmed by a coupled enzyme assay of the crude plant extracts.

Reproduced with permission of the copyright owner. Further reproduction prohibited without permission.

ACKNOWLEDGEMENTS

I gratefully acknowledge my supervisor, Professor John C. Vederas, for his continual encouragement, support and guidance throughout this research experience. I am grateful to Dr. Matt Clay and Dr. Viji Moorthie for their insightful suggestions and for the proofreading of my thesis. I would also like to acknowledge Dr. Sandra Marcus and Dr. Marco van Belkum for their contributions towards this manuscript.

I would like to thank all members of the Vederas research group, past and present, for their helpful advice. In particular, I would like to extend my gratitude to Dr. Chris Diaper for helping me become acquainted with the DAP project. Furthermore, I would like to thank Professor Michael Deyholos (Dept. of Biology) for collaborative efforts.

The staff in spectral and analytical services at the Department of Chemistry is gratefully acknowledged for their technical expertise and aid in identification and characterization of compounds. Specifically, I would like to thank Don Morgan for his generous donation of time in the mass spectrometry lab.

Finally, I would like to thank all my friends and family for their unfailing support. I would also like to thank my girlfriend Melissa for her optimism and words of encouragement during the past three years.

Financial assistance from the Natural Sciences and Engineering Research Council of Canada, the Alberta Heritage Foundation for Medical Research and the University of Alberta is gratefully acknowledged.

Reproduced with permission of the copyright owner. Further reproduction prohibited without permission.

TABLE OF CONTENTS

Reproduced with permission of the copyright owner. Further reproduction prohibited without permission.

Reproduced with permission of the copyright owner. Further reproduction prohibited without permission.

Reproduced with permission of the copyright owner. Further reproduction prohibited without permission.

Reproduced with permission of the copyright owner. Further reproduction prohibited without permission.

Reproduced with permission of the copyright owner. Further reproduction prohibited without permission.

Reproduced with permission of the copyright owner. Further reproduction prohibited without permission.

Reproduced with permission of the copyright owner. Further reproduction prohibited without permission.

LIST OF SCHEMES

Reproduced with permission of the copyright owner. Further reproduction prohibited without permission.

Reproduced with permission of the copyright owner. Further reproduction prohibited without permission.

Reproduced with permission of the copyright owner. Further reproduction prohibited without permission.

LIST OF FIGURES

Reproduced with permission of the copyright owner. Further reproduction prohibited without permission.

Reproduced with permission of the copyright owner. Further reproduction prohibited without permission.

Reproduced with permission of the copyright owner. Further reproduction prohibited without permission.

LIST OF ABBREVIATIONS

[α]	specific rotation
A	ampere
abs	absorbance units
Ac	acetyl
AcOH	acetic acid
app.	apparent
aq	aqueous
Ar	aryl
Asp	aspartic acid
AT	aminotransferase
ATP	adenosine triphosphate
azi-DAP	2-(4-amino-4-carboxybutyl)-2-aziridine-carboxylate
Bn	benzyl
Boc	*tert*-butoxycarbonyl
Boc_2O	di-*tert*-dicarbonate
br	broad
tert-Bu	*tertiary*-butyl
Calcd	calculated
Cbz	benzyloxycarbonyl
CbzCl	benzyl chloroformate
Conc.	concentrated

Reproduced with permission of the copyright owner. Further reproduction prohibited without permission.

Cys	cysteine
δ	chemical shift in parts per million downfield from tetramethylsilane
DAP	2,6-diaminopimelic acid
DCC	1,3-dicyclohexylcarbodiimide
DCM	dichloromethane
DMAP	4-(dimethylamino)pyridine
DMF	dimethylformamide
DMSO	dimethylsulfoxide
DTT	dithiothreitol
EDTA	ethylenediaminetetraacetic acid
ee	enantiomeric excess
EI	electron impact ionization
ES	electrospray ionization
ET	electron transfer
Et	ethyl
Et_2O	diethyl ether
EtOAc	ethyl acetate
eq.	equivalence
GlcNAc	*N*-acetylglucosamine
Glu	glutamic acid
GC	gas chromatography
HEPESKOH	4-(2-hydroxyethyl)-1-piperazineethanesulfonic acid potassium hydroxide salt

Reproduced with permission of the copyright owner. Further reproduction prohibited without permission.

HPLC	high performance liquid chromatography
HRMS	high resolution mass spectrometry
IC_{50}	concentration causing 50% inhibition
IR	infrared
IPA	isopropyl alcohol
J	coupling constant
Lpm	liters per minute
Lys	lysine
m/z	mass to charge ratio
Me	methyl
MeCN	acetonitrile
MeOH	methanol
meso	mesomeric
MHz	megahertz
m.p.	melting point
MS	mass spectrometry
MurNAc	*N*-acetylmuramic acid
MWCO	molecular weight cut-off
$NAPH^+$	nicotinamide adenine dinucleotide phosphate (oxidized form)
NADPH	nicotinamide adenine dinucleotide phosphate (reduced form)
NMR	nuclear magnetic resonance
NOE	nuclear Overhouser effect
NMM	*N*-methylmorpholine

Reproduced with permission of the copyright owner. Further reproduction prohibited without permission.

OAB	*ortho*-aminobenzaldehyde
2-OG	2-oxyglutarate
OPA	*ortho*-phthalaldehyde
PET	photoinduced electron transfer
PFPA	pentafluoropropionic anhydride
Ph	phenyl
Phe	phenylalanine
PLP	pyridoxyl-5'-phosphate
PyBOP®	benzotriazol-1-yl-oxytripyrrolidinophosphonium hexafluorophosphate
quant.	quantitative
rac-	racemic
RP	reverse phase
rt	room temperature
TFA	trifluoroacetic acid
THDP	tetrahydropicolinate
THF	tetrahydrofuran
TLC	thin layer chromatography
TMS	tetramethylsilane
TMSCl	trimethylsilyl chloride
Tris-HCl	tris-(hydroxymethyl)aminomethane hydrochloride
Trp	tryptophan
UV	ultraviolet

Reproduced with permission of the copyright owner. Further reproduction prohibited without permission.

Chapter 1: Introduction

This thesis consisted of two related projects. One project involves the decarboxylation of amino acid derivatives. The other project investigates the biosynthetic pathway to L-lysine in plants. Chapter 1 (Introduction) and Chapter 4 (Experimental) have the two projects combined. Chapter 2 consists of the results and discussion of the decarboxylation project, whereas Chapter 3 consists of the L-lysine project.

1.1. Importance of Diaminopimelic Acid and L-Lysine

Diaminopimelic acid (2,6-diaminoheptanedioic acid, DAP, **1-3**) (Figure 1) was discovered in the late 1940's and was first isolated in 1951 from *Corynebacterium diphtheria.*[1] It is an important constituent of bacterial cell wall peptidoglycan and is a biosynthetic precursor to L-lysine (**4**).

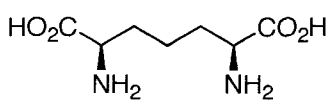

***meso*-DAP, 1**

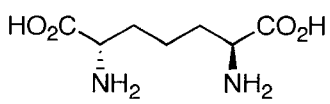

LL-DAP, 2

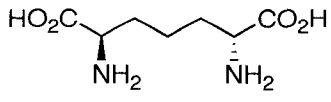

DD-DAP, 3

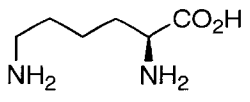

L-lysine, 4

Figure 1. Structures of the DAP isomers (**1-3**) and L-lysine (**4**).

Reproduced with permission of the copyright owner. Further reproduction prohibited without permission.

Peptidoglycan is a continuous covalent macromolecular structure located on the outside of the cytoplasmic membrane of almost all bacteria.[2] Its main function is to preserve cell integrity by withstanding the internal osmotic pressure along with defining the cell shape of both Gram-positive and Gram-negative bacteria.[3] The peptidoglycan layer of the bacterial cell wall consists of linear chains of alternating *N*-acetyl glucosamine (GlcNAc) and *N*-acetylmuramic acid (MurNAc) residues, cross linked by short peptides attached to the muramyl moiety[4] (Figure 2). The carboxyl group at the end of each *N*-acetylmuramic acid residue is substituted by a peptide subunit, which is most often L-alanine, γ-D-glutamate, *meso*-DAP or L-lysine, followed by two D-alanines. The pentapeptide side chain contains D-amino acids that stabilize peptidoglycan against enzymatic hydrolysis. Gram-negative bacteria contain *meso*-DAP (**1**)[5, 6] whereas its biosynthetic product, L-lysine (**4**), along with LL-DAP (**2**) has analogous functions in many Gram-positive bacterial species. [2, 6] DD-DAP (**3**) occurs less frequently, however it has been found in the peptidoglycan of *Bacillus megaterium*.[7]

To give peptidoglycan its necessary rigidity, neighboring glycan strands are interlinked either by a direct peptide linkage between a peptide subunit of the chains with one another or by a short peptide bridge between two peptide subunits.[8, 9] The composition of this peptide linkage varies greatly between bacteria.[2] Formation of the peptidoglycan layer is a primary target for many antibiotics, including β-lactams (e.g. penicillins, cephalosporins) as well as glycopeptides (e.g. vancomycin).[10] The absence of lysine or DAP production in mammals, implies that inhibitors of the DAP biosynthetic pathway should provide drugs with selective toxicity against bacteria.

Reproduced with permission of the copyright owner. Further reproduction prohibited without permission.

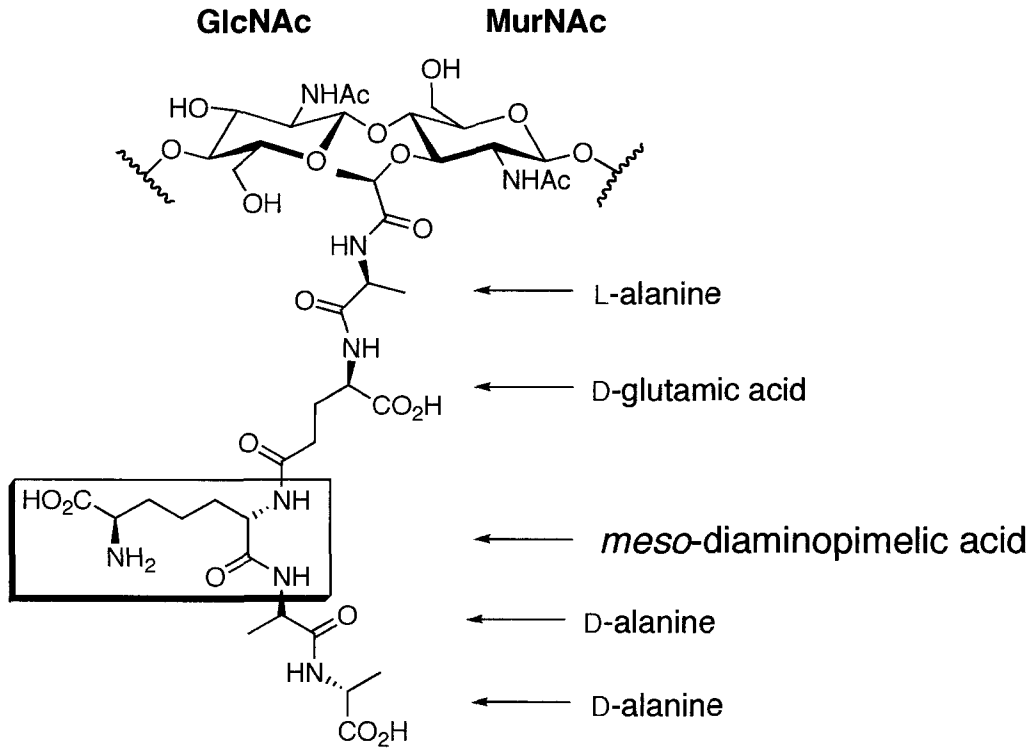

Figure 2. Peptidoglycan unit in Gram-negative bacteria.

Human and monogastric mammals cannot synthesize nine of the amino acids found in proteins and therefore need to obtain them from their diet. Among these "essential" amino acids, lysine is the most limiting in the major cereal grains, and is considered as a nutritionally significant amino acid.[11] It is hoped that structural and mechanistic information of the enzymes involved in the biosynthetic pathway to lysine will facilitate the rational design of bioengineered plants with increased quantities of essential amino acids such as L-lysine.

Reproduced with permission of the copyright owner. Further reproduction prohibited without permission.

1.2. L-Lysine Biosynthesis in Bacteria

The biosynthesis of L-lysine (**4**) from aspartic acid in most bacteria proceeds *via* a series of nine enzyme-catalyzed reactions (Scheme 1).[12] The first step in the pathway involves the condensation of pyruvate with L-aspartate-semialdehyde (**5**), resulting in the formation of L-1,2-dihydrodipicolinate (L-DHDP, **6**) by dihydrodipicolinate synthase (*DapA*).[13] Reduction of **6** by dihydrodipicolinate reductase (*DapB*) leads to the formation of L-tetrahydrodipicolinate (L-THDP, **7**).

Two different pathways from **7** to L-lysine have been identified in a variety of bacterial species.[14] The more common of the two routes proceeds *via* acylation of L-THDP (**7**), producing the acyl-blocked α-amino-ε-ketopimelate **8** by tetrahydrodipicolinate *N*-succinyltransferase (*DapD*). Succinate is the acyl group used in most bacterial species, including *Escherichia coli*, however in some species such as *Bacillus*, acetate is used.[14, 15] The ketopimelate **8** then undergoes transamination by a pyridoxal phosphate (PLP) dependant *N*-acyl-DAP aminotransferase (*DapC*) using glutamate as the amino donor.[16] Removal of the acyl group from **9** by DAP desuccinylase (*DapE*) then affords LL-DAP (**2**), which is epimerized by DAP epimerase (*DapF*) to form *meso*-DAP (**1**).[17] In the less common pathway, *meso*-DAP (**1**) is produced directly from L-THDP (**7**) by *meso*-DAP dehydrogenase (*Ddh*). In the final step of the lysine pathway, **1** is decarboxylated by the PLP-dependant *meso*-DAP decarboxylase (*LysA*) to give L-lysine (**4**).[18] In several bacterial species, both pathways operate. For example, the

Reproduced with permission of the copyright owner. Further reproduction prohibited without permission.

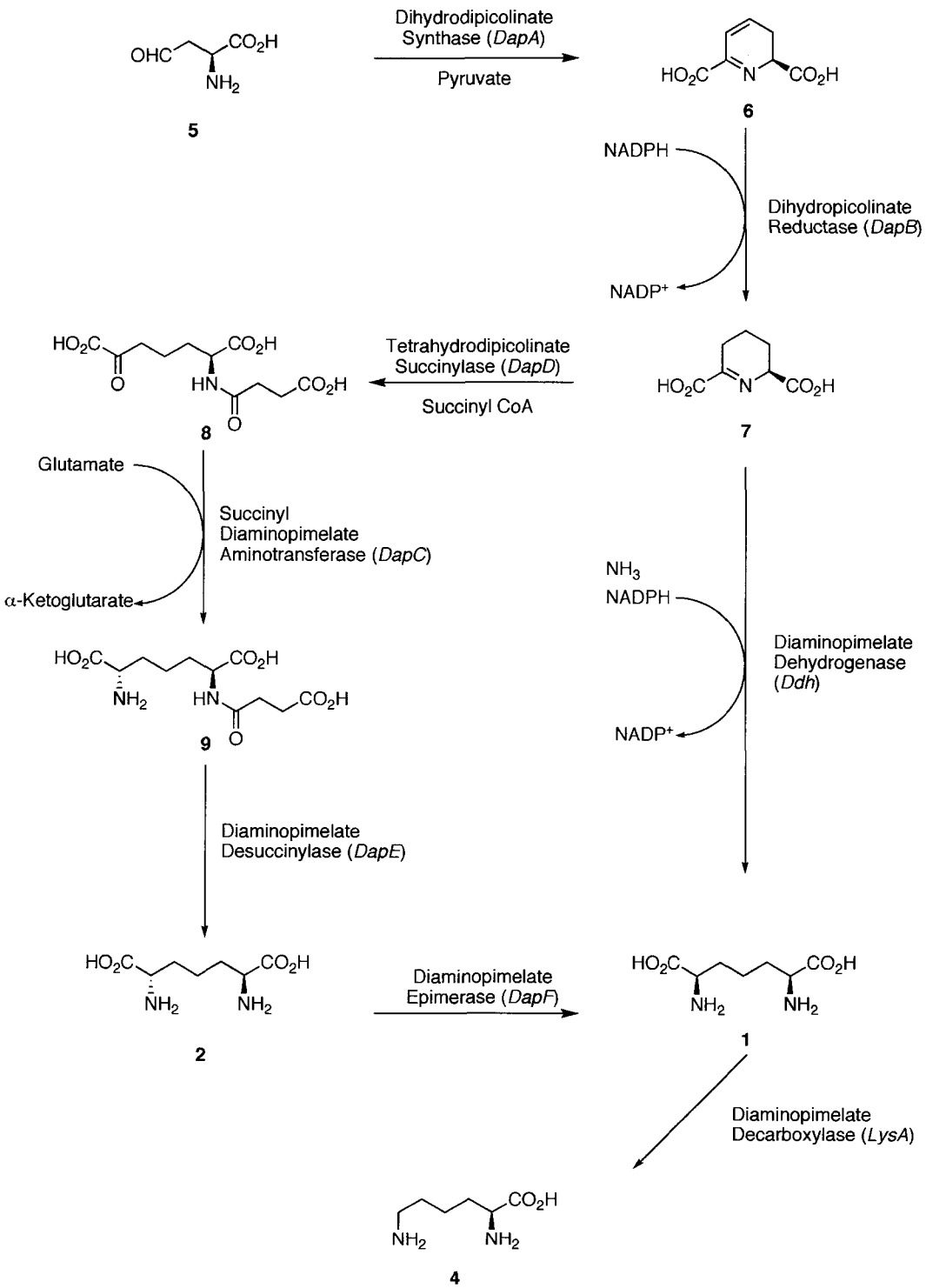

Scheme 1. L-Lysine biosynthetic pathway in bacteria.

Reproduced with permission of the copyright owner. Further reproduction prohibited without permission.

industrially important lysine producer, *Corynebacterium glutamicum*, utilizes both the *N*-succinyl and the dehydrogenase pathways.[19, 20] The presence of multiple lysine biosynthetic pathways suggests the importance of DAP and lysine in bacterial survival.

1.3. L-Lysine Biosynthesis in Fungi

In fungi, L-lysine biosynthesis proceeds through the intermediacy of L-α-aminoadipate (**15**) in a series of transformations entirely unrelated to the bacterial DAP route.[21] Lysine biosynthesis in fungi requires eight steps involving seven free intermediates, beginning with 2-oxyglutarate (2-OG, **10**) (Scheme 2). The first step of the pathway involves the condensation of **10** and acetyl-CoA catalyzed by homocitrate synthase.[22] The resulting homocitric acid (**11**) undergoes a dehydration yielding *cis*-homoaconitic acid (**12**), which in turn is converted to homoisocitric acid (**13**) by the same enzyme, homoaconitase.[23] Oxidation of homoisocitric acid by homoisocitrate dehydrogenase results in the transient formation of a β-keto acid followed by loss of carbon dioxide to yield α-ketoadipic acid (**14**).[24] Glutamate dependant transamination of **14** by aminoadipate aminotransferase gives rise to L-α-aminoadipic acid (**15**).[25] Reduction of the side chain carboxy group of **15** by aminoadipate reductase, in a process requiring ATP and NADPH, gives rise to L-α-aminoadipic acid-δ-semialdehyde (**16**).[26] Saccharopine reductase then catalyses the condensation of **16** with L-glutamate and subsequent reduction of the imine to give L-saccharopine (**17**).[27] The last step of the

Reproduced with permission of the copyright owner. Further reproduction prohibited without permission.

pathway is the cleavage of the carbon-nitrogen bond within the glutamate moiety of **17** carried out by saccharopine dehydrogenase to yield L-lysine (**4**).[28]

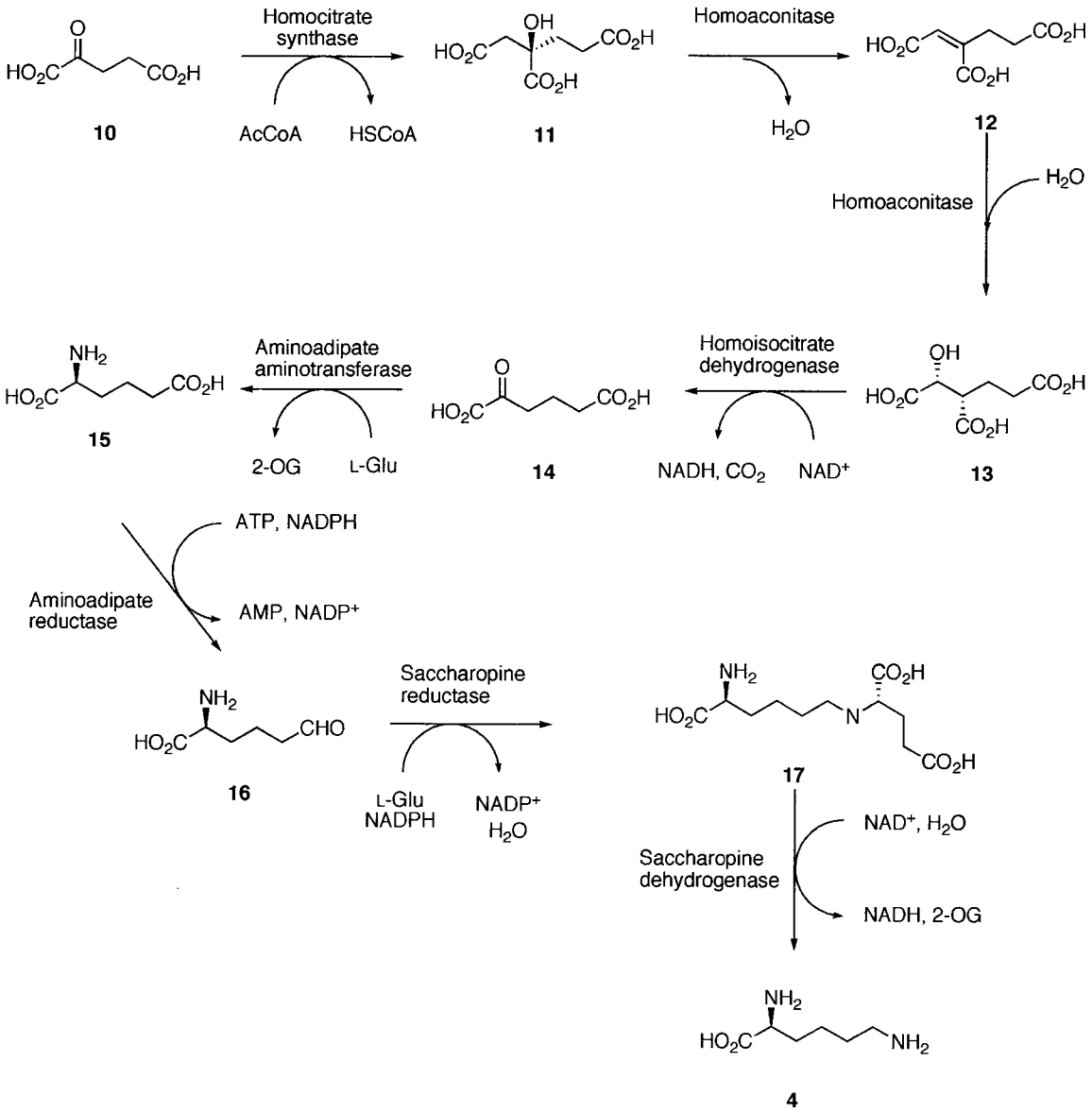

Scheme 2. L-Lysine biosynthetic pathway in fungi.

Reproduced with permission of the copyright owner. Further reproduction prohibited without permission.

1.4. L-Lysine Biosynthesis in Plants

Four pathways to L-lysine in bacteria and fungi have been discussed in the literature. The pathway from fungi utilizes aminoadipate (**15**) while the variants of the bacterial pathway utilize DAP. Since 1959, it has been known that lysine formation in plants occurs *via* a pathway that utilizes DAP as an intermediate.[29] Hence, the lysine pathway in plants is likely to be a variant of one of the three found in bacteria (Scheme 3). The first step that is specific to the DAP pathway in plant lysine biosynthesis is the condensation of pyruvate with L-aspartate-semialdehyde (**5**), resulting in the formation of L-1,2-dihydrodipicolinate (L-DHDP, **6**) by dihydrodipicolinate reductase (*DapA* ortholog).[30] Like its counterpart in the bacterial pathway, dihydrodipicolinate reductase has a feedback mechanism to the lysine pathway and is inhibited by lysine upon overproduction.[31] Reduction of **6** by L-DHDP reductase (*DapB* ortholog) leads to the formation of L-tetrahydrodipicolinate (L-THDP, **7**).[32-34] However, using plant extracts, Leustek and coworkers[32] were unable to detect enzyme activity corresponding to tetrahydrodipicolinate acyltransferase (*DapD* ortholog), *N*-succinyl-α-amino-ε-ketopimelate-glutamate aminotransferase (*DapC* ortholog), *N*-acyldiaminopimelate deacylase (*DapE* ortholog) or *meso*-diaminopimelate dehydrogenase (*Ddh* ortholog). This suggested that lysine production in plants proceeds by a distinctly different route compared to the known bacterial enzymes.[32] Leustek and coworkers were then able to identify that the next step of the pathway involves the direct conversion of **7** to LL-DAP (**2**) by LL-diaminopimelate aminotransferase (LL-DAP-AT), which bypasses the acylation

Reproduced with permission of the copyright owner. Further reproduction prohibited without permission.

and deacylation steps of the bacterial pathway.[35] LL-DAP (**2**) is then epimerized to *meso*-DAP (**1**) by DAP epimerase (*DapF* ortholog) in a similar fashion to the bacterial pathway.[32] The final step of the pathway involves decarboxylation of *meso*-DAP by *meso*-DAP decarboxylase (*LysA* ortholog) to give L-lysine (**4**).[32]

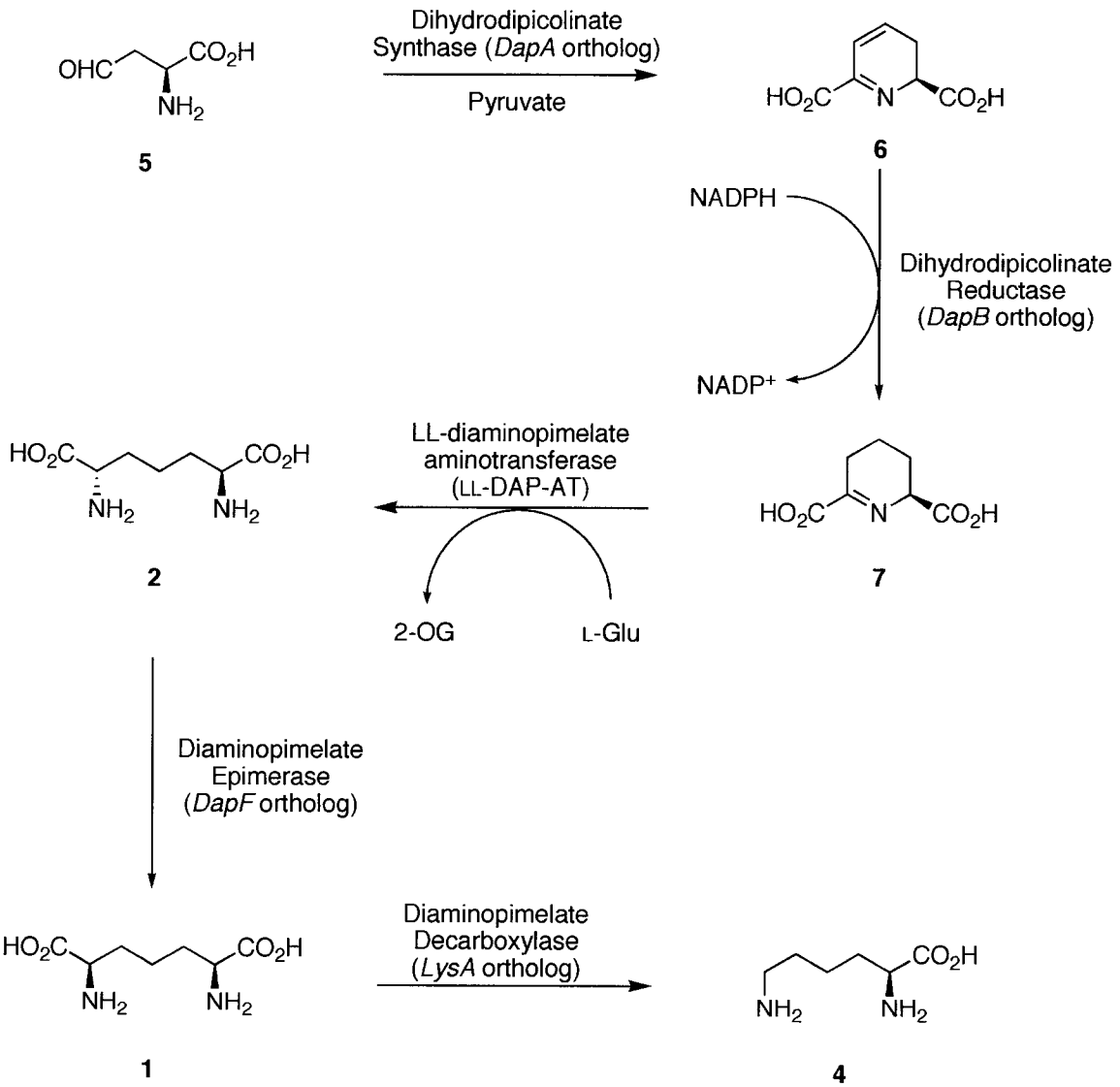

Scheme 3. L-Lysine biosynthetic pathway in plants.

Reproduced with permission of the copyright owner. Further reproduction prohibited without permission.

Recently, the cloning of the biosynthetic genes and overexpression of many of the enzymes involved in the plant lysine biosynthesis has facilitated detailed studies regarding the mechanism of action of these enzymes. Two enzymes of interest in the DAP pathway, DAP epimerase and LL-DAP aminotransferase, utilize substrates having either an imine bond or have transient intermediates wherein the α-carbon center of the amino acid moiety becomes planar.[32, 35]

At the beginning of this project, the plant DAP epimerase and LL-DAP aminotransferase were not well understood in terms of their structure and the mechanism of action. A better understanding of these enzymes can be achieved by constructing inhibitors to probe the chemical and biochemical properties. Protein crystal structures of such enzymes having inhibitors in their active sites can also help in the elucidation of their mechanism.

1.5. Key Plant Enzymes Involved in Lysine Biosynthesis.

1.5.1. Diaminopimelate Epimerase

An understanding of the bacterial DAP epimerase will shed light on the mechanistic and structural properties of the plant DAP epimerase. Bacterial DAP epimerase, a member of the non-pyridoxal phosphate-dependant amino acid racemase family, catalyzes the interconversion of LL-DAP (**2**) and *meso*-DAP (**1**) without the use of cofactors, metals, or keto or imine intermediates.[36] The enzyme is not inhibited by hydrazine or hydroxylamine, and an imine is not an intermediate as the enzyme is not

Reproduced with permission of the copyright owner. Further reproduction prohibited without permission.

inhibited by sodium borohydride.[37] Like other well-studied PLP-independent racemases, such as proline racemase,[38] glutamate racemase[39, 40] and aspartate racemase,[41] early mechanistic studies indicated that DAP epimerase (*DapF*) uses two cysteine residues for catalytic activity.[36] The thiolate of one cysteine residue acts as a base, abstracting the α-proton from one face while the second thiol acts as an acid and delivers a proton to the opposite face, resulting in an inversion of stereochemistry at the α-position[36, 38] (Scheme 4). The primary kinetic isotope effect observed as the α-hydrogen exchanges with deuterated solvent *via* the thiol, also supports this mechanism.[36, 42]

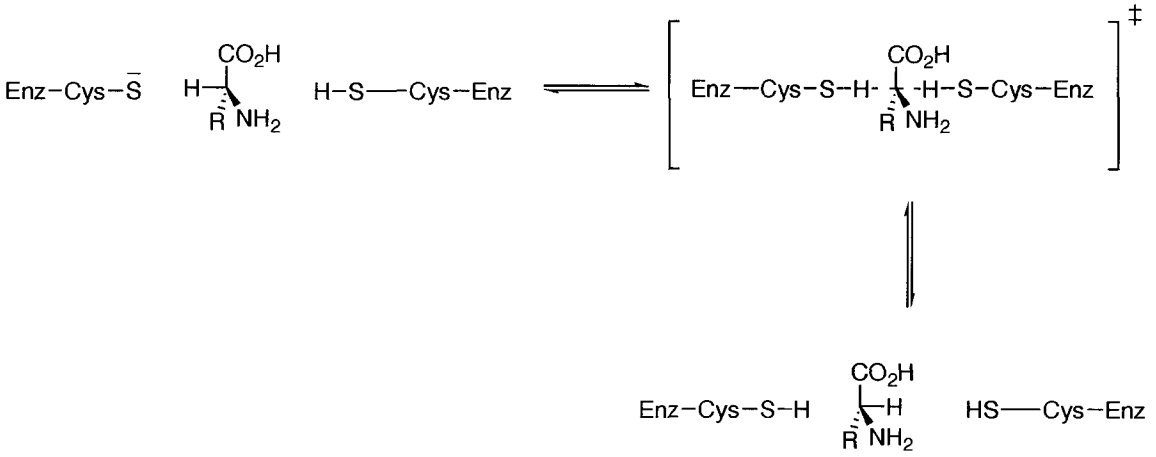

Scheme 4. Thiol thiolate mediated epimerization mechanism.

Studies into the substrate specificity of DAP epimerase shows that the stereochemistry at the distal (non-reacting) site of the substrate is critical for substrate recognition along with the specific carboxyl and amino groups. DD-DAP (**3**) was shown not to be a substrate along with both D- and L-isomers of lysine (**4**) and α-aminopimelic acid (**18**) (Figure 3).[17]

Reproduced with permission of the copyright owner. Further reproduction prohibited without permission.

An early mechanistic study of DAP epimerase supported the formation of α-anionic character at the α-carbon by investigating the elimination of hydrogen fluoride from the pure β-fluoro-DAP stereoisomers.[43] A subsequent study confirmed that Cys73 and Cys217 were the general bases for proton abstraction in the LL to *meso* and the *meso* to LL directions, respectively.[44]

The three-dimensional structure of an inactive form of DAP epimerase from *Haemophilus influenzae* in which Cys73 and Cys217 have formed a disulfide bond reveals a monomeric enzyme, consisting of 274 amino acids with an unusual pseudo twofold symmetry axis around the central cleft that forms the active site.[45, 46]

Recently, DAP epimerase from *Haemophilus influenzae* was crystallized after reaction with enantiomerically pure isomers of 2-(4-amino-4-carboxybutyl)aziridine-2-carboxylic acid (azi-DAP) (**19**, **20**) (Figure 3).[17, 47] Previous studies have shown that isomeric mixtures of azi-DAP were irreversible inhibitors of DAP epimerase.[48]

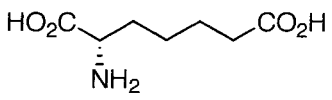

18

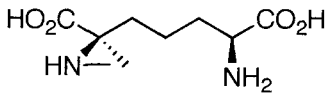

19

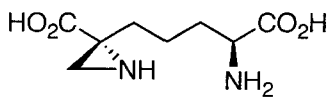

20

Figure 3. Chemical structures of **18** and DL- and LL- azi-DAP (**19**, **20**).

Reproduced with permission of the copyright owner. Further reproduction prohibited without permission.

The crystal structures confirmed that Cys73 and Cys217 were the general bases for proton abstraction in the LL to *meso* and the *meso* to LL directions respectively. Analysis of the crystal structures found LL-azi-DAP (**20**) covalently bound to Cys73 in the LL-azi-DAP inhibited enzyme and the DL-azi-DAP (**19**) covalently bound to Cys217 in the DL-azi-DAP inhibited enzyme (Figure 4).[17]

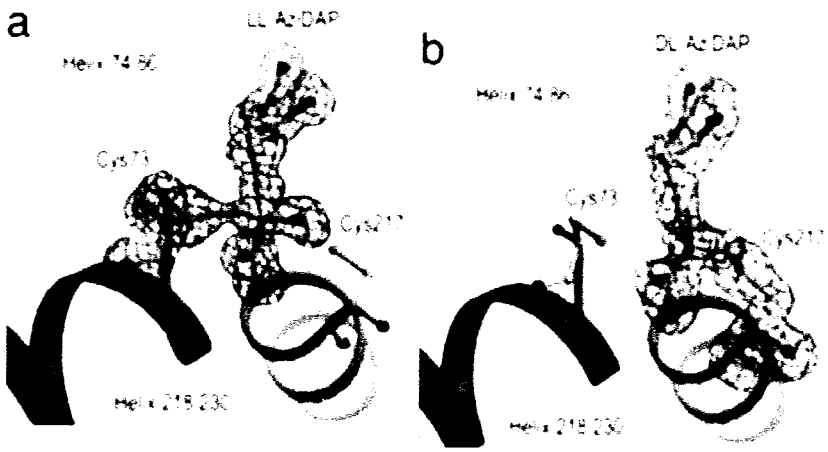

Figure 4. The active site of DAP epimerase in the LL-azi-DAP-epimerase complex (a) and the DL-azi-DAP-epimerase complex (b). (Reproduced with permission from *Proc. Natl. Acad. Sci.*, Pillai, 2006).[17]

Recently, Leustek and coworkers[32] isolated and identified the ortholog of *DapF* from *Arabidopsis thaliana* and showed it to be 31.2% identical with the protein sequence from *E. coli*. The crude protein was found to be active in the conversion of LL-DAP to *meso*-DAP by a coupled assay developed by Wiseman and Nichols.[36]

Reproduced with permission of the copyright owner. Further reproduction prohibited without permission.

1.5.2. LL-DAP Aminotransferase (LL-DAP-AT)

Plant LL-DAP-AT, a pyridoxal phosphate dependant aminotransferase, catalyzes the direct conversion of L-THDP (**7**) to LL-DAP (**2**) with the use of glutamic acid and PLP (**21**) as cofactors.[35] Recently, Leustek and coworkers[35] isolated and purified LL-DAP aminotransferase from *Arabidopsis thaliana* and showed that the enzyme is specific towards the LL-DAP isomer.

Aminotransferases are an important and diverse group of enzymes. The reactions catalyzed by aminotransferases are involved in a variety of metabolic pathways, including amino acid biosynthesis and catabolism, vitamin metabolism, carbon and nitrogen assimilation and shuttling, secondary metabolism, photorespiration, glyoxylate detoxification, and gluconeogenesis.[49] These enzymes catalyze amino group transfers from an amino donor to an amino acceptor. In general, amino acids serve as the amino donor and 2-oxoacids are the amino acceptors. The products of the process are the corresponding 2-oxoacids and amino acids (Scheme 5).

Scheme 5. General scheme in an aminotransferase reaction.

The aminotransferase reactions are freely reversible with the use of a versatile cofactor, pyridoxal-5'-phosphate (PLP, **21**), which is necessary for activity in most

Reproduced with permission of the copyright owner. Further reproduction prohibited without permission.

aminotransferases. PLP-dependant enzymes catalyze a number of reactions depending on which bond at the α-carbon is broken (Figure 5). Cleavage of bond *a* is affected by aminotransferases and certain racemases, bond *b* by decarboxylases, and bond *c* by aldolases.

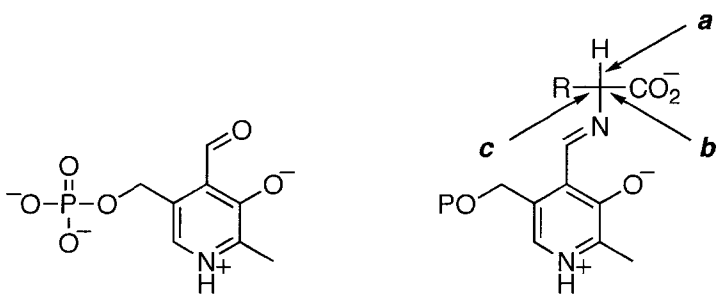

21

Figure 5. Structure of **21** and bond cleavages associated with PLP-dependant enzymes.

A number of PLP-dependant enzymes are irreversibly inhibited by *N*-hydroxy analogs, which form stable nitrones by transamination with PLP. Hydrazino analogs are also well known competitive inhibitors of PLP-dependant enzymes through formation of hydrazone intermediates, which are less susceptible to hydrolysis than the regular aldimine (Figure 6). Like nearly all enzymes, PLP enzymes are susceptible to simple competitive inhibition, but the catalytic versatility and mechanism of the PLP cofactor enhances their potential susceptibility to natural or designed mechanism-based inhibitors.

Reproduced with permission of the copyright owner. Further reproduction prohibited without permission.

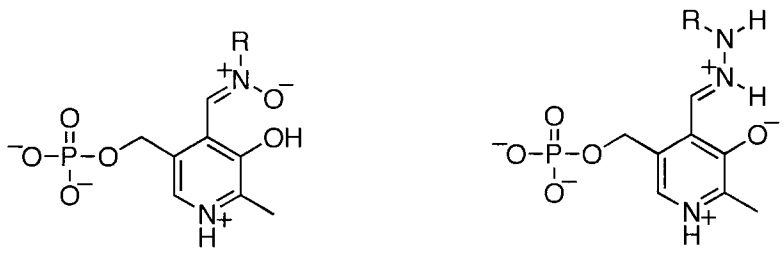

Nitrone Hydrazone

Figure 6. Stable PLP complexes formed from treatment with *N*-hydroxamines and hydrazines.

The general mechanism of PLP-dependant aminotransferases is shown in Scheme 6. Pyridoxal-5'-phosphate acts as an electron sink to stabilize the negative charge development at the α-carbon of the transition state. This occurs when the amino acid substrate (e.g. glutamate in Scheme 6) condenses with PLP to form a Schiff base (**23**) (also referred to as the external aldimine). Initial proton abstraction of the glutamate aldimine **23** at the α-carbon forms the quinonoid intermediate **24**. This intermediate then tautomerizes to the ketimine intermediate **25**. The imine moiety of **25** then hydrolyzes to release α-ketoglutarate (2-OG), leaving the enzyme in the pyridoxamine-5'-phosphate (PMP, **26**) form. Pyridoxamine-5'-phosphate (**26**) then condenses with a ketoacid to form the ketimine intermediate **27**. Proton abstraction at the C_4' position of the cofactor followed by reprotonation at the α-carbon yields the aldimine **28**. Hydrolysis of the imine then yields the PLP form of the enzyme (**22**) and the newly formed amino acid. Potential side reactions of aminotransferases involve racemization of the amino acid α-center. To minimize racemization, the enzyme closes around the substrate to prevent solvent water

Reproduced with permission of the copyright owner. Further reproduction prohibited without permission.

molecules from accessing the quinonoid intermediates.[50] This is a general property of the entire class of aminotransferases.[49]

Under normal physiological conditions and in the absence of PLP, the pK_a of the α-proton of an amino acid is approximately 30.[51] The addition of PLP stabilizes the negative charge by delocalizing it through the π-system of the cofactor, enabling the enzyme to react under ordinarily inaccessible conditions. The function of the protein apoenzyme is to enhance the catalytic potential and to enforce selectivity of substrate binding and reaction type.

The prominent role of PLP enzymes in biochemical reactions has generated a great deal of interest in the mechanism of their inhibition. Understanding the mechanism of inhibition is crucial in the design of better inhibitors for this important class of enzymes. It is also interesting how these enzymes, whose natural reaction pathways includes reactive intermediates such as aldimines and ketimines, manage to avoid inactivation.

Reproduced with permission of the copyright owner. Further reproduction prohibited without permission.

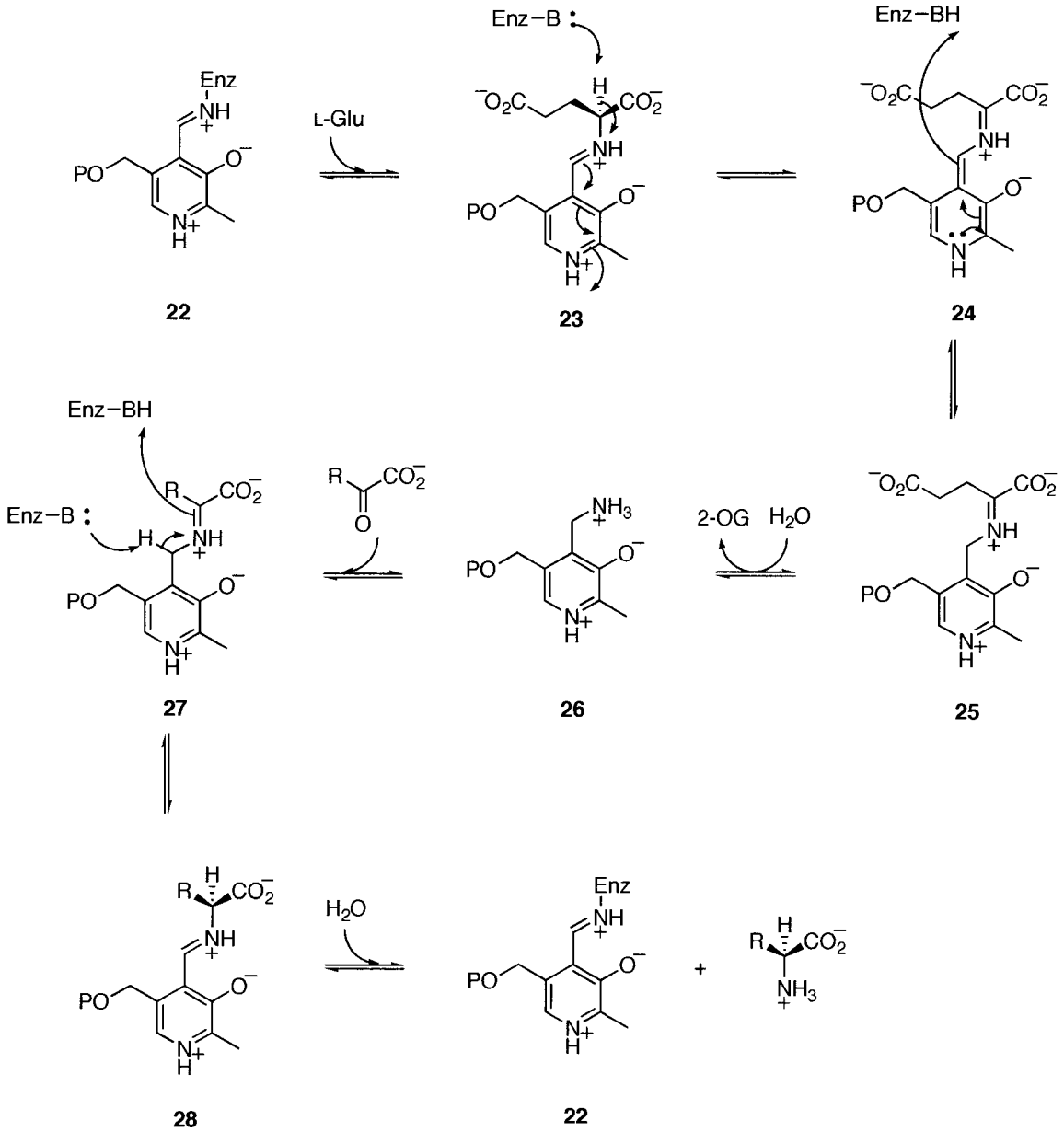

Scheme 6. General mechanism of aminotransferases using glutamic acid as the amino donor.

Reproduced with permission of the copyright owner. Further reproduction prohibited without permission.

1.6. Decarboxylation of Amino Acids

Amines represent one of nature's key functionalities. Their abundance in both natural and synthetic systems makes development of new methods for the preparation of chiral amines desirable.

Decarboxylation of α-amino acids is a well-known reaction. The most common decarboxylation methods involve thermolysis of the amino acid in the presence of a catalytic amount of an aldehyde or ketone.[52-54] Other methods involve irradiation with UV light,[55] heating in diphenylmethane solvent[56] or thermolysis in a high boiling solvent in the presence of a peroxide catalyst.[57]

The synthesis of optically active amines from amino acids has drawn even more attention due to their wide range of usages as chiral building blocks for the synthesis of various pharmaceuticals.[58, 59] Among the methods that have been used for the synthesis of optically active amines, the use of transaminases, chiral reduction of cyanides and kinetic resolutions of racemic amines have been most widely employed.[60]

In the past few years, a great deal of work has gone into the development of chemistry involving radical reactions.[61] As a result, the efficiency of the radical reactions has been improved and many multicomponent catalytic processes have been developed. Selectivity has also become a predictable feature. There are numerous ways to generate radicals, including thermal, electrochemical, metal catalyzed, as well as photochemical processes.

Reproduced with permission of the copyright owner. Further reproduction prohibited without permission.

Photoinduced electron transfer (PET) reactions are very similar to homolytic photochemical reactions, but in order to reach the ground state closed-shell products, the charges produced in the electron transfer must be annihilated via charge recombination or elimination of a negatively or positively charged fragment. However, PET processes become inherently different than homolytic processes when the influences of solvent polarity, donor and/or acceptor redox potential and geometry factors are considered.[61]

Oda and coworkers[62] reported a simple PET method for photodecarboxylation of carboxylic acids that used aza aromatic compounds as electron acceptors (Scheme 7). This method produced moderate yields when using simple hydrocarbon carboxylic acid derivatives in solution phase and a hydrogen donor such as *tert*-butyl thiol. Functionalized carboxylic acids (eg. those containing heterocycles) produced unselective results with a variety of byproducts.

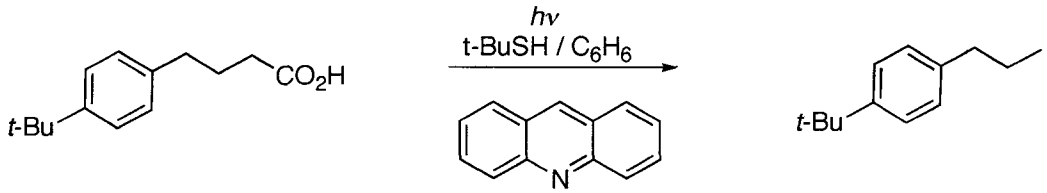

Scheme 7. Photoreaction of simple carboxylic acids in the presence of an aza aromatic compound.

Koshima and coworkers[63-65] found that the solid-state photodecarboxylation occurred with a remarkable selectivity compared to that in solution phase. The solid-state photolysis was conducted in the crystalline state. The crystals were comprised of a stoichiometric mixture of the carboxylic acid and aza aromatic compound and the

Reproduced with permission of the copyright owner. Further reproduction prohibited without permission.

reaction proceeded without the use of a hydrogen donor such as tributyltin hydride in moderate yields. Their proposed mechanism is similar to that suggested by Oda and coworkers.[62] Irradiation of the crystal causes a PET process in which a proton transfer followed by an electron transfer affords the carboxylate radical and the hydroacridine radical. Radical decarboxylation followed by hydrogen abstraction from the N-H yields the product (Scheme 8).[66]

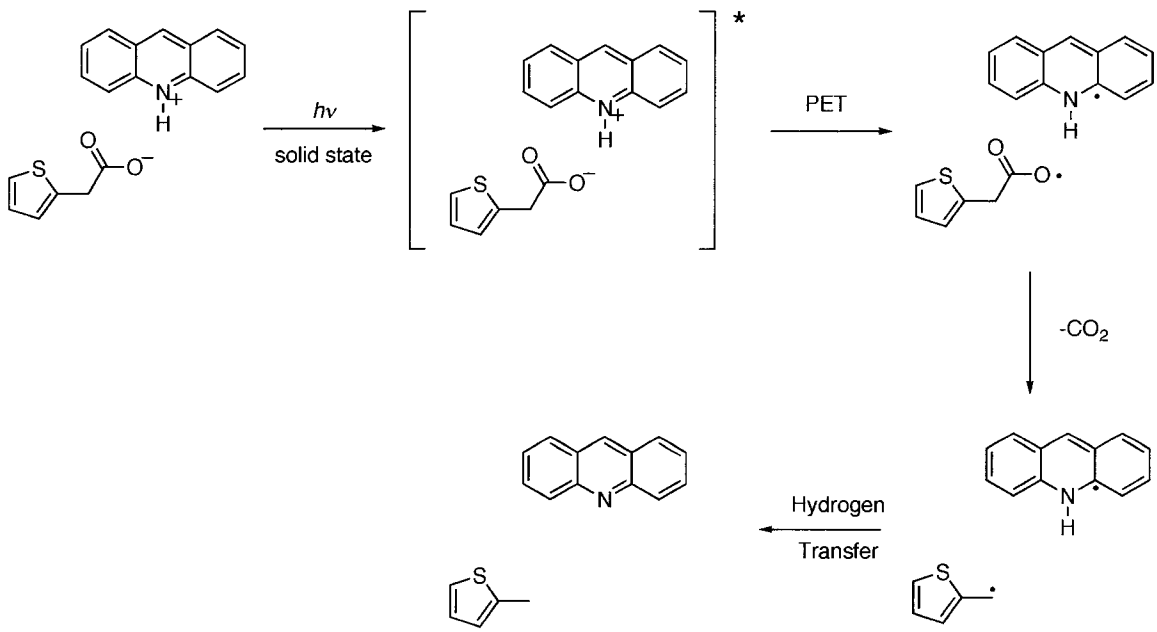

Scheme 8. Photoreaction of two-component molecular crystals in solid state.

Reproduced with permission of the copyright owner. Further reproduction prohibited without permission.

1.7. Objectives

Two separate projects will be presented within this thesis. The first project to be presented involves the photodecarboxylation of amino acid derivatives in the presence of aza aromatic compounds.

Photoinduced decarboxylation has been used with simple carboxylic acids using aza aromatics, and provides a novel method for the preparation of alkane compounds. Decarboxylation in the solid state provides a remarkable selectivity towards formation of the product without unselective recombination, disproportionation or interaction with the solvent molecules. The current methods involved with the decarboxylation of amino acids do not investigate the chirality of the product.

The objective of the first project is to extend this methodology towards the preparation of chiral amines *via* decarboxylation of amino acid derivatives. The stereochemical outcome of this decarboxylation has not previously been investigated and could provide access to chiral amines from chirally pure amino acids.

The second project presented involves investigation into the plant lysine biosynthetic pathway. Previous mechanistic, kinetic and crystallographic studies of enzymes involved in the bacterial lysine biosynthesis have provided valuable tools and insight into the function and mechanism of enzymes involved in the plant lysine biosynthesis. Elucidation of the mechanism of bacterial DAP epimerase by our group suggests that the plant DAP epimerase should function in a similar manner. Furthermore, the proposed mechanism for LL-DAP aminotransferase and aminotransferases in general implies the design of inhibitors that may interfere with the formation of the external

Reproduced with permission of the copyright owner. Further reproduction prohibited without permission.

aldimine or competitively bind in the enzyme active site without undergoing a nitrogen transfer.

The objective of this work is to examine the interaction of several DAP analogs with key enzymes in the plant DAP pathway utilizing synthetic organic chemistry and biochemistry tools. The synthetic DAP analogs prepared will possess either an L- or D-distal configuration to test the requirements for enzyme recognition. The research will focus on the investigation of plant DAP epimerase and LL-DAP aminotransferase.

It is hoped that the investigations presented in this thesis will provide new information concerning the mechanisms of these plant enzymes and lead to novel and more potent inhibitors.

Reproduced with permission of the copyright owner. Further reproduction prohibited without permission.

Chapter 2. Decarboxylation of α-Amino Acids to Yield Amines

As previously described, photolysis in the solid state is shown to occur with remarkable selectivity compared to that in the solution phase, so the latter method will be applied to the current work.[63-66] Koshima and coworkers[63] developed the solid state decarboxylation methodology using simple aliphatic carboxylic acids. Decarboxylation of amino acids using this methodology is unknown in the literature and could lead to a useful method for the synthesis of biologically interesting amine compounds.

2.1. Preliminary Screening

In order to determine useful experimental conditions for the decarboxylation, some preliminary experiments were done using (*S*)-2-(*N*-benzyloxycarbonylamino)-3-phenylpropanoic acid (**29**) and 1,10-phenanthroline (**30**) as an electron acceptor (Scheme 9). The UV spectrum of **30** shows an intense absorption at 254 nm, hence medium pressure mercury lamps were chosen to excite this chromophore since they have an emission band in the same region of the UV spectrum.

Reproduced with permission of the copyright owner. Further reproduction prohibited without permission.

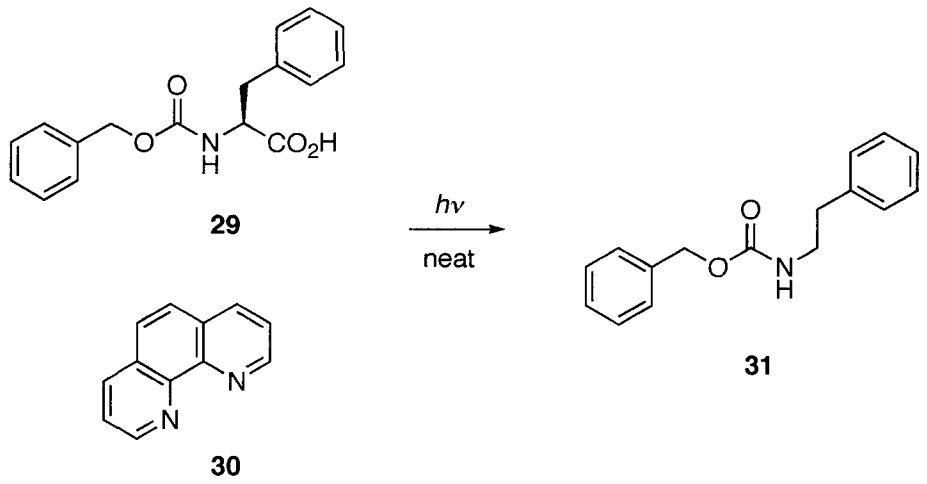

Scheme 9. Photoinduced decarboxylation of amino acid **29** using **30** as the aza aromatic base.

Initial attempts directed at crystallizing the reaction mixture by slow crystallization techniques along with diffusion crystallization proved unsuccessful in forming crystals. Therefore the photolysis was conducted with the substrates in a thin film of uncrystallized material. The thin film can be successfully prepared by dissolving the two components in DCM and varying amounts of MeOH (if needed) and allowing the mixture to evaporate under a stream of argon.

Typically, one of two methods are employed. In method A, a solution of approximately 60-100 mg of amino acid and 1 equivalent of the aza aromatic compound is evaporated to a thin film and irradiated using a 0.9 A mercury lamp for 1-2 days through a quartz plate at 4 °C. If yields are higher than 10% using method A, then method B is employed. Method B is similar, except that the thin film is re-dissolved in DCM and reformed every few hours. This is done to eliminate possible photoprotection of the lower layers of the film by the strata above it.

Reproduced with permission of the copyright owner. Further reproduction prohibited without permission.

Irradiation of equimolar amounts of **29** and **30** as a thin film, gives **31** in 12% yield with a 41% conversion of starting material using method A. An increase in photolysis time to 48 h did slightly improve the yield to 20%, however, prolonged photolysis times (3-5 days) does not improve the yield significantly. Using method B, the yield of **31** increases to 32% with complete conversion of the starting material and also shows a decreased reaction time from 48 h to 8 h. This shows that the photoprotection due to the upper strata of the film lowers the yield of the reaction unless mixed by reforming the film every couple of hours.

The temperature also influences the reaction rate. Photolysis of **29** at -78 °C shows a 53% conversion of starting material in 24 h and a yield of 18%, whereas photolysis at 70 °C shows a conversion of 100% in a 6 h period and a yield of 24%. An increase in the amount of side products is also seen as the temperature is increased.

In addition to 1,10-phenanthroline (**30**), various other commercially available aza aromatic compounds successfully induce the decarboxylation of **29**, albeit in much lower yields than **30** (Figure 7). Koshima and coworkers[63-66] reported that acridine (**32**) can induce decarboxylation with simple carboxylic acids, but it is unsuccessful in the decarboxylation of **29** in this study and only starting material is recovered. Compounds **33**, **34**, and **35** induce decarboxylation to give **31** in 10%, 5% and 9% yields, respectively using method A. Non-aza aromatic compound such as **36, 37**, and **38** also show decarboxylation product in 5%, 7% and 8% yields, respectively.

Reproduced with permission of the copyright owner. Further reproduction prohibited without permission.

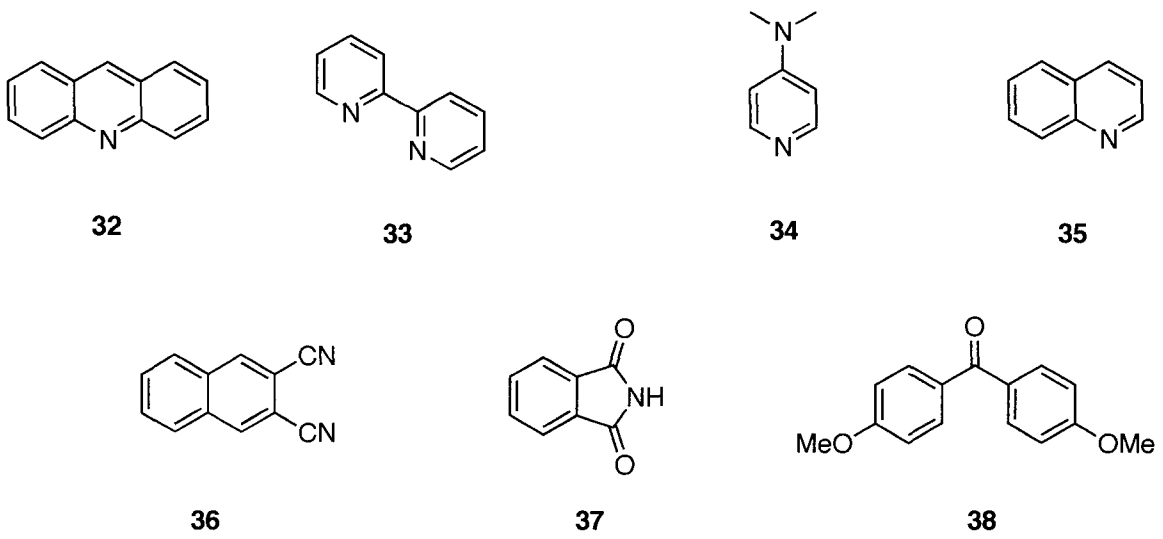

32 33 34 35

36 37 38

Figure 7. Commercially available aza aromatic compounds **32-38** to be tested as aza aromatic compounds for the decarboxylation of **29**.

Koshima and coworkers[63-66] along with Oda and coworkers[62] reported the formation of small amounts of alkylated derivatives of acridine (**41**, **42**) as byproducts in the photolysis reactions when using acridine (Scheme 10). Attempts were made to purify similar byproducts that may arise when using 1,10-phenanthroline as the aza aromatic base. However, these were unsuccessful due to the large number of products formed with similar R_f values on silica gel.

Reproduced with permission of the copyright owner. Further reproduction prohibited without permission.

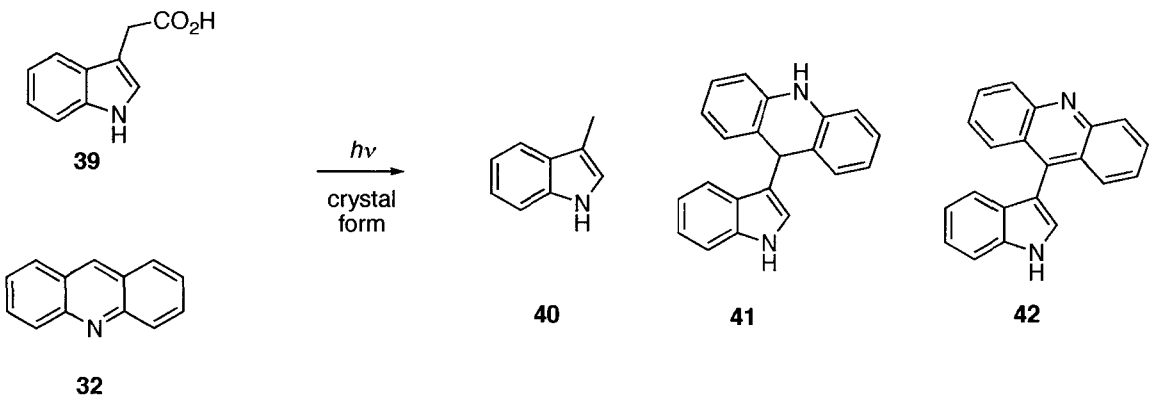

Scheme 10. Formation of byproducts **41** and **42** in the decarboxylation of **39** using **32** as the aza aromatic base.[63-66]

A possible explanation for the poor yields is that our experiments are not conducted in the crystalline state. Since the photolysis is done as a thin film, the resulting radical is in close proximity to a variety of randomly positioned molecules. As such, the ability of the radical to either abstract a proton or undergo radical recombination with these nearby molecules may give rise to the many byproducts in the photolysis. In a crystalline state, the radical intermediate is in a rigid conformation and only a small variety of byproducts are possible.

In order to determine if one particular component of the reaction is causing the majority of the side reactions, control experiments can be conducted. Deletion of each component of the photolysis reaction mixture at a time shows no observable side products in the absence of either the aza aromatic or the amino acid. This ensures that the observed decarboxylation requires the aza aromatic compound and that the side products of the decarboxylation only occur when the two components are present. Photolysis of

Reproduced with permission of the copyright owner. Further reproduction prohibited without permission.

product **31** shows no decomposition, suggesting that the side products are not forming from the decomposition of the decarboxylation products.

2.2. Influence of the *N*-Protecting Groups and Amino Acid Substituents on the Decarboxylation.

It was supposed that the electron donating capabilities of the α-nitrogen group may play a role in the formation of the vast amount of side products observed in the photolysis reaction, hence various *N*-protected phenylalanines (**29, 43-45**) were synthesized and subjected to the decarboxylation conditions (Figure 8). The required *N*-benzyloxycarbonyl protected **29** and *N*-amide protected **43** are commercially available, whereas *N*-benzyl protected **44** and **45** can be synthesized as outlined in Scheme 11.

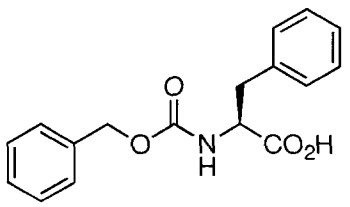

29

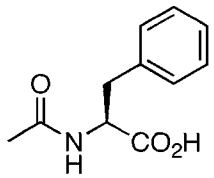

43

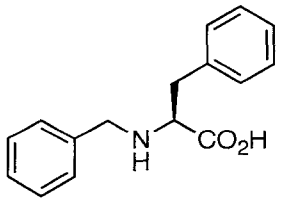

44

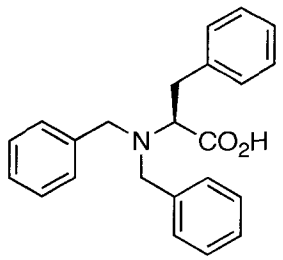

45

Figure 8. Structures of *N*-protected phenylalanines **29, 43-45.**

Reproduced with permission of the copyright owner. Further reproduction prohibited without permission.

Treatment of **46** with sodium carbonate and benzyl bromide gives **47** in 95% yield.[67] Hydrolysis of **47** is then achieved using 2 N KOH to give **45** in 88% yield. The synthesis of the mono-benzylated **44** is achieved by first forming the imine of **46** with benzaldehyde, followed by reduction of the imine with sodium borohydride to yield **44** in 90% yield.[68]

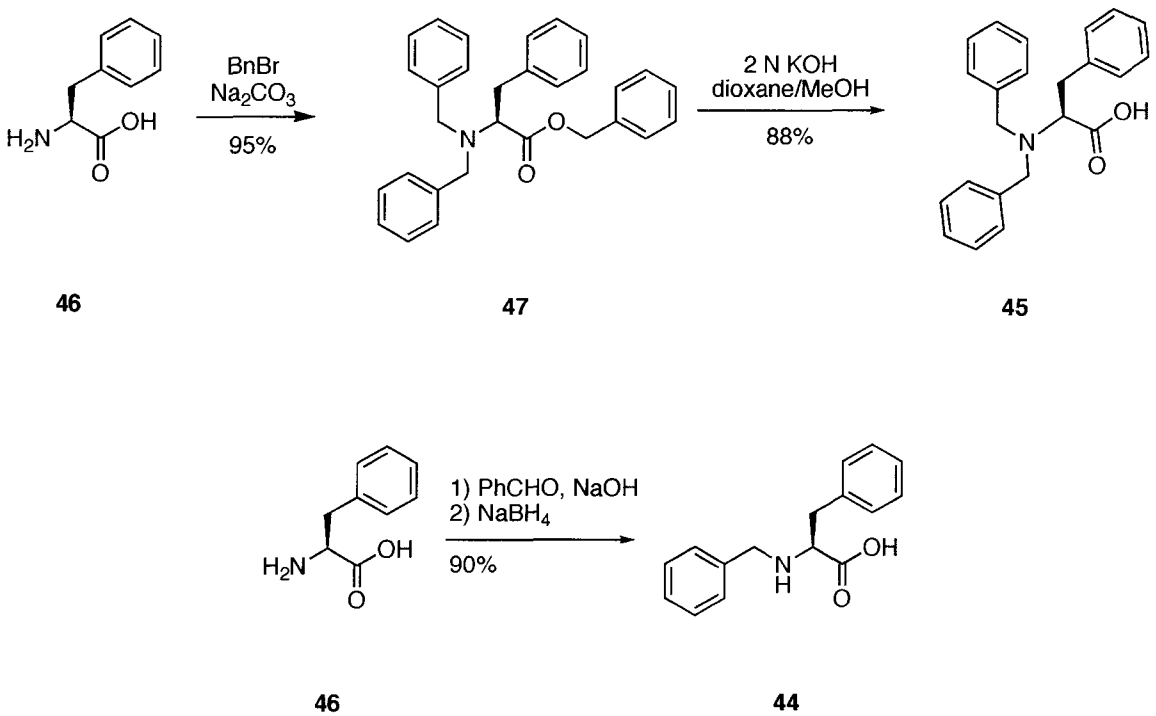

46 **47** **45**

46 **44**

Scheme 11. Synthesis of *N*-benzyl protected phenylalanines **44** and **45**.

Comparing the decarboxylation of **29** and **43-45** with **30** shows that the *N*-protecting group greatly affects the yield. The carbamate **29** and amide **43** show yields of 32% and 27%, respectively, using method B. However, compounds **44** and **45** show no

Reproduced with permission of the copyright owner. Further reproduction prohibited without permission.

reaction as only starting material is recovered. This is most likely due to the electron donating ability of the nitrogen next to the α-carbon upon decarboxylation (Scheme 12).

When the carboxylate radical is formed, donation of electron density from the nitrogen lone pair into the α-carbon produces a negatively charged center. This would inhibit the radical decarboxylation from occurring. On the other hand, using a carbamate or amide protecting group draws electron density away from the α-carbon producing a positively charged center, which provides the electron sink required for the radical decarboxylation to occur.

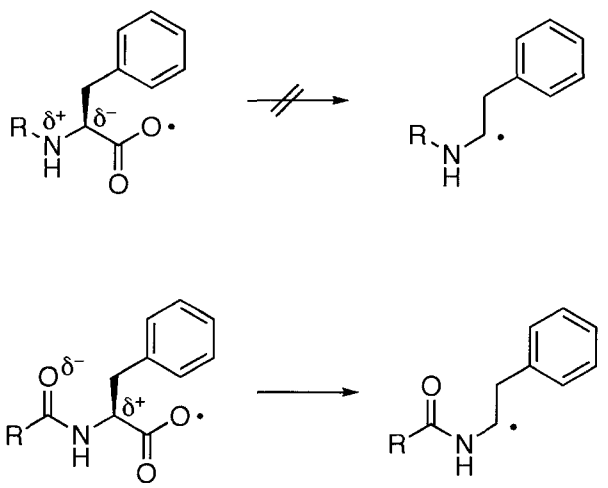

Scheme 12. Influence of *N*-protecting groups on decarboxylation.

The influence of the amino acid substituent can also be seen with the decarboxylation of **48** which has a phenyl substituent compared with **29** which has a benzylic substituent (Scheme 13). Photolysis of **48** in the presence of **30** gives **49** in 11% yield. The low yield can be attributed to the stability of the α-radical intermediate in the benzylic position. The abstraction of the N-H proton to yield the product is a kinetic

Reproduced with permission of the copyright owner. Further reproduction prohibited without permission.

process due to the close proximity of the proton. Stabilizing this radical allows it an opportunity to undergo other processes including radical recombination and proton abstraction from the molecules around it in the thin film. In comparison, the relative instability of the α-radical intermediate formed during the decarboxylation of **29** makes it more prone to kinetic proton abstraction from the N-H.

Steric crowding at the α-amino acid center is also shown to affect the decarboxylation. The decarboxylation of **50** in the presence of **30** gives **51** in 15% yield (Scheme 13). A reason for the lower yield could be attributed to the increased steric bulk at the α-center, but is more likely caused by the increased stability of the radical.

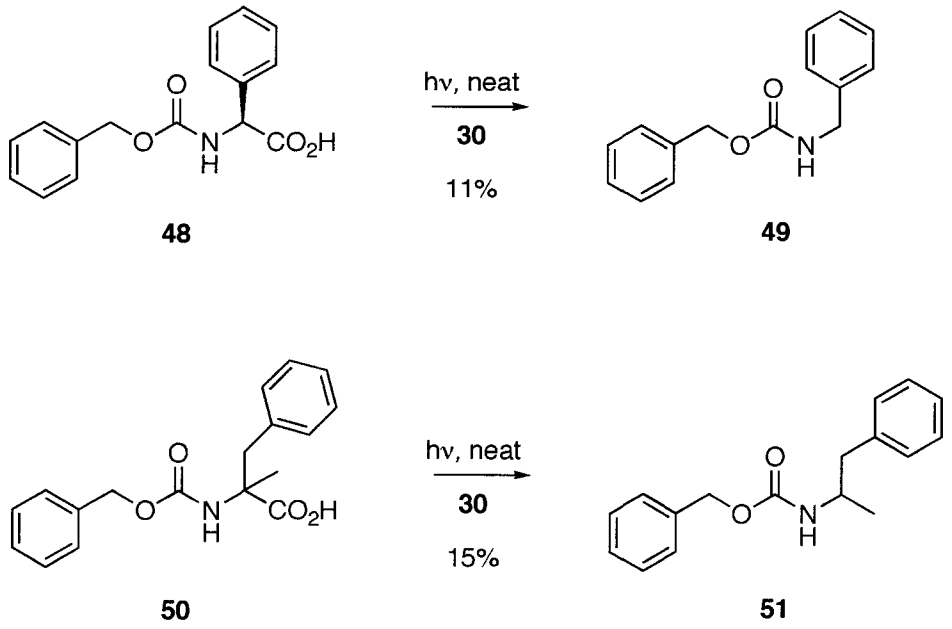

Scheme 13. Photoinduced decarboxylation of **48** and **50**.

Reproduced with permission of the copyright owner. Further reproduction prohibited without permission.

2.3. Retention of Chirality During Photolytic Decarboxylation of Acids

The mechanism of decarboxylation for the two-component system using simple carboxylic acids and aza aromatic compounds is well documented.[61-66] However, the mechanism has not been thoroughly investigated using chirally pure amino acids. If a radical intermediate is present in the decarboxylative process, the resultant photoproduct should suffer loss of chiral integrity.

To study the stereochemistry of this methodology, we investigated the photodecarboxylation of (*S*)-2-(*N*-tert-butoxycarbonylamino)-3-phenylpropanoic acid d_5,α,β,β-d_8 (**52**). According to the mechanism, decarboxylation of **52** will replace the carboxylate functionality with the N-H proton from the hydro-aza aromatic, which can then be analyzed for chiral integrity (Scheme 14). Photolysis of **52** and **30** at 4 °C gives the photoproduct **53** in 31% yield with a 100% conversion of the starting acid using method B. Unfortunately, the enantiomeric excess (*ee*) of **53** could not be determined using chiral NMR shift reagents.[69] Chiral HPLC was similarly unhelpful in resolving the enantiomers, hence an alternative method was sought.

Reproduced with permission of the copyright owner. Further reproduction prohibited without permission.

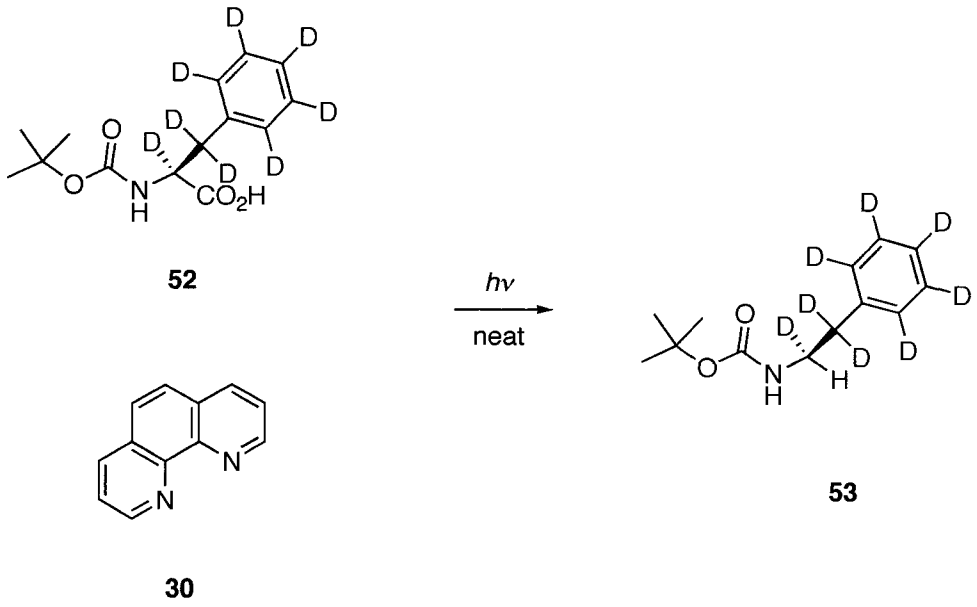

Scheme 14. Photoinduced decarboxylation of **52**.

Derivatization of the two enantiomers using a chiral derivatizing agent should lead to a diasteromeric mixture that can be differentiated by NMR. Mosher and coworkers[70] introduced the derivatizing agent (*S*)-α-methoxy-α-(trifluoromethyl)phenylacetic acid ((*S*)-MTPA, **54**) in 1969 (Figure 9), which has been useful in the determination of the *ee* in a variety of amino acids, terpenoids and amine compounds.[71-73]

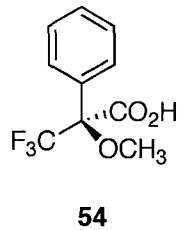

Figure 9. Structure of (*S*)-MTPA (**54**).

Reproduced with permission of the copyright owner. Further reproduction prohibited without permission.

To test this method, the Mosher amide of phenethylamine (**55**) is prepared as a model substrate. Treatment of phenethylamine (**55**) with (*S*)-MTPA acid chloride gives **56** in 86% yield (Scheme 15).[71] Proton NMR analysis of the **56** reveals no baseline separation of the NCH_2-protons in $CDCl_3$, C_6D_6, toluene-d_8, or $(CD_3)_2CO$. However, baseline resolution of the two protons is observed with CD_3CN as a solvent (Figure 10).

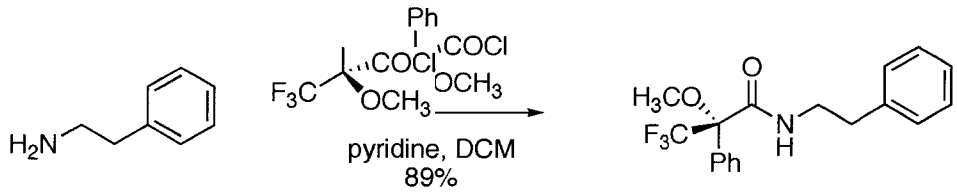

55 **56**

Scheme 15. Synthesis of Mosher amide **56**.

Reproduced with permission of the copyright owner. Further reproduction prohibited without permission.

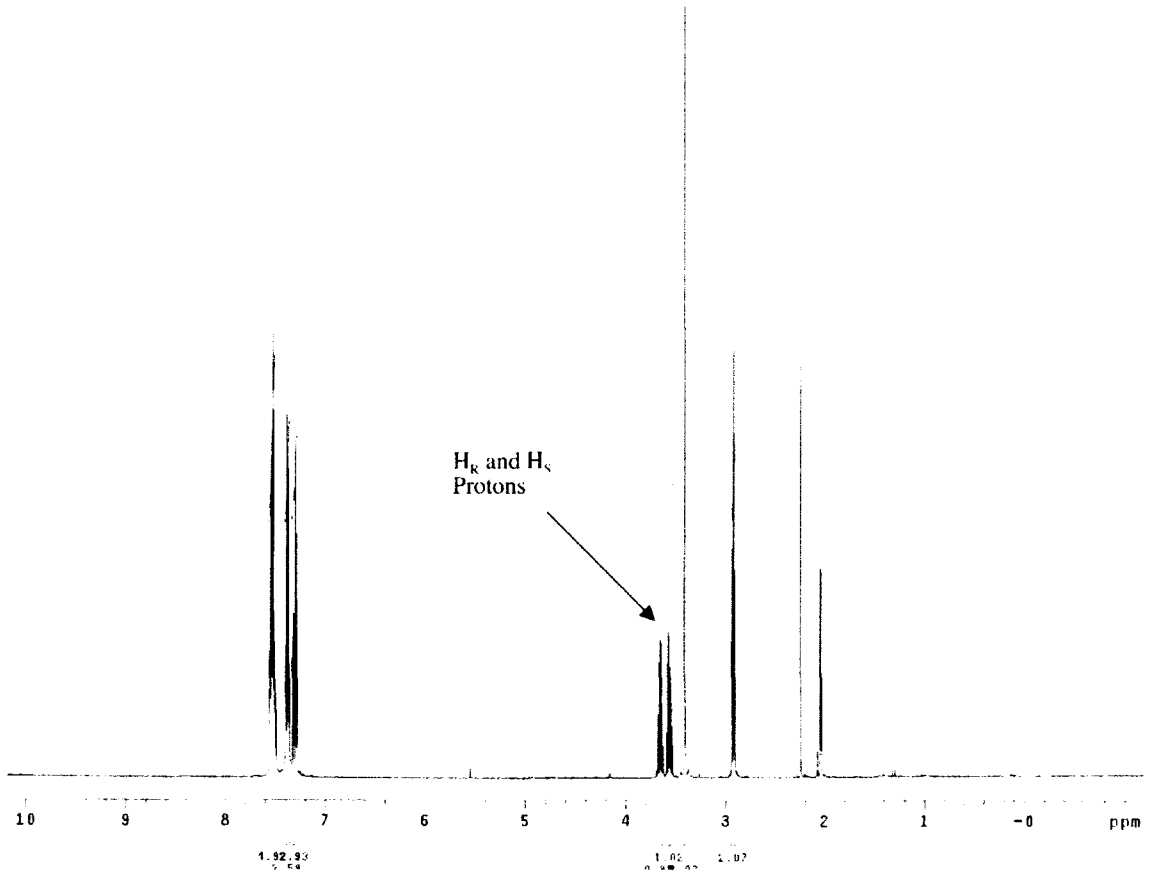

Figure 10. Proton NMR spectrum of **56** in CD_3CN.

Assignment of the two protons can be accomplished using the general model outlined by Mosher.[74] In the MTPA model, the α-trifluoromethyl and carbonyl oxygen are eclipsed so that the preferred conformation has the carbinyl hydrogen eclipsed with the carbonyl group (Figure 11). This places the R_1 group in close proximity to the phenyl ring. Being close to the shielding influence of the anisotropic aromatic group, the R_1 group resonates to lower frequency.

Reproduced with permission of the copyright owner. Further reproduction prohibited without permission.

Figure 11. Eclipsed conformation in the Mosher Model.[74]

The two protons of interest in **56** can be assigned in a similar fashion (Figure 12). Eclipsing the H_R-proton with the α-trifluoromethyl group leaves the H_S-proton close to the shielding influence of the phenyl group and would therefore be expected to be further upfield. Rotating the Newman projection to put the H_S-proton eclipsed with the α-trifluoromethyl group leaves the H_R-proton close to the methoxy group and would cause this proton to be more downfield than the H_S-proton.

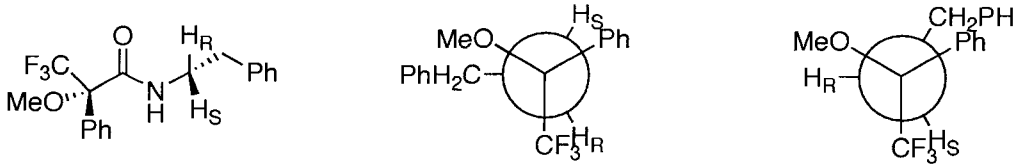

Figure 12. Assignment of diatereomeric protons in **56**.

Treating compound **53** with a 1:1 solution of TFA:DCM followed by exchange of the trifluoroacetate anion with chloride by treatment with 1 M HCl yields **57** (Scheme 16). Conversion of **57** to the chloride salt allows for easier handling of the product as a solid instead of an oil. Without purification, **58** is prepared in 65% yield using the acid chloride of (*S*)-MTPA and pyridine (Scheme 16). Proton NMR analysis of **58** in CD_3CN

Reproduced with permission of the copyright owner. Further reproduction prohibited without permission.

shows that the decarboxylation occurs with loss of chiral integrity (66% *ee*) and with retention of stereochemistry in the major isomer.

One would expect the degree of stereochemical retention to vary with the temperature of the photolysis. However, photolysis of **52** with **30** at -78 °C or rt, shows a similar result to the photolysis at 4 °C, with 66% *ee* and 62% *ee*, respectively, for the corresponding Mosher amides.

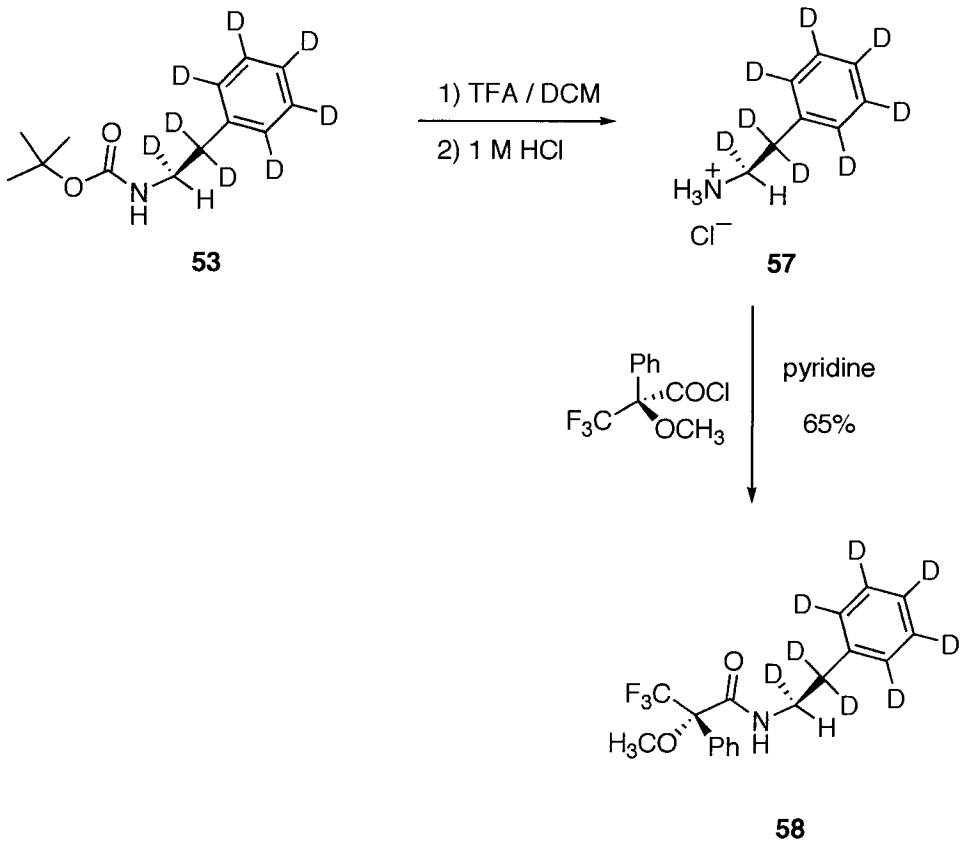

53 **57** **58**

Scheme 16. Synthesis of Mosher amide **58**.

Reproduced with permission of the copyright owner. Further reproduction prohibited without permission.

2.4. Synthesis and Decarboxylation of Other Aza Aromatics

Attempts to increase the yield of the decarboxylation by varying the amino acid protecting group or by using a variety of aza aromatic compounds was somewhat successful. The best yields are obtained using 1,10-phenanthroline (**30**) along with a carbamate or amide protecting group on the amino acid. The increased yield, using **30** as the aza aromatic, is likely due to the increased basicity of the two nitrogen systems as compared to the single nitrogen aza aromatics (**32, 34, 35**) and the rigidity of the aromatic system, in contrast to the more flexible 2,2'-bipyridyl system (**33**) previously employed. A more detailed study on the influence of the donating or withdrawing capacity of the aza aromatic upon decarboxylation is needed.

To increase the yield as well as decrease the number of byproducts formed, additional aza aromatic compounds were synthesized with either the 1,10-phenanthroline or acridine skeletons and tested with (*S*)-2-(*N*-benzyloxycarbonylamino)-3-phenylpropanoic acid (**29**) for decarboxylation (Figure 13). Comparison of the yields against 1,10-phenanthroline will show the affects of these modifications.

Reproduced with permission of the copyright owner. Further reproduction prohibited without permission.

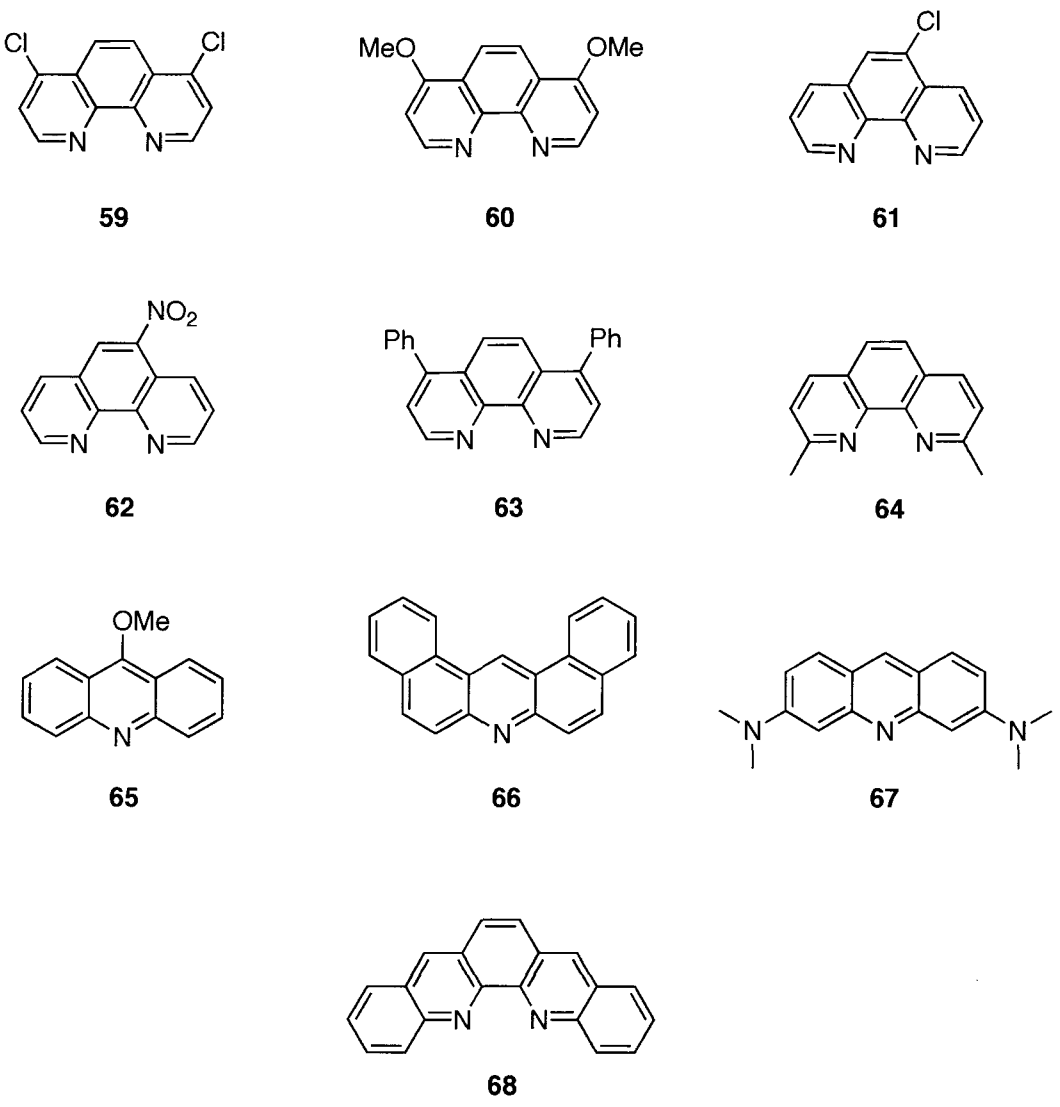

Figure 13. Additional aza aromatic bases to be tested for decarboxylation.

2.4.1. Synthesis of Electron Rich and Benzo-Fused Aza Aromatics

From a retrosynthetic perspective, 4,5-dimethoxy-1,10-phenanthroline (**60**) may be formed *via* displacement of the chloride groups of the corresponding 4,5-dichloro-

Reproduced with permission of the copyright owner. Further reproduction prohibited without permission.

1,10-phenanthroline (**59**) (Scheme 17). Synthesis of compound **59** involves displacement of the hydroxyl groups in the corresponding 4,5-dihydroxy-1,10-phenanthroline (**69**).

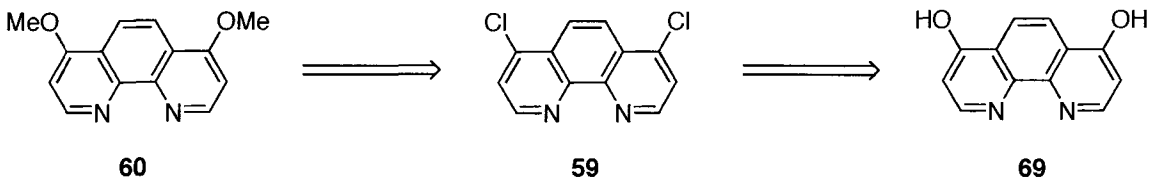

60 **59** **69**

Scheme 17. Retrosynthetic analysis for the synthesis of **60**.

The required dichloro compound **59** can be synthesized as outlined in Scheme 18. Treatment of **69** with $POCl_3$ and PCl_5 gives **59** in 0.05% yield.[75]

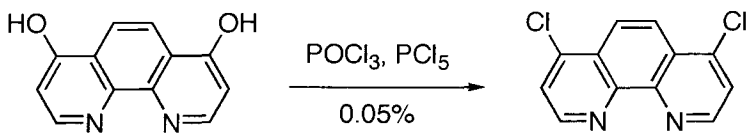

69 **59**

Scheme 18. Synthesis of dichloro compound **59**.

Due to the low yield obtained by this route, an alternate approach to **59** was taken as outlined in Scheme 19. Treatment of diamine **70** with Meldrum's acid in trimethyl orthoformate gives the bis-adduct **71** in 88% yield. The thermal decarboxylation/cyclization occurs under reflux at 210 °C in diphenyl ether to give the crude phenanthrolone **72**. Treatment with phosphoryl chloride then gives **59** in 56% yield.[76]

Reproduced with permission of the copyright owner. Further reproduction prohibited without permission.

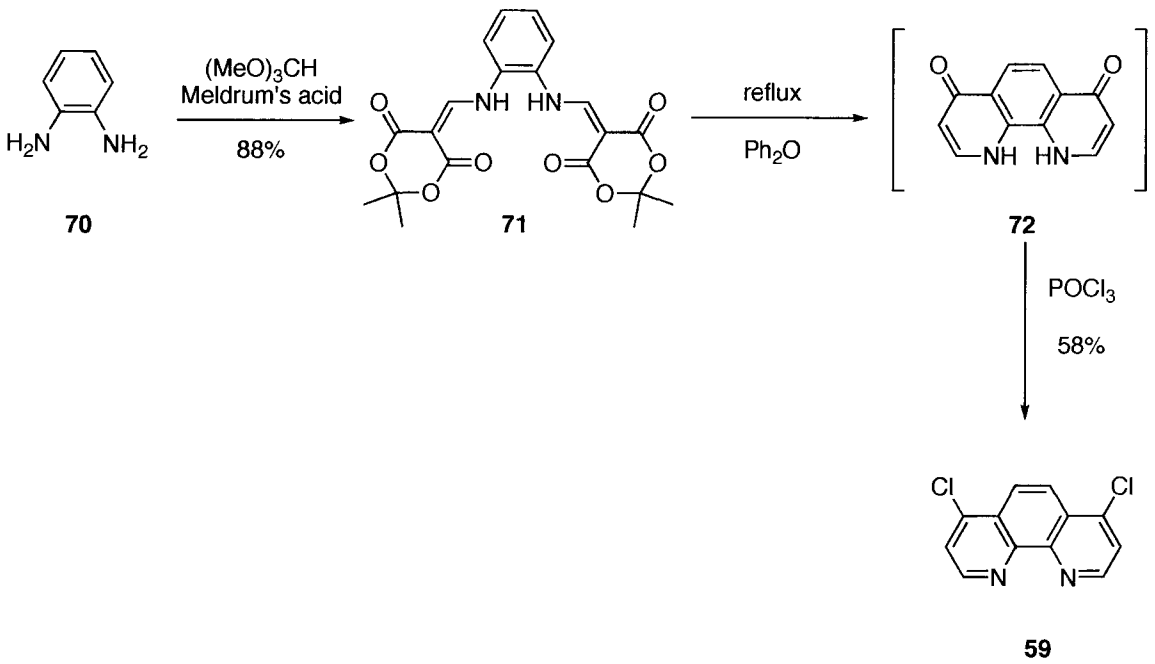

Scheme 19. An alternate synthesis of **59**.

Compound **59** is a convenient starting material for the synthesis of other 4,7-disubstituted 1,10-phenanthrolines. The chloride substituents can easily be replaced with methoxy groups under the influence of sodium methoxide in methanol to give **60** in quantitative yield (Scheme 20).[77] Previous studies within this thesis showed that acridine was not a strong enough PET agent to affect the decarboxylation of **29** due to the lack of basic character. Addition of a methoxy group *para* to the nitrogen should increase the basic character of the nitrogens and improve the decarboxylation. Using the same methodology as was used in the synthesis of **60**, compound **65** can be prepared from **73** in quantitative yield (Scheme 20).[77]

Reproduced with permission of the copyright owner. Further reproduction prohibited without permission.

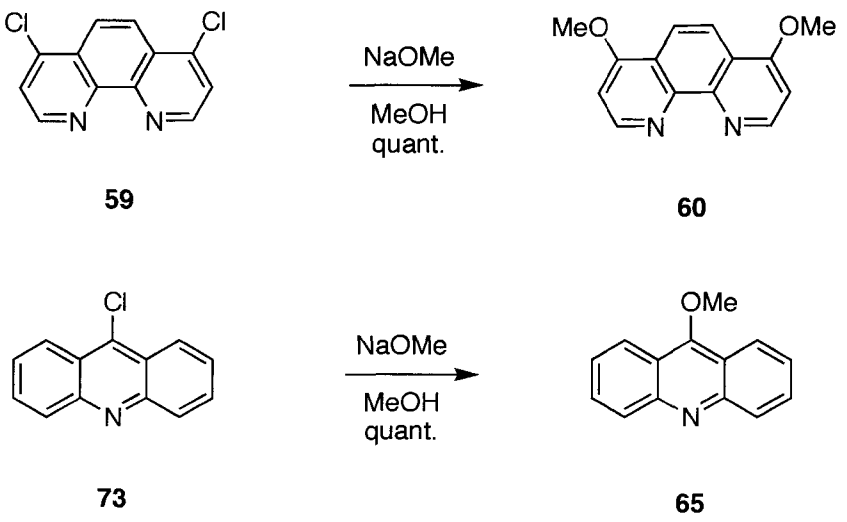

Scheme 20. Synthesis of methoxy substituted aza aromatics **60** and **65**.

The inability to crystallize any of the decarboxylation mixtures led to the synthesis of bisbenzo[2,3:9,8]-1,10-phenanthroline (**68**). This crescent-shaped aromatic molecule might interact in an ordered π-stacking manner and thus assist crystallization. An increased π-system also gives **68** an expanded chromophore and the ability to absorb more UV radiation. The route proceeds by using the Friedlander synthesis of quinolines from *o*-aminobenzaldehyde (OAB, **75**) (Scheme 21).[78] Addition of **74** and **75** to a saturated ethanolic potassium hydroxide solution under reflux gives the biquinoline **76** in quantitative yield. Dehydrogenation of **76** with 10% Pd/C in refluxing nitrobenzene then gives **68** in 47% yield.[79]

Reproduced with permission of the copyright owner. Further reproduction prohibited without permission.

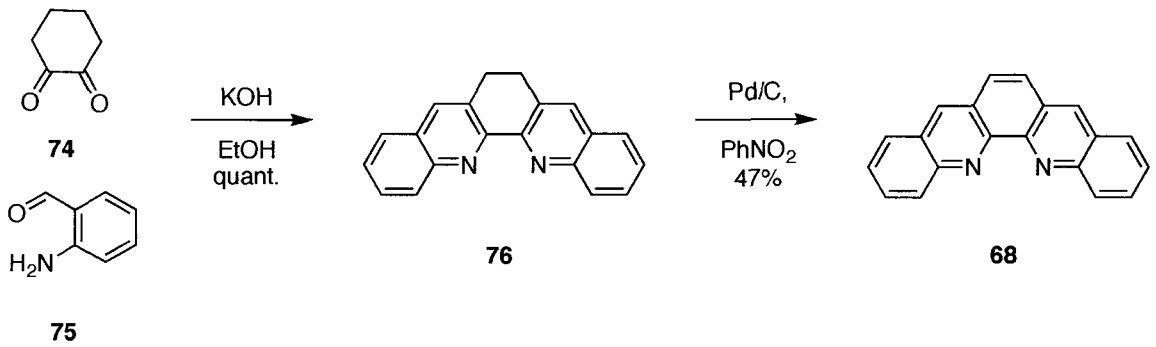

Scheme 21. Synthesis of benzo-fused phenanthroline **68**.

2.4.2. Decarboxylation

The decarboxylation of **29** can be achieved using the compounds in Figure 13 to determine the optimum electronic structure of the aza aromatic compound for efficient decarboxylation. Electron rich aza aromatics such as methoxy derivatives **60** and **65** show an increased conversion of starting material but lower yields of 10% and 14% respectively, due to the increased amount of side products formed. The addition of a methoxy group to acridine sufficiently increases the basicity to allow the decarboxylation to take place, but forms an unstable aza aromatic radical that is prone to undergo side reactions. Compound **67** shows no decarboxylation product, as this is possibly due to the carboxylic acid forming a salt with the $-N(CH_3)_2$ group instead of the ring nitrogen. The dimethyl-substituted phenanthroline **64** gives a decarboxylation yield of 29%. The electronic structure of **64** is similar to that of **30**, except for a small inductive donation of the methyl groups, which is a possible explanation for the similar yields.

Reproduced with permission of the copyright owner. Further reproduction prohibited without permission.

Dichloro **59** and monochloro **61** show yields of 10% and 18% respectively, possibly due to the electron withdrawing capabilities of the chloride substituents. Addition of a nitro group in **62** shows a decarboxylation yield of 10%. It can be concluded that the presence of electron withdrawing substituents on the aza aromatic lowers the yield of the reaction as compared to using **30** as the aza aromatic.

To investigate if an increase in conjugation increases the yield of the decarboxylation, compounds **63, 66, 68,** and **76** can be tested in the decarboxylation of **29** using method A. The benzo-substituted acridine (**66**) shows a yield of 5%. The bridged diquinoline **76** and benzo fused 1,10-phenantholine **68**, show yields of 5% and 6% respectively. Compound **63** shows a decarboxylation yield of 15%. The use of method B in the decarboxylation did not improve the yield of the products significantly. The low yields are possibly due to the photoprotection of the conjugated aza aromatics on the lower layers of the thin film.

2.5. Mechanism of Decarboxylation

The reaction mechanism for decarboxylation (Scheme 22) follows a pathway outlined by Koshima and coworkers except that the photolysis is done as a thin film of uncrystallized material.[63-66] The loss of chirality during the decarboxylation confirms a radical based mechanism, first suggested by Oda and coworkers.[62] This radical is stabilized with electron withdrawing protecting groups such as amides and carbamates on the nitrogen. It is also stabilized as a benzylic radical in compound **48**. The aza aromatic radical is readily formed in electron rich aromatics **60** and **64**, but is shown to be too

Reproduced with permission of the copyright owner. Further reproduction prohibited without permission.

reactive as a vast amount of side products form. Electron withdrawing substituents on the aza aromatic (**59, 61** and **62**) show a more stabilized radical than **60** and **64**, but do not produce a yield greater than with **30**. Photolysis as a thin film has a random distribution of compounds within it, which is the possible reason why recombination of the radicals produces the vast amount of side products.

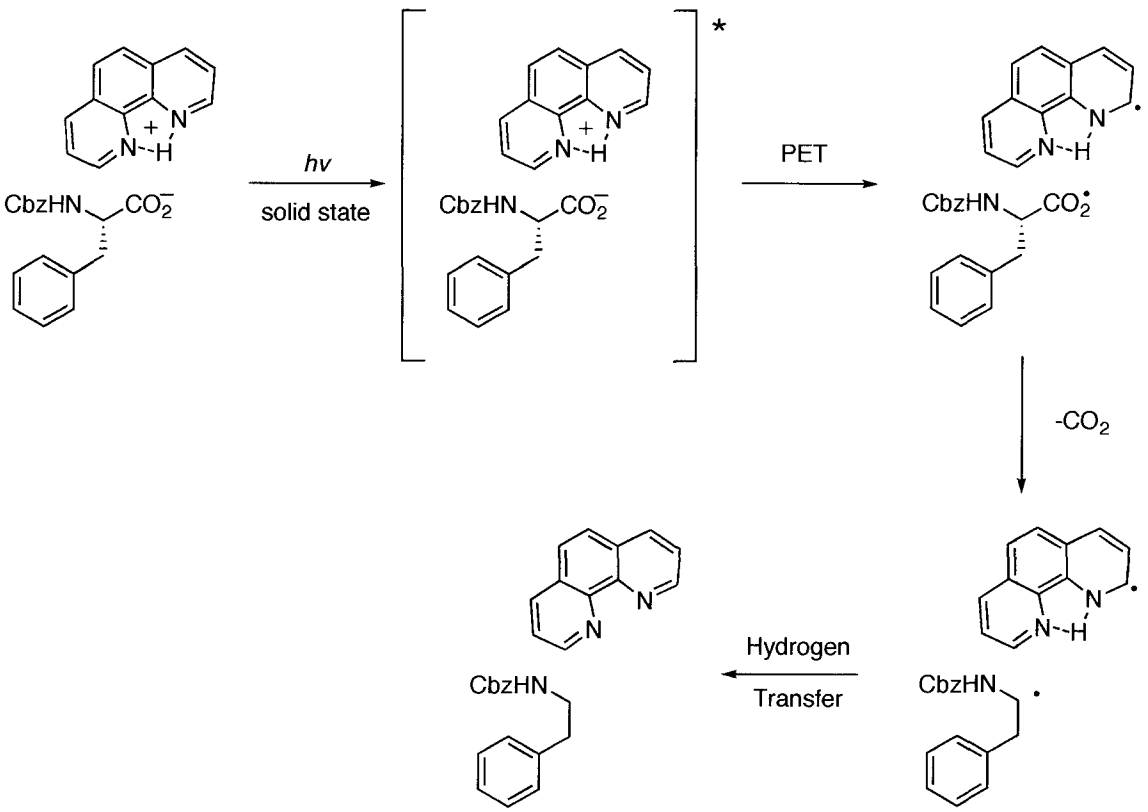

Scheme 22. Decarboxylative reaction mechanism of α-amino acids.

Reproduced with permission of the copyright owner. Further reproduction prohibited without permission.

2.6. Synthesis of Other Amino Acids

To further investigate the stability of the radical intermediate formed on the amino acid, two amino acid analogs (**77, 78**) will be synthesized (Figure 14). Compound **77** will be used to determine if a vinylic radical can be formed, whereas **78** will be used to further investigate the radical based mechanism. The cyclopropyl group has been used in the past as a trap for radical intermediates, since it involves the rapid cyclopropylcarbinyl to homoallylcarbinyl radical rearrangement (Scheme 23).[80, 81]

77 **78**

Figure 14. Structures of amino acids **77** and **78.**

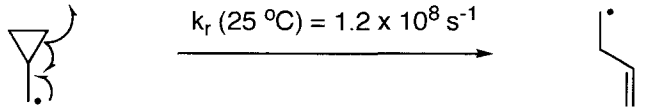

Scheme 23. Mechanism of the cyclopropylcarbinyl to homoallylcarbinyl radical rearrangement.

A retrosynthetic analysis of **77** is shown in Scheme 24. The unsaturated amino acid **77** can be obtained by using a Wittig type reaction with an aldehyde that could come

Reproduced with permission of the copyright owner. Further reproduction prohibited without permission.

from L-glutamic acid (**79**). Manipulation of the protection group would also allow the vinylic acid to be selectively deprotected.

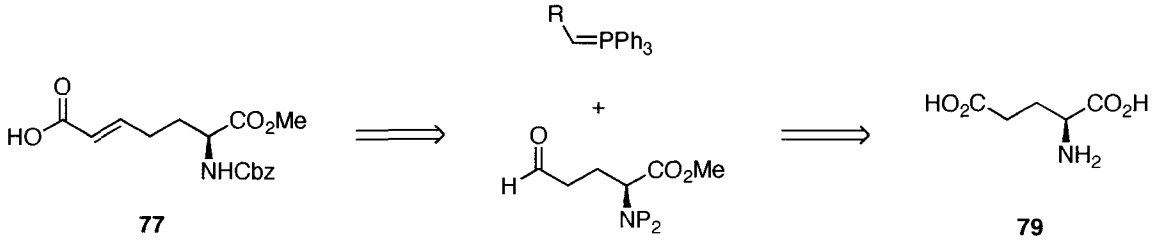

Scheme 24. Retrosynthetic analysis for the synthesis of **77**.

The required aldehyde is synthesized as outlined in Scheme 25.[82] Protection of L-glutamic acid (**79**) as its *N*-Boc dimethyl ester derivative (**80**) is achieved in 99% yield *via* treatment with chlorotrimethylsilane in dry MeOH, followed by the addition of triethylamine and Boc_2O. To reduce the ester to the required aldehyde, Padron and coworkers[82] found that di-Boc protection of the nitrogen minimized its nucleophilic power, hence it allows the subsequent reduction to occur. The dimethyl *N*-Boc-glutamate **80** is treated with Boc_2O and DMAP to give the di-protected **81** in 84% yield. Reduction of **81** with DIBAL in diethyl ether then leads to the formation of the required aldehyde **82** in 83% yield.[82]

Reproduced with permission of the copyright owner. Further reproduction prohibited without permission.

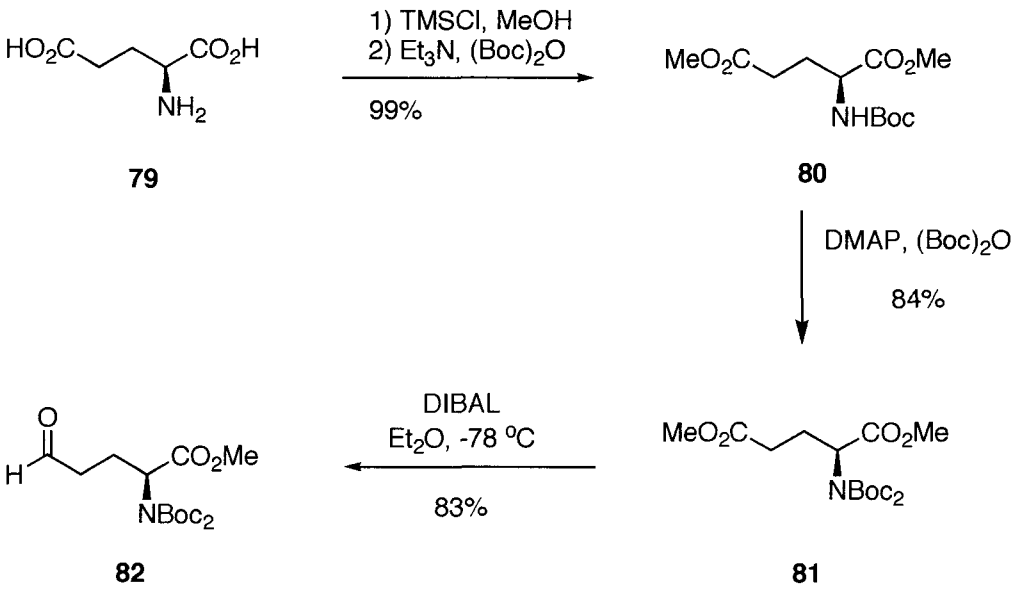

Scheme 25. Synthesis of aldehyde **82**.

With the aldehyde moiety in place, a Wittig reaction is required to furnish the unsaturated α-amino diacid (Scheme 26).[82, 83] Aldehyde **82** was submitted to a Wittig reaction with (*tert*-butoxycarbonylmethylene)triphenyl phosphorane to obtain the corresponding *E*-unsaturated ester **83** in 87% yield. Treatment of **83** with TFA removes the *tert*-butyl protecting group along with both Boc groups to give **84** in 99% yield.[83] The (*tert*-butoxycarbonylmethylene)triphenyl phosphorane was used to allow for specific deprotection of the vinylic acid over the α-carboxylic acid. Protection of **84** as its *N*-Cbz derivative provides **77** in 77% yield.

Reproduced with permission of the copyright owner. Further reproduction prohibited without permission.

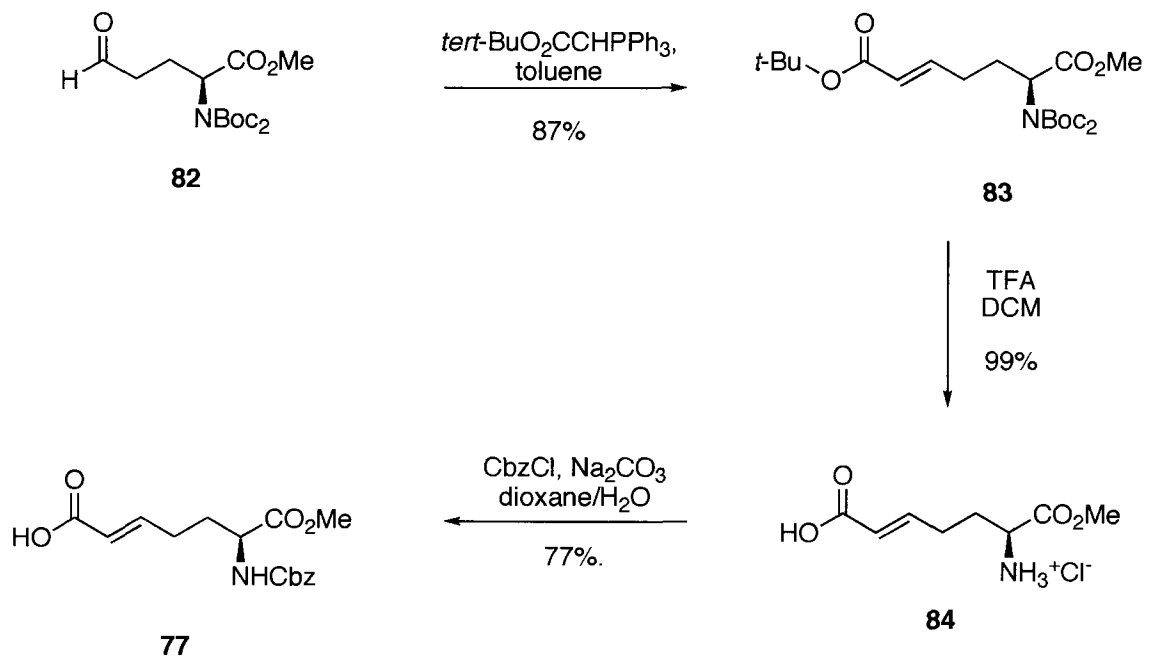

82 83 84 77

Scheme 26. Synthesis of vinyl acid **77**.

From a retrosynthetic perspective, cyclopropylglycine **78** may be formed *via* a Strecker type reaction from cyclopropylcarboxaldehyde (**85**) (Scheme 27).

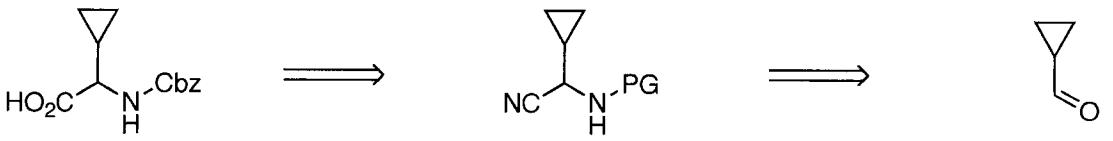

78 **85**

Scheme 27. Retrosynthetic analysis for the synthesis of **78**.

The synthesis of **78** is outlined in Scheme 28.[84] Imine formation of cyclopropylcarboxaldehyde (**85**) with benzylamine followed by potassium cyanide attack gives derivative **86** in 74% yield. Hydrolysis of the cyanide with conc. HCl leads to the

Reproduced with permission of the copyright owner. Further reproduction prohibited without permission.

formation of **87** in 63% yield. Hydrogenation with 10% Pd/C in MeOH then gives **88** in quantitative yield.[84] Protection of **88** as its *N*-Cbz derivative provides **78** in 67% yield.

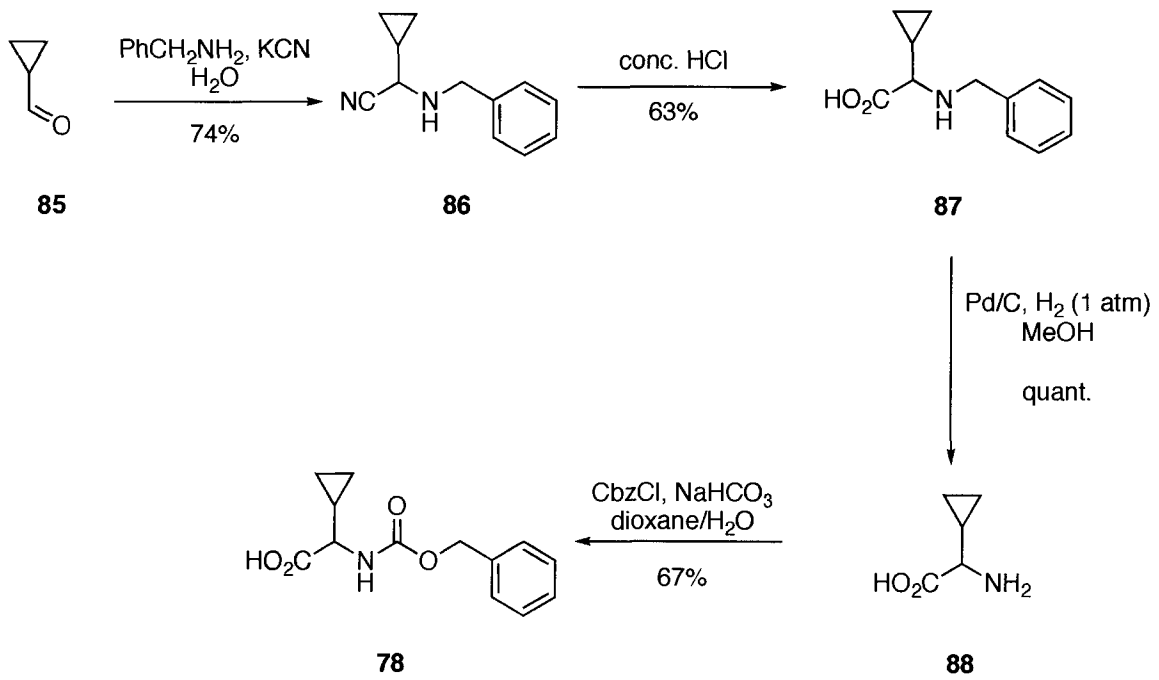

Scheme 28. Synthesis of cyclopropyl derivative **78**.

In summary, the syntheses of compounds **77** and **78** have been achieved. Unfortunately, the project was abandoned due to poor yields before these compounds could be tested using the decarboxylation methodology.

Reproduced with permission of the copyright owner. Further reproduction prohibited without permission.

2.7. Conclusions

The photodecarboxylation of α-amino acids with aza aromatic compounds in the solid state has been described. The best yields were obtained using the carbamate and the amide protecting groups with 1,10-phenanthroline (**30**) as the aza aromatic compound. The increased basicity and rigidity of the two-nitrogen system of **30**, compared to the single-nitrogen aromatics, promotes the decarboxylation, while both the amide and carbamate protecting groups can draw electron density away from the nitrogen and hence assist with the decarboxylation. Decarboxylation at high temperatures increased the conversion of the starting material, but decreased the yield due to the amount of side products formed.

An investigation into the optimum electronic structure of the aza aromatic revealed that electron rich aromatics produced a large amount of side products whereas electron deficient aromatics produced lower yields than the decarboxylation involving **30**.

The stereochemistry of the decarboxylation reaction revealed that the product **53** is formed in 66% *ee* from optically pure starting material **52** by analysis of the Mosher amide.[70] The decarboxylation occurs predominantly with the retention of stereochemistry. The temperature of the decarboxylation did not significantly affect the enantiomeric excess of the product.

Overall, this methodology using amino acids produced lower yields and less selectivity than that obtained by Koshima and coworkers[63-66] with simple carboxylic acids. Thus, further investigation into this methodology was abandoned.

Reproduced with permission of the copyright owner. Further reproduction prohibited without permission.

Chapter 3. Studies Directed Towards the Plant Lysine Biosynthesis Pathway

In recent years, a large number of diaminopimelic acid (DAP) derivatives have been synthesized and studied for inhibition of key bacterial enzymes involved in lysine biosynthesis.[37] The isolation of similar enzymes found in plants allows for the characterization and comparison of these enzymes against their bacterial counterparts.[29, 30, 33-35, 85] Some deviations of the bacterial pathway that are found in plants include the absence of the succinyl pathway or dehydrogenase pathway and direct conversion of L-THDP (**7**) to LL-DAP (**2**) by LL-DAP aminotransferase (LL-DAP-AT).[32, 35]

DAP epimerase in plants and bacteria is believed to function by a similar mechanism whereby planar character develops at the α-carbon of DAP in the transition state (Scheme 4). As a consequence, amino acid derivatives showing inhibitory activity towards the bacterial epimerase may inhibit the plant epimerase as well.

To further investigate the interaction and selectivity of DAP with DAP epimerase, the synthesis of all three isomers of DAP (**1-3**) was proposed (Figure 15). These isomers may provide additional information with regards to the stereochemical requirements in binding with plant DAP epimerase.

Reproduced with permission of the copyright owner. Further reproduction prohibited without permission.

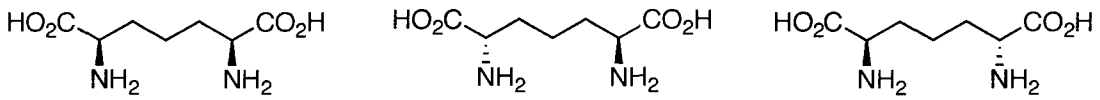

meso-DAP, **1** LL-DAP, **2** DD-DAP, **3**

Figure 15. Structures of the three DAP isomers.

Furthermore, the synthesis of the DAP isomers will also allow for an investigation into the stereochemical requirements of LL-DAP-AT. To further investigate the interaction of L-THDP analogs with LL-DAP-AT, the synthesis of 1*R*-*cis*-**89** was proposed (Figure 16). This cyclic derivative may provide additional information with regards to both the stereochemical requirements and the importance of particular amino acid moieties in binding to LL-DAP-AT. This derivative may also allow for crystallization and characterization of the enzyme-**89** adduct, and thus provide information about structural features that confer selectivity.

7 1*R*-*cis*-**89**

Figure 16. Structures of L-THDP (**7**) and L-THDP analogue 1*R*-*cis*-**89**.

Reproduced with permission of the copyright owner. Further reproduction prohibited without permission.

3.1. Synthesis of DAP Isomers

The study of DAP analogs and their activity with key bacterial enzymes in lysine biosynthesis is extensive, and the variety of chemistry used to access these compounds reflects this. Purification of DAP isomers from the statistical mixture (1:1:2 ratio of **2**:**3**:**1**) of unprotected DAP stereoisomers,[9] along with the biochemical production of these isomers[86] is often quite difficult. Early synthetic methods included the Kolbe electrolysis, but yields were often very low (10-13%).[87] Slightly improved methods to obtain only one specific isomer of DAP include a Diels-Alder reaction[88] and the use of organozinc chemistry[89] to obtain *meso*-DAP (**1**). The syntheses of orthogonally protected DAP derivatives can be achieved using ene chemistry[90] and olefin metathesis,[91] but only provide the DAP isomers with moderate *ee*. The use of chiral synthons in the synthesis of DAP has been shown to occur in high *ee* by Williams,[92] Jurgens,[93] Bold,[94] and Sandri.[95] Another method of DAP synthesis involves the use of diacyl peroxides, which can be obtained from enantiomerically pure starting material already bearing orthogonal protecting groups. Photolysis of diacyl peroxides has been reported to give coupled products under mild conditions.[96, 97] Recently our group has used this methodology towards the synthesis of orthogonally protected LL-DAP (**1**).[98, 99]

From a retrosynthetic perspective, the DAP isomers may be formed *via* photolysis of diacyl peroxides formed from suitably protected aspartic and glutamic acids (Scheme 29).

Reproduced with permission of the copyright owner. Further reproduction prohibited without permission.

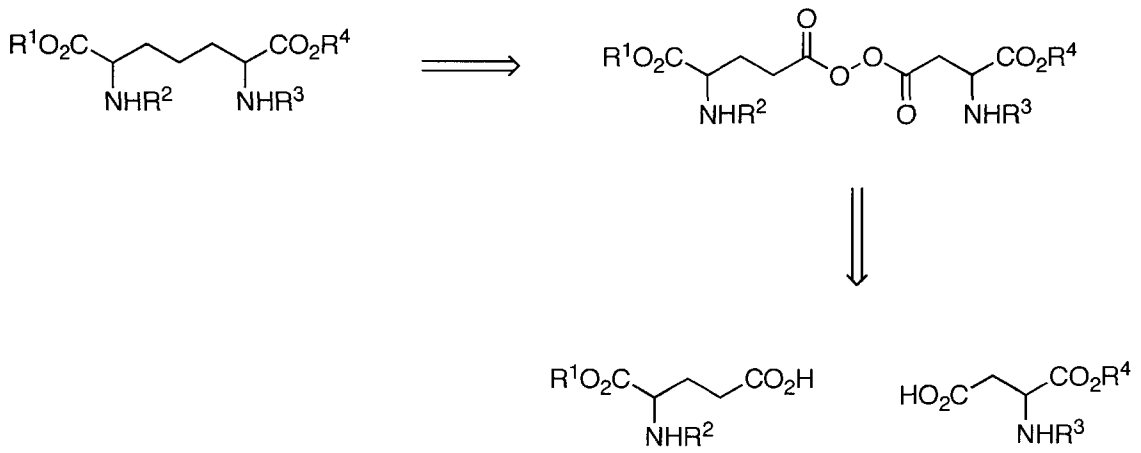

Scheme 29. Retrosynthetic analysis for the synthesis of DAP isomers.

The syntheses of diacyl peroxides **95**, **100** and **104** are outlined in Schemes 30-32.[98] The perester of the suitably protected glutamic acid (**90**, **96** and **101**) can be synthesized by activation of the carboxyl group with DCC followed by coupling with 2-methoxyprop-2-yl hydroperoxide[100] (**91**) to yield the peresters **92**, **97** and **102** in 99%, 89% and 94% yields, respectively. Acidic deprotection of the peresters with TFA then yields the peracids **93**, **98** and **103**, which can only be stored at -20 °C for 1-2 days before noticeable decomposition back to the corresponding glutamic acid is observed. Coupling of the suitably protected aspartic acid (**94** or **99**) with the peracid then yields the diacyl peroxides **95**, **100** and **104** in 89%, 93% and 65% (unoptimized) yields, respectively. The diacyl peroxides are relatively stable and can be stored at -20 °C without decomposition for several weeks.

Reproduced with permission of the copyright owner. Further reproduction prohibited without permission.

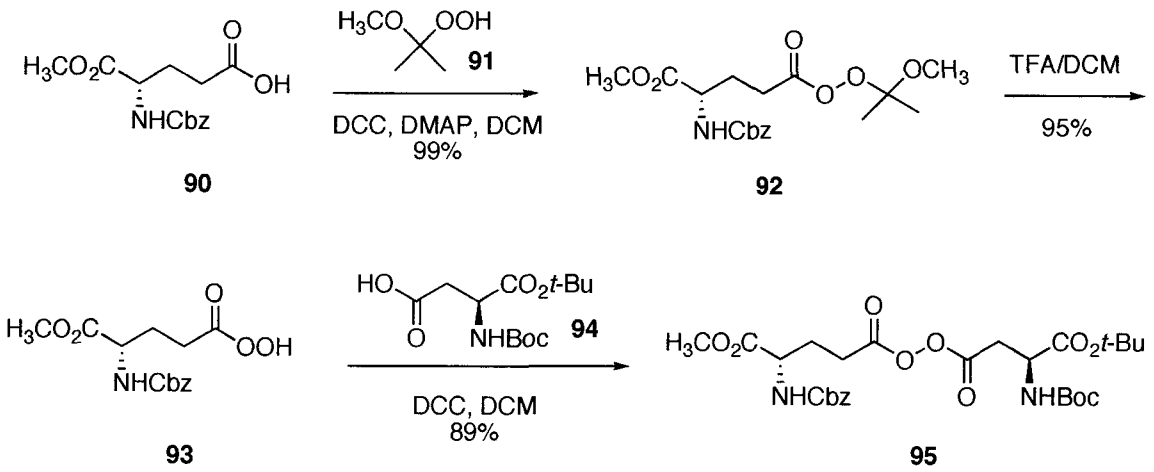

Scheme 30. Synthesis of LL-DAP diacyl peroxide **95** by Dr. Rajendra Jain.

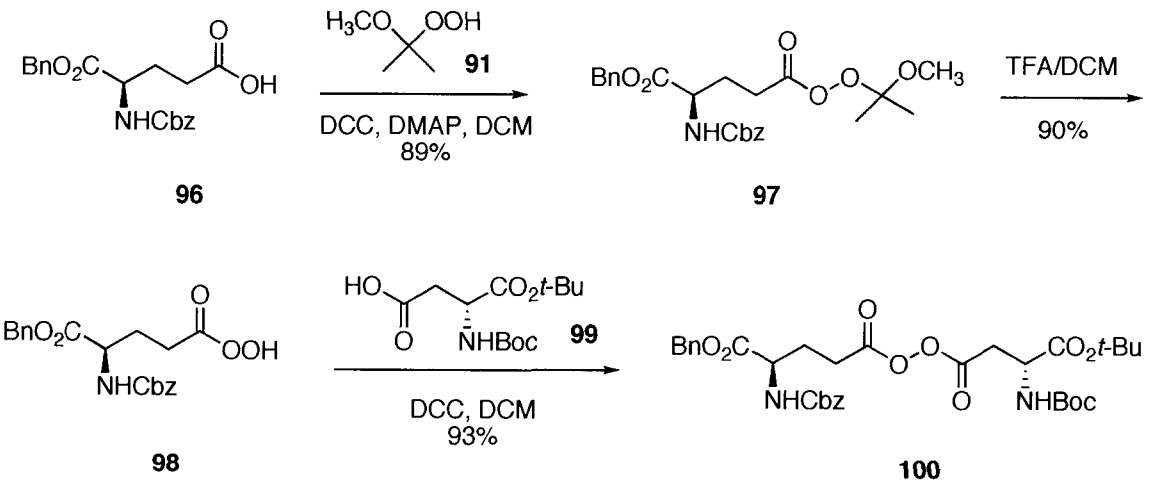

Scheme 31. Synthesis of DD-DAP diacyl peroxide **100**.

Reproduced with permission of the copyright owner. Further reproduction prohibited without permission.

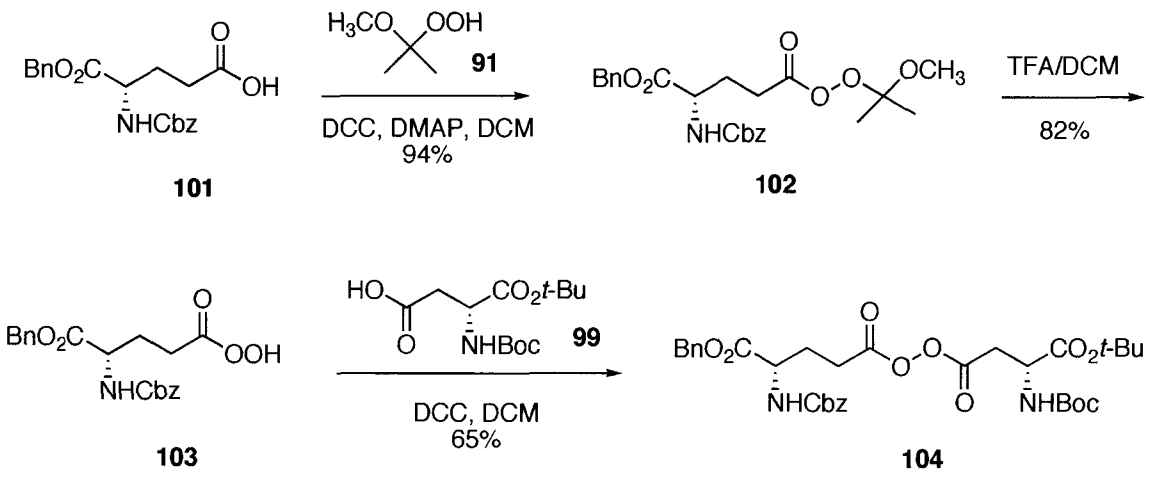

Scheme 32. Synthesis of *meso*-DAP diacyl peroxide **104**.

The formation of pure DAP isomers from the corresponding diacyl peroxides is outlined in Schemes 33-35.[98] Our group has shown that photolysis of diacyl peroxides is best done with neat substrates at -78 °C under an argon atmosphere. At low temperature, cage recombination of the alkyl radicals is more likely due to the restricted movement of the reactive partners.[98] Photolysis of **95**, **100** and **104** with one 254-nm UV lamp gives the orthogonally protected DAP derivatives **105-107** in 49%, 49% and 30% yields respectively. The use of two UV lamps decreased the required photolysis time, but also decreased the yield significantly due to decomposition. The yields of the photolysis are also increased as the thickness of the thin film is decreased. This is possibly due to photoprotection of the lower layers of the thin film by the strata above them. Complete deprotection of the protected DAP derivatives is achieved with 6 M HCl to yield the pure DAP isomers **1**, **2** and **3** in 83%, 90%, and 52% (unoptimized) yields respectively.

Reproduced with permission of the copyright owner. Further reproduction prohibited without permission.

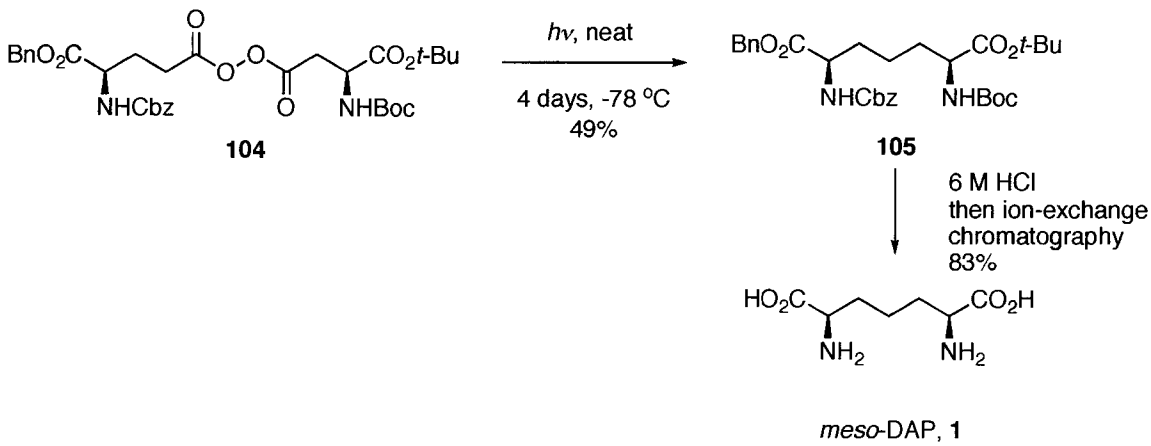

Scheme 33. Synthesis of *meso*-DAP (**1**).

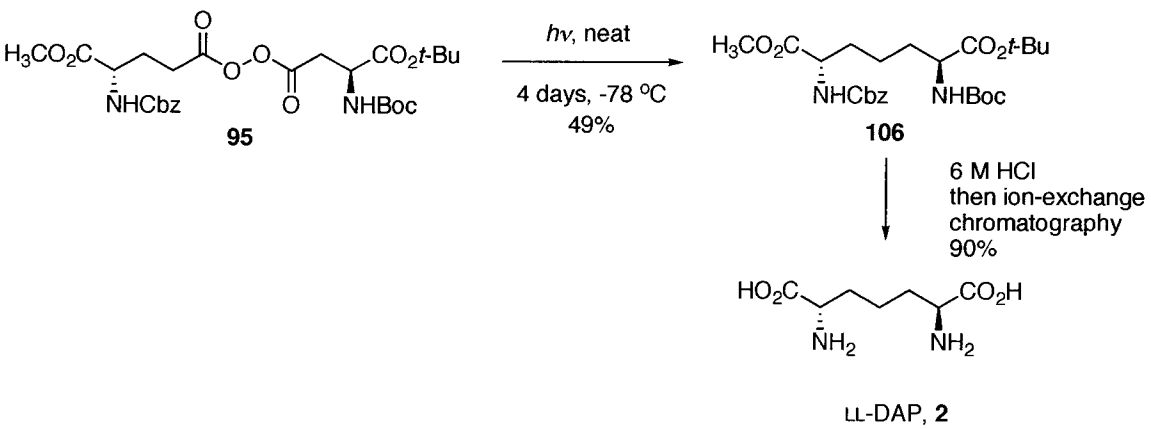

Scheme 34. Synthesis of LL-DAP (**2**).

Reproduced with permission of the copyright owner. Further reproduction prohibited without permission.

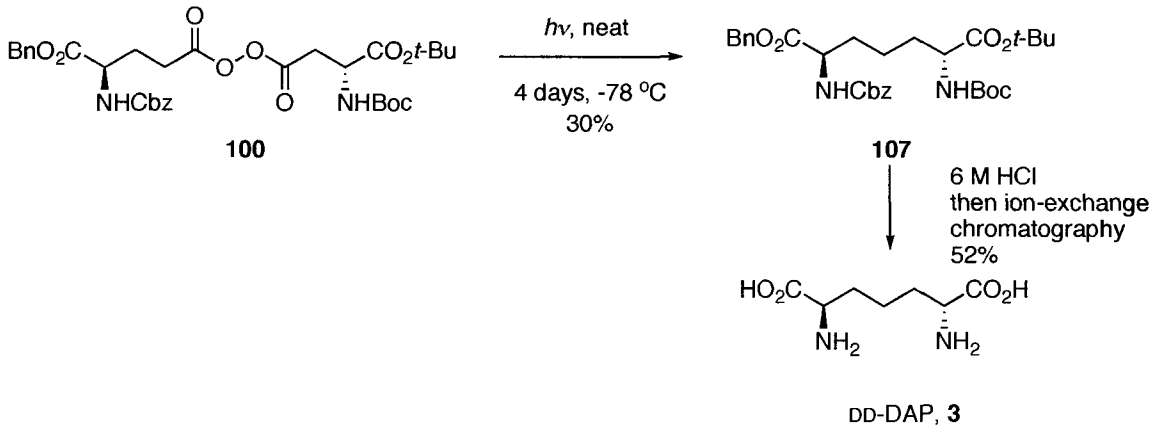

Scheme 35. Synthesis of DD-DAP (**3**).

Many methods, including preparative TLC and paper chromatography, have been used in the separation of DAP isomers, but suffer from poor sensitivity, long analysis times and the inability to separate DD- and LL- isomers.[101, 102] Separation of all DAP isomers can be achieved using HPLC and supercritical fluid chromatography based on either diastereomeric derivatives of DAP,[103] chiral mobile phases,[36] or chiral stationary phases.[104, 105]

To determine the *ee* of each of **1**-**3**, the method described by McKerrow and coworkers can be employed.[106] This technique utilizes the separation of diastereomeric isoindole derivatives of amino acids by their reaction with *o*-phthalaldehyde **108** (OPA) and a chiral thiol such as *N*-acetyl cysteine (**109**) under basic conditions (Scheme 36).

Reproduced with permission of the copyright owner. Further reproduction prohibited without permission.

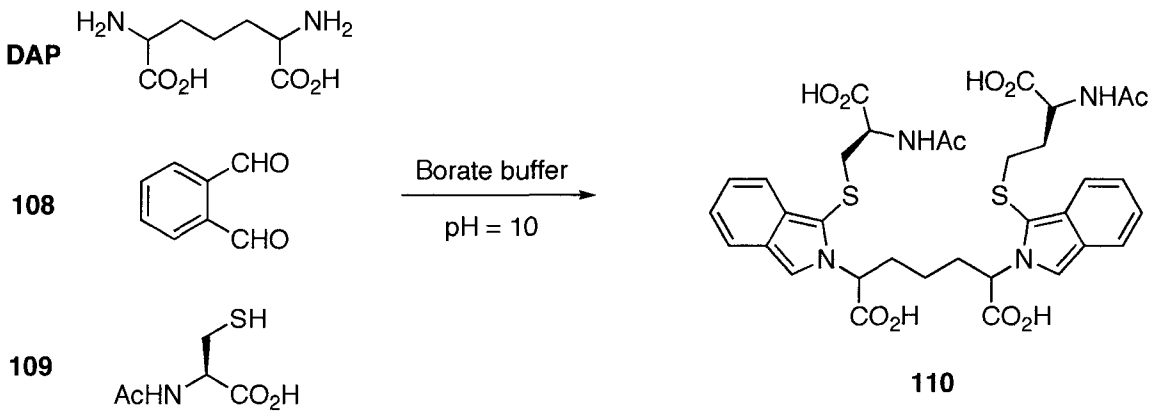

Scheme 36. Synthesis of isoindole **110** for HPLC separation of DAP isomers.

The OPA derivatives of DAP (1:1:2 mixture of **2**:**3**:**1**) are completely separated using a C18 Varian RP-HPLC column with a mobile phase of 15% acetonitrile in phosphate buffer at a flow rate of 0.4 mL/min. Assignment of the peaks is achieved by comparison with the pure DAP isomers to be LL:DD:*meso* in a 1:1:2 ratio at retention times of 17.3, 19.8, and 21.4 minutes respectively (Figure 17). Analysis of each of the peaks shows the DAP isomers **1**, **2** and **3** in >99% *ee* each.

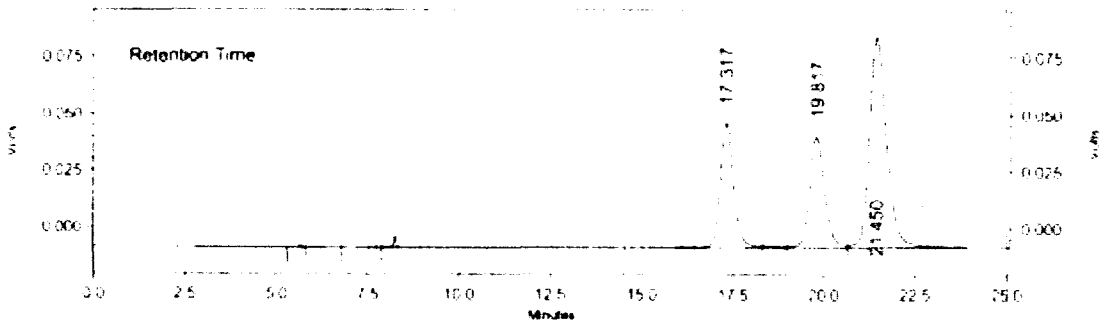

Figure 17. HPLC trace of separated DAP isomers using OPA derivatization.

Reproduced with permission of the copyright owner. Further reproduction prohibited without permission.

3.2. Enzyme Substrate and Inhibition Studies of DAP Isomers 1, 2 and 3 with Plant DAP Epimerase

3.2.1. Substrate Specificity Studies with DAP Epimerase

Upon completion of the synthesis of DAP isomers **1**-**3**, the substrate specificity of the plant DAP epimerase can be analyzed by the coupled enzyme assay described by Wiseman and Nichols.[36] The coupled assay at pH 7.8 employs the reverse reaction wherein $NADP^+$ along with bacterial *meso*-DAP dehydrogenase oxidatively deaminates the D-amino acid center of *meso*-DAP (**1**) to L-THDP (**7**) with generation of NADPH. The required *meso*-DAP is generated by the plant epimerase from LL-DAP (**2**) and the assay is followed spectrophotometrically with the production of NADPH (Scheme 37). *meso*-DAP dehydrogenase was purified from *Bacillus spaericus* IFO 3525.[107] The plant DAP epimerase used was isolated by Dr. Sandra Marcus from *Escherichia coli* M15[pREP4].[108] The *E. coli* strain was transformed by Dr. Marco van Belkum with pQE60 plasmid[32] containing plant DAP epimerase DNA donated by Professor Thomas Leustek (Rutgers University) from *Arabidopsis thaliana*. The first 51 amino acids of the epimerase precursor were removed by amplifying the mature part of the epimerase with PCR and the PCR product was cloned into pQE60.

Reproduced with permission of the copyright owner. Further reproduction prohibited without permission.

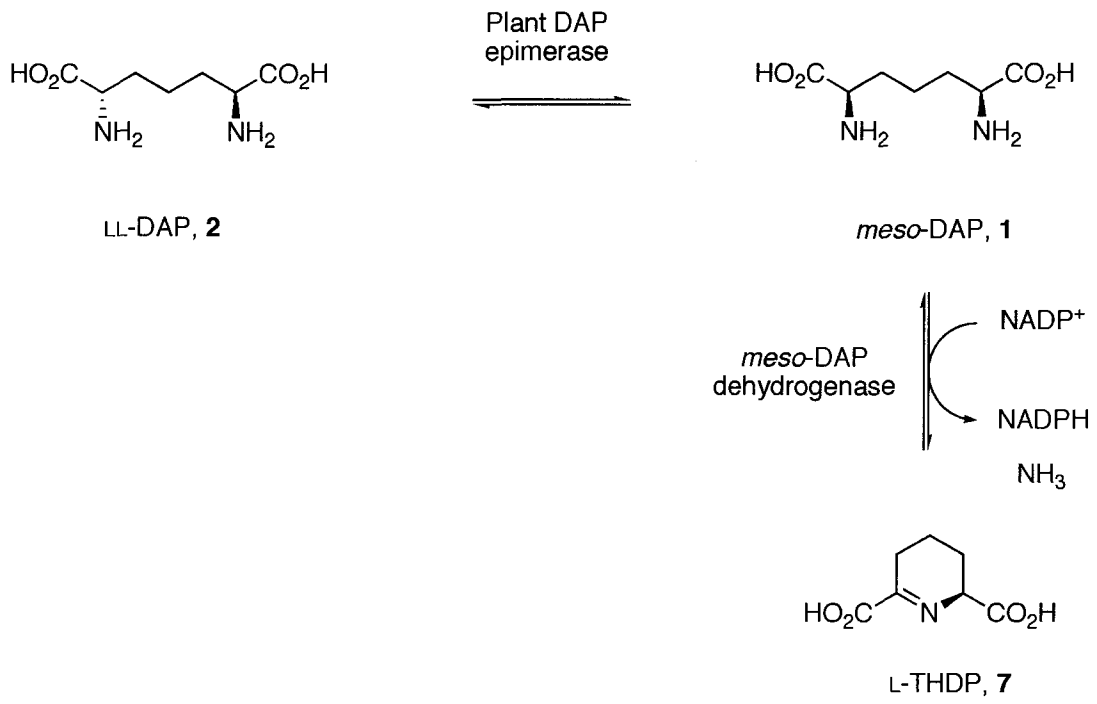

Scheme 37. Spectrophotometric coupled assay for plant DAP epimerase activity.

The DAP isomers **1-3**, were tested as both substrates and inhibitors for the DAP epimerase. The DAP isomers were first tested as substrates for the epimerase, as described in the experimental section. LL-DAP (**2**) is a substrate for the epimerase by the coupled assay whereas DD-DAP (**3**) is not a substrate (Figure 18). LL-DAP (**2**) is added to the DD-DAP assay after 12 minutes to ensure the enzyme is still active. *meso*-DAP (**1**) could not be tested in the coupled assay as it is a direct substrate for the dehydrogenase. To test **1**, the substrate test for the epimerase is performed in deuterated Tris buffer. After incubation with the enzyme for 3 days, anion exchange chromatography is employed to recover the compound and a proton NMR spectrum is obtained. If the compound being tested is a substrate for DAP epimerase, then racemization will result in replacement of the α-hydrogen for deuterium in the buffer solution. LL-DAP (**2**) and *meso*-DAP (**1**) each

Reproduced with permission of the copyright owner. Further reproduction prohibited without permission.

show deuterium incorporation at the α-center by proton NMR. DD-DAP (**3**) does not show any deuterium incorporation at the α-center indicating that the distal site (non-reacting site) of the substrate is very important for enzyme recognition.

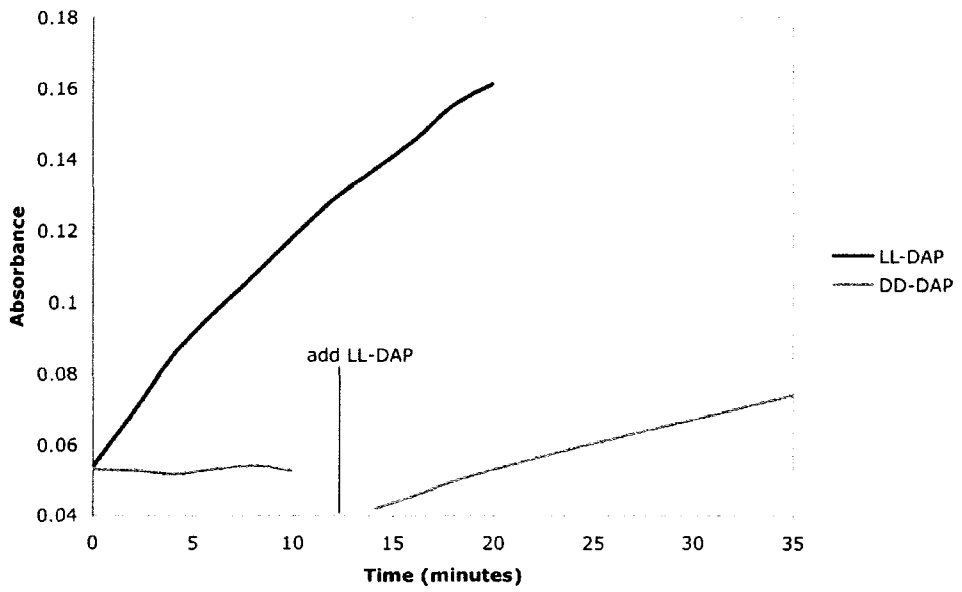

Figure 18. UV spectrum showing NADPH production of coupled assay containing, 0.4 mM of DD- or LL-DAP, 0.3 mM $NADP^+$, 50 mU of DAP dehydrogenase and 32 μg of DAP epimerase in a total volume of 1 mL Tris buffer.

Recent work from our group has shown the bacterial DAP epimerase from *Haemophilus influenzae* to be very specific in accepting only DAP isomers having the L-configuration at the distal site. The crystal structure reveals that the tight packing of the active site residues surrounding the distal site prevents the binding of a D-isomer at that position.[17] Unpublished results from Dr. Viji Moorthie in collaboration with Dr. Bindu

Reproduced with permission of the copyright owner. Further reproduction prohibited without permission.

Pillai and Dr. Maia Cherney show very similar structural features between the bacterial and plant epimerases with preliminary crystal structures of the plant DAP epimerase irreversibly inhibited with azi-DAP (**19** and **20**).[17, 47] The tertiary structures of the bacterial epimerase from *Haemophilus influenzae* and the plant epimerase transformed by Dr. Marco van Belkum from *Arabidopsis thaliana* expressed in *E.* coli show a large similarity, in spite of the modest sequence identity of 40.2%.

As an extension on the requirements of substrate recognition of the plant DAP epimerase, L-lysine (**4**), L-aminoadipic acid (**15**), and L-aminopimelic acid (**18**) can also be tested as substrates and inhibitors for the plant DAP epimerase (Figure 19).

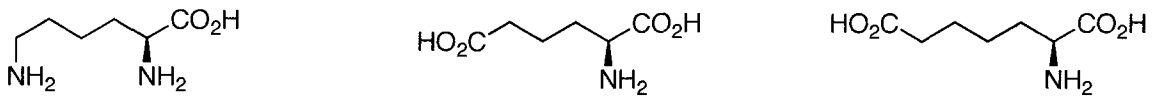

4 **15** **18**

Figure 19. Structure of amino acids **4**, **15** and **18**.

After incubation with the epimerase in deuterated buffer, no deuterium incorporation into substrates **4**, **15**, and **18** is detected by proton NMR. This indicates that both the carboxyl group and the amino group at the distal center are needed for substrate recognition. Inhibition studies were conducted by the addition of 1 mM of **4**, **15**, and **18** to the coupled assay described in the experimental section. Unfortunately, they fail to exhibit any inhibition against the enzyme even in concentrations of 10 mM. The failure of **4** to inhibit the enzyme suggests that the epimerase is not involved in the regulatory mechanism of lysine biosynthesis.[32]

Reproduced with permission of the copyright owner. Further reproduction prohibited without permission.

3.3. Detection of DAP Isomers in Plants

Amino acids are among the most important molecules in nature and come in the L- and D- forms. Despite almost identical chemical and physical properties, L-amino acids were primarily selected during evolution for the formation of polypeptides and proteins.[109] The selection of L-amino acids was generally thought to be a result of chance.[110] The resulting homochirality is essential for life, as it dictates the spatial architecture of biological polymers and therefore plays a role in enzymatic specificity and structural interactions. The presence and study of D-amino acids first emerged with the isolation of D-alanine and D-glutamine from peptidoglycan.[111] The formation of D-amino acids obviously increases the diversity of products that can be synthesized *in vivo*. In several cases of vertebrate and invertebrate peptides, the secreted products contain a D-amino acid, whereas the codon for the corresponding L-isomer is found encoded by the mRNA.[112]

Separation of the L- and D- isomers of amino acids has been accomplished with both gas chromatography and liquid chromatography. Some of the disadvantages of direct or indirect liquid chromatography separation of amino acid enantiomers is the incomplete separation of all amino acid enantiomers (or diastereomers), the presence of unusual amino acids or the interference of other compounds in the crude physiological samples, as well as problems resulting from matrix effects. These problems are overcome by the use of isopropyl *N*-pentafluoropropionic amide derivatives of amino acids analyzed with gas chromatography techniques.[113, 114] Derivatization of DAP as the

Reproduced with permission of the copyright owner. Further reproduction prohibited without permission.

isopropyl *N*-pentafluoropropionic amide **111** was proposed for analysis of DAP isomers present in crude plant samples.

3.3.1. Synthesis of the GC-MS Standard 111

The synthesis of the GC-MS standard **111** is outlined in Scheme 38.[114] The required standard can be obtained by the addition of isopropyl alcohol and catalytic conc. HCl to DAP (1:1:2 mixture of **2:3:1**). The mixture is then heated at 100 °C in a sealed reaction vessel for 16 h to give the isopropyl ester. Evaporation of the solvent followed by treatment with pentafluoropropionic anhydride (PFPA) then gives **111** in 42% yield over two steps. Use of conc. H_2SO_4 as the catalytic acid gives a lower yield of 32%.

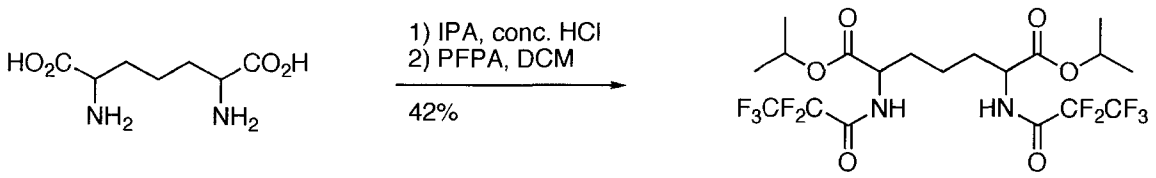

DAP **111**

Scheme 38. Synthesis of the GC-MS standard **111**.

3.3.2. Analysis of 111 and Crude Plant Samples by GC-MS

Upon completion of the synthesis of **111**, the separation of the DAP isomers can be done by GC analysis on a Chirasil-Val capillary column described by Schieber and coworkers.[114] Initial MS analysis of **111** shows two major ion fragments at m/z 274 and

Reproduced with permission of the copyright owner. Further reproduction prohibited without permission.

316 corresponding to molecular formulas of $C_9H_9O_3F_5N$ and $C_{12}H_{15}O_3F_5N$, respectively (Figure 20). Monitoring these fragments by MS can help verify the presence of DAP in the crude plant samples. Mass spectrometry peaks due to the DAP fragment m/z 274 and m/z 316 should be of the same intensity relative to each other. Selective analysis for these fragments shows a 1:1:2 ratio at retention times of 46.0, 46.1, and 46.2 minutes, respectively (Figure 20). Initial experiments by Dr. Chris Diaper showed that the order of the isomers proceed as LL:DD:*meso* by spiking the standard sample with the corresponding derivative of LL-DAP.

Bundles of *Arabidopsis thaliana*, *Brassica napus* (canola), *Triticum aestivum* (wheat), *Linum usitatissimum* (flax), and *Nicotiana benthamiana* (tobacco) can also be analyzed in a similar fashion for DAP. The extracts are obtained by crushing the plant material in liquid nitrogen with a mortar and pestle to break open the cells followed by treatment with 6 M HCl. Partial purification by ion-exchange chromatography and derivatization as described above gives samples ready for GC-MS analysis. Samples from *Arabidopsis thaliana* and canola both contain LL- and *meso*-DAP. Canola is also found to contain DD-DAP. To confirm the results in *Arabidopsis thaliana*, the sample was spiked with **111** to verify that DD-DAP is not present (Figures 22-24). Dr. Diaper also found LL-, DD- and *meso*-DAP in *Brassica nigra* in a 1:1:2 (LL:DD:*meso*) ratio of isomers. No DAP can be detected in wheat by GC-MS, but *meso*-DAP can be detected in tobacco. LL-DAP and *meso*-DAP are found to be present in flax (Figures 25-27). A slight deviation in the retention times is noticed over time due to degradation of the GC column. This is possibly due to an excess of pentafluoropropionic acid left over after the derivatization or due to the vast amount of compounds present in the plant material after partial

Reproduced with permission of the copyright owner. Further reproduction prohibited without permission.

purification that do not completely go through the GC column. This leads to decreased separation of the isomers and deviations in retention times. DAP isomers could still be identified according to their major ion fragments at m/z 274 and 316. To combat the degradation, sections at the start of the column are removed to allow for a clean injection onto the column. Removal of sections of the column produce shorter retention times with lower resolution of the DAP isomers. The presence of certain DAP isomers may give insight into the substrate specificity of the DAP epimerase present in the various species.

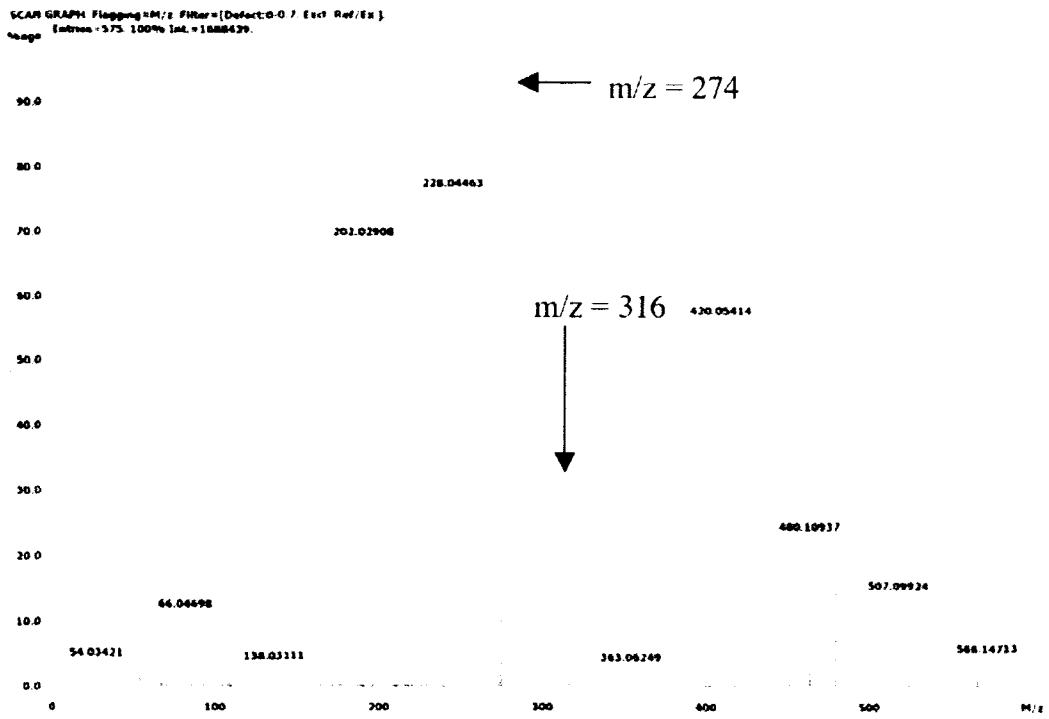

Figure 20. Mass spectrum of **111** by electron impact ionization.

Reproduced with permission of the copyright owner. Further reproduction prohibited without permission.

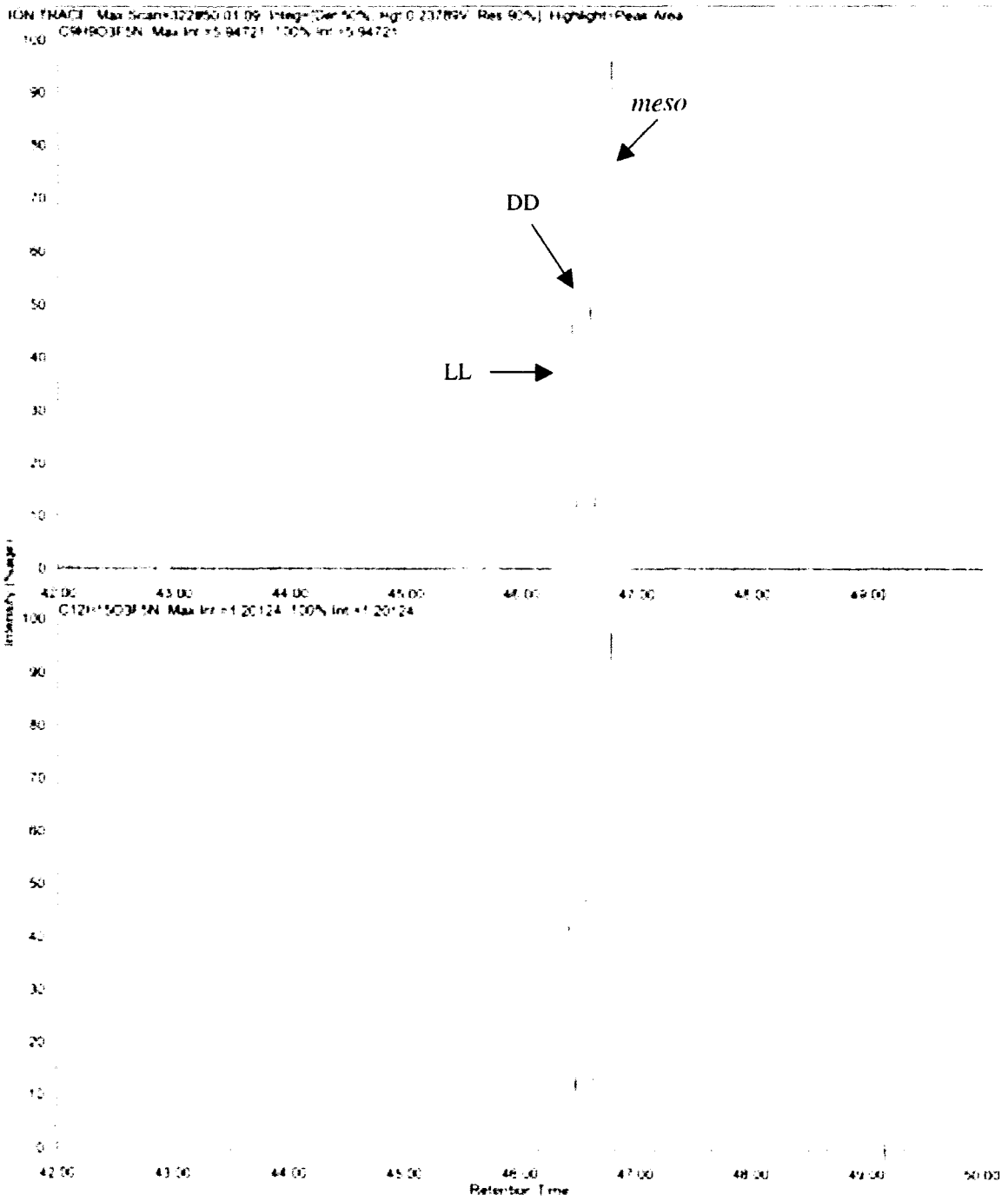

Figure 21. GC-MS trace of **111** with single ion selection for m/z = 274 (top) and m/z = 316 (bottom).

Reproduced with permission of the copyright owner. Further reproduction prohibited without permission.

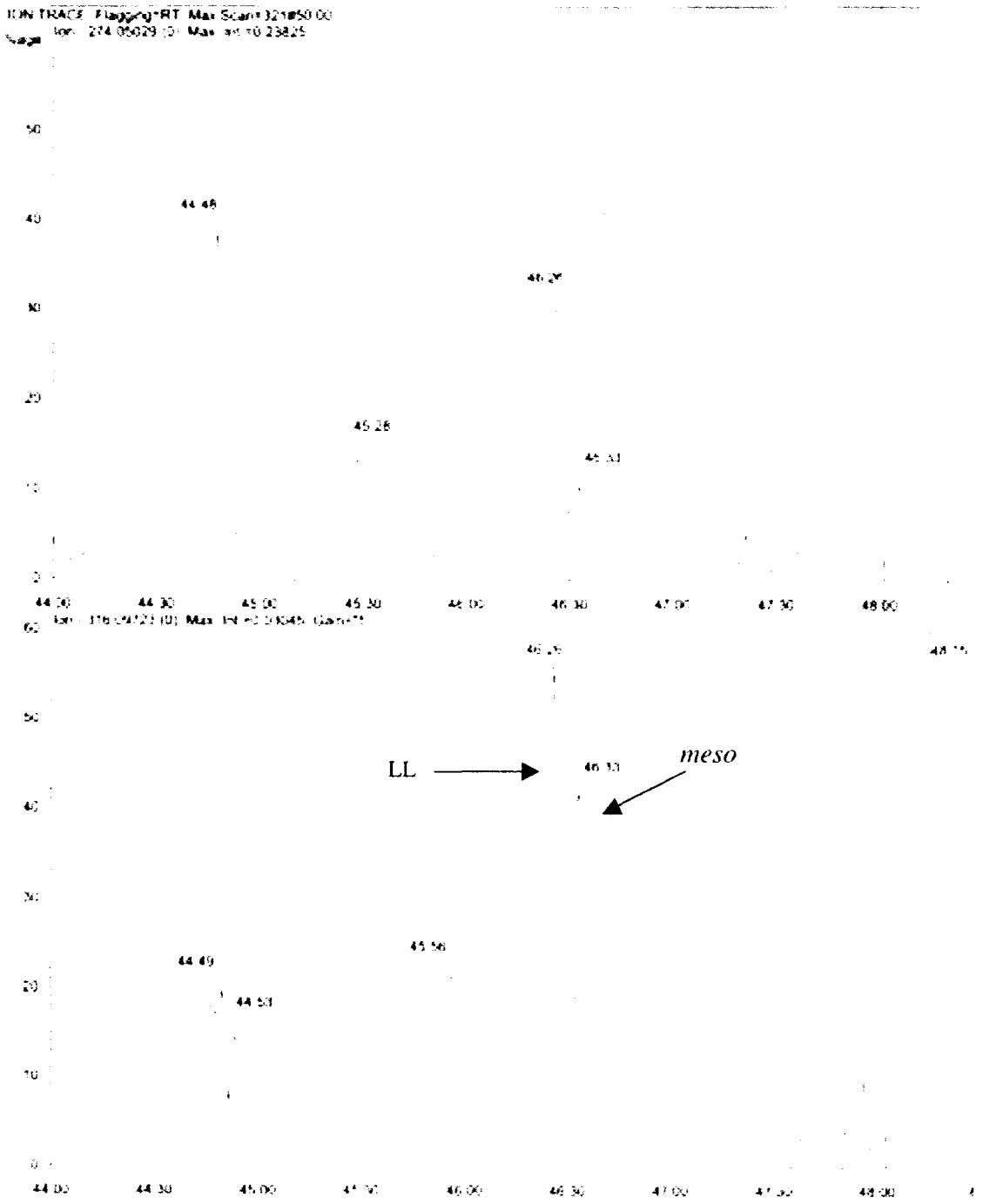

Figure 22. GC-MS trace of the derivatized crude plant extract from *Arabidopsis thaliana* with single ion selection for m/z = 274 (top) and m/z = 316 (bottom).

Reproduced with permission of the copyright owner. Further reproduction prohibited without permission.

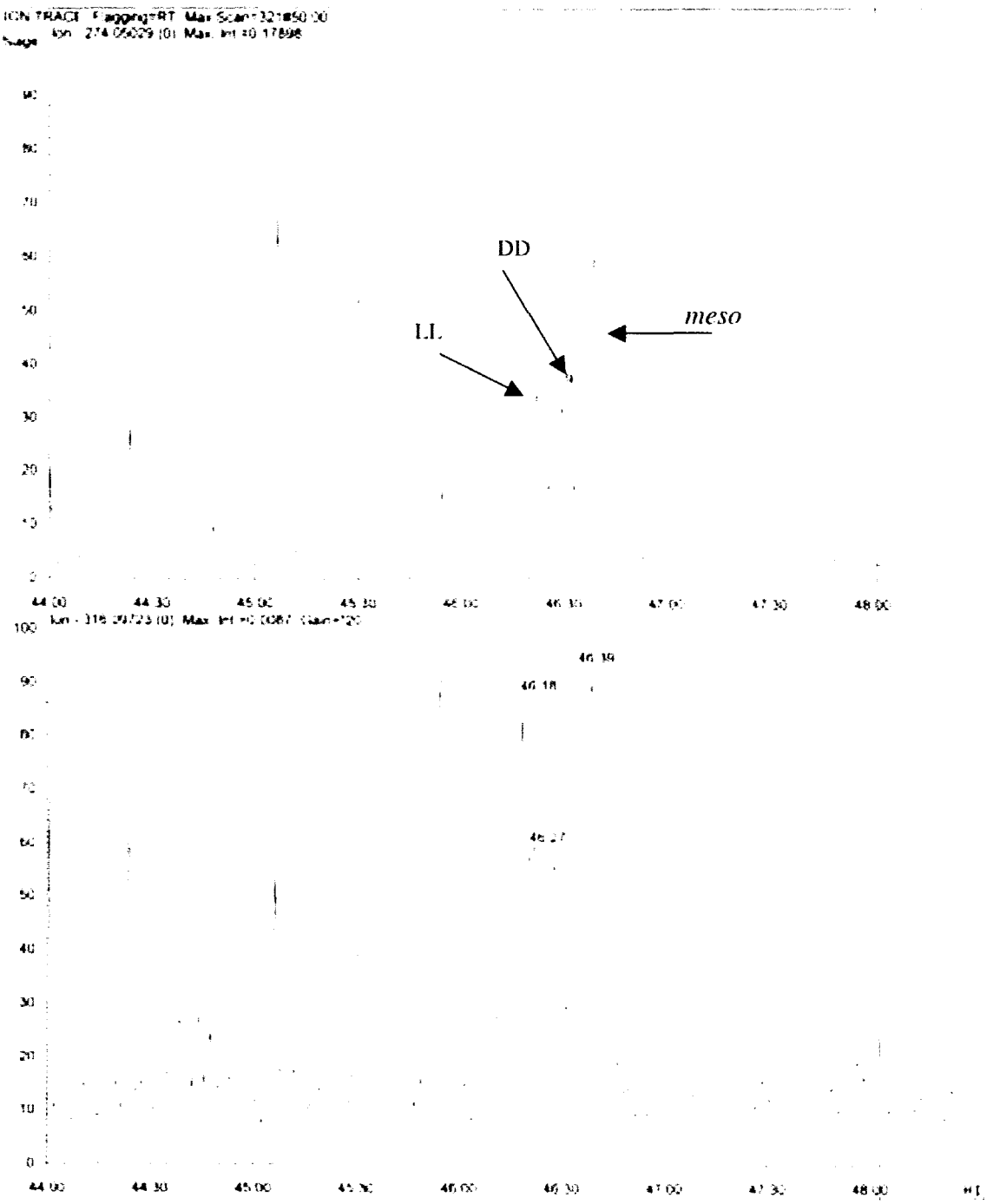

Figure 23. GC-MS trace of the derivatized crude plant extract from *Arabidopsis thaliana*, spiked with **111** with single ion selection for m/z = 274 (top) and m/z = 316 (bottom).

Reproduced with permission of the copyright owner. Further reproduction prohibited without permission.

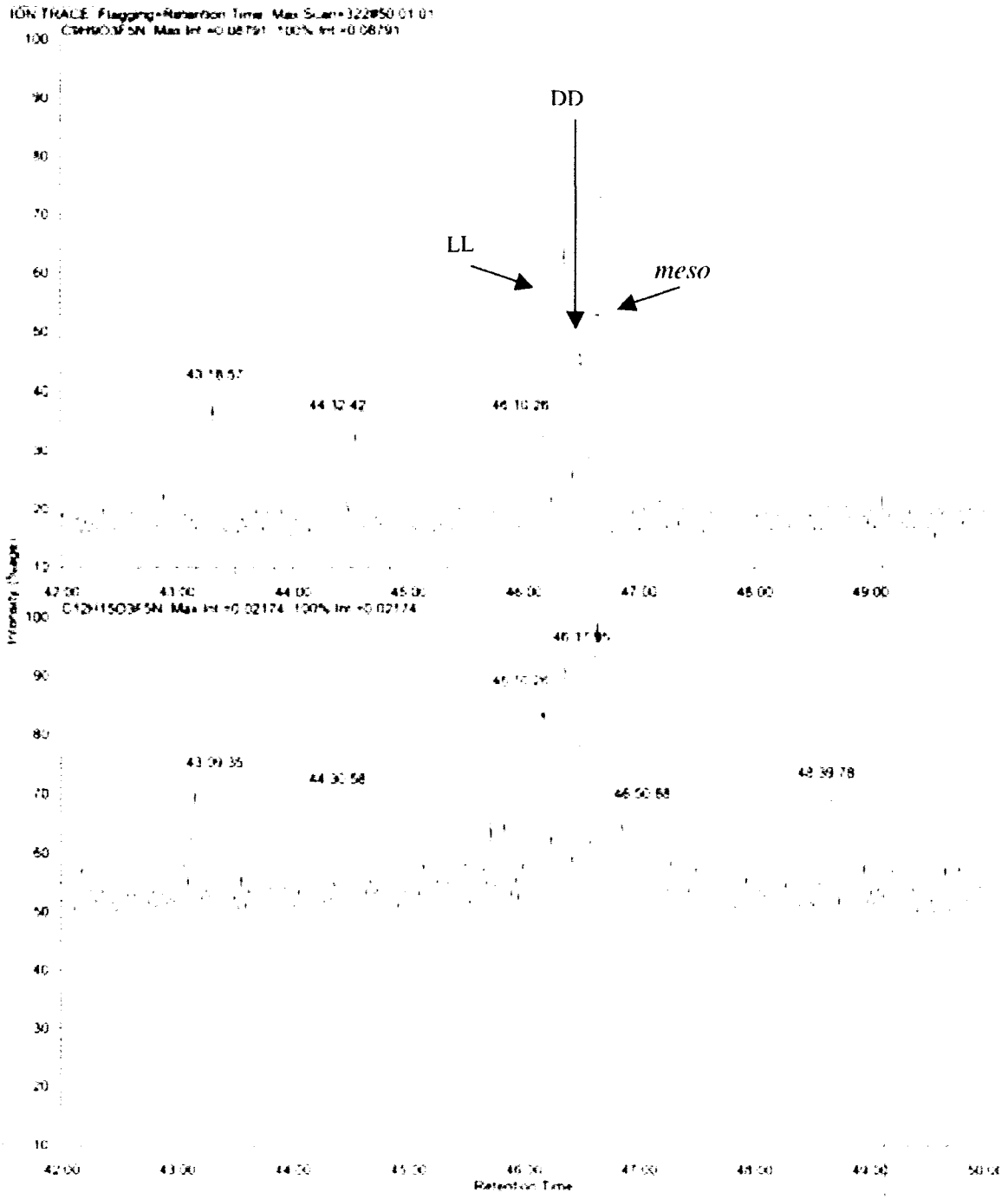

Figure 24. GC-MS trace of the crude plant extract from *Brassica napus* (canola) with single ion selection for m/z = 274 (top) and m/z = 316 (bottom).

Reproduced with permission of the copyright owner. Further reproduction prohibited without permission.

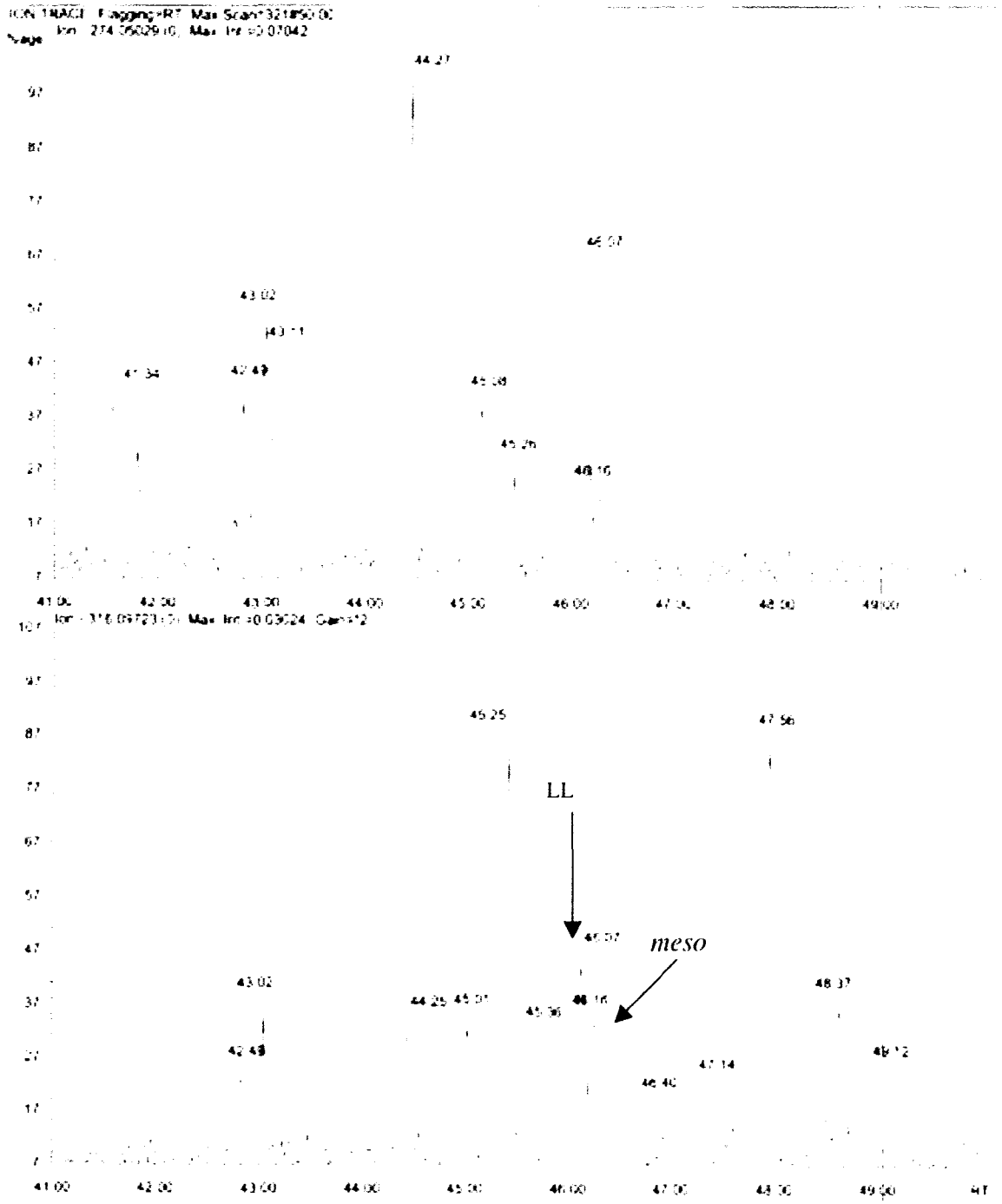

Figure 25. GC-MS trace of the derivatized crude plant extract *Linum usitatissimum* (flax) with single ion selection for m/z = 274 (top) and m/z = 316 (bottom).

Reproduced with permission of the copyright owner. Further reproduction prohibited without permission.

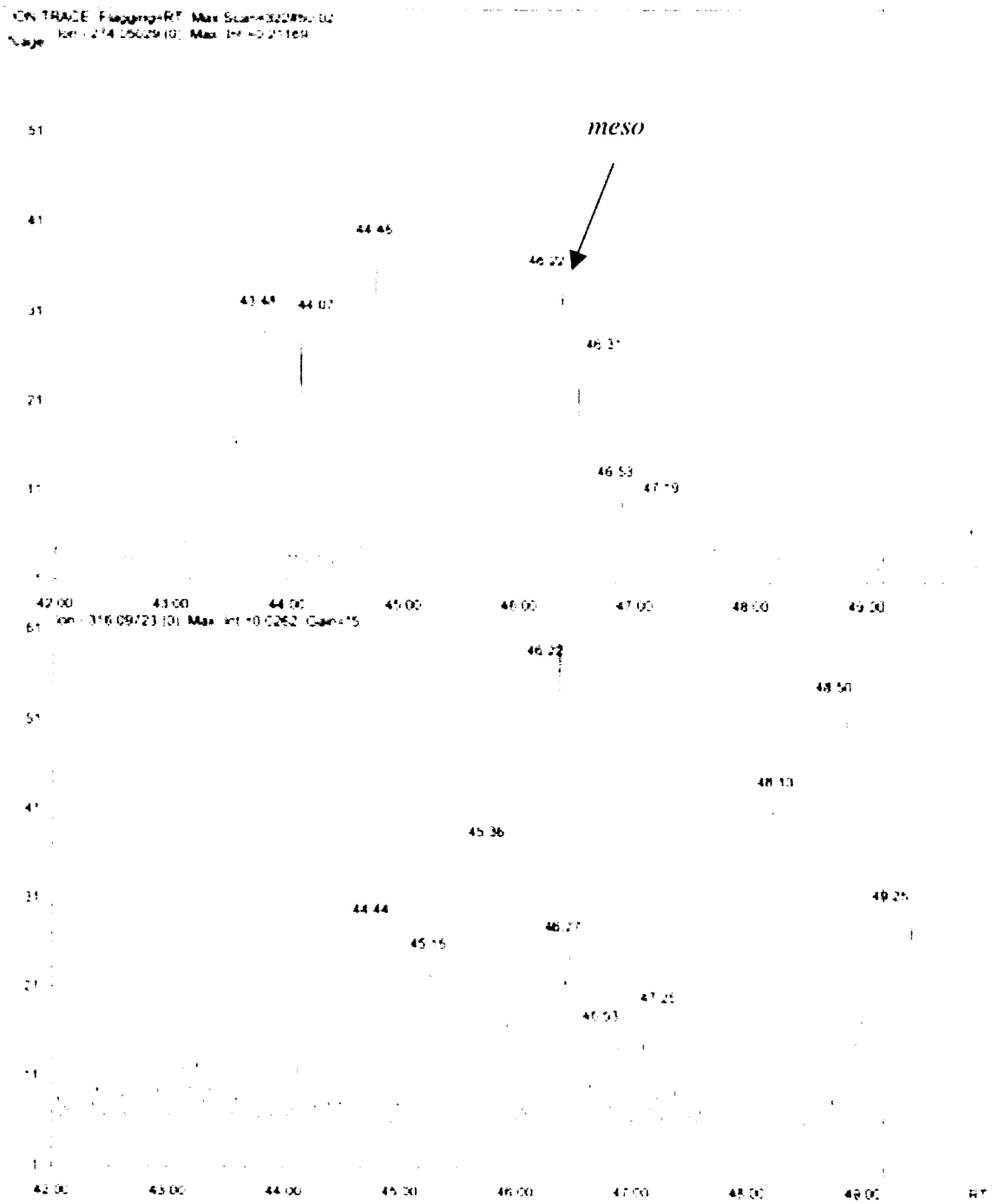

Figure 26. GC-MS trace of the derivatized crude plant extract from *Nicotiana benthamiana* (tobacco) with single ion selection for m/z = 274 (top) and m/z = 316 (bottom).

Reproduced with permission of the copyright owner. Further reproduction prohibited without permission.

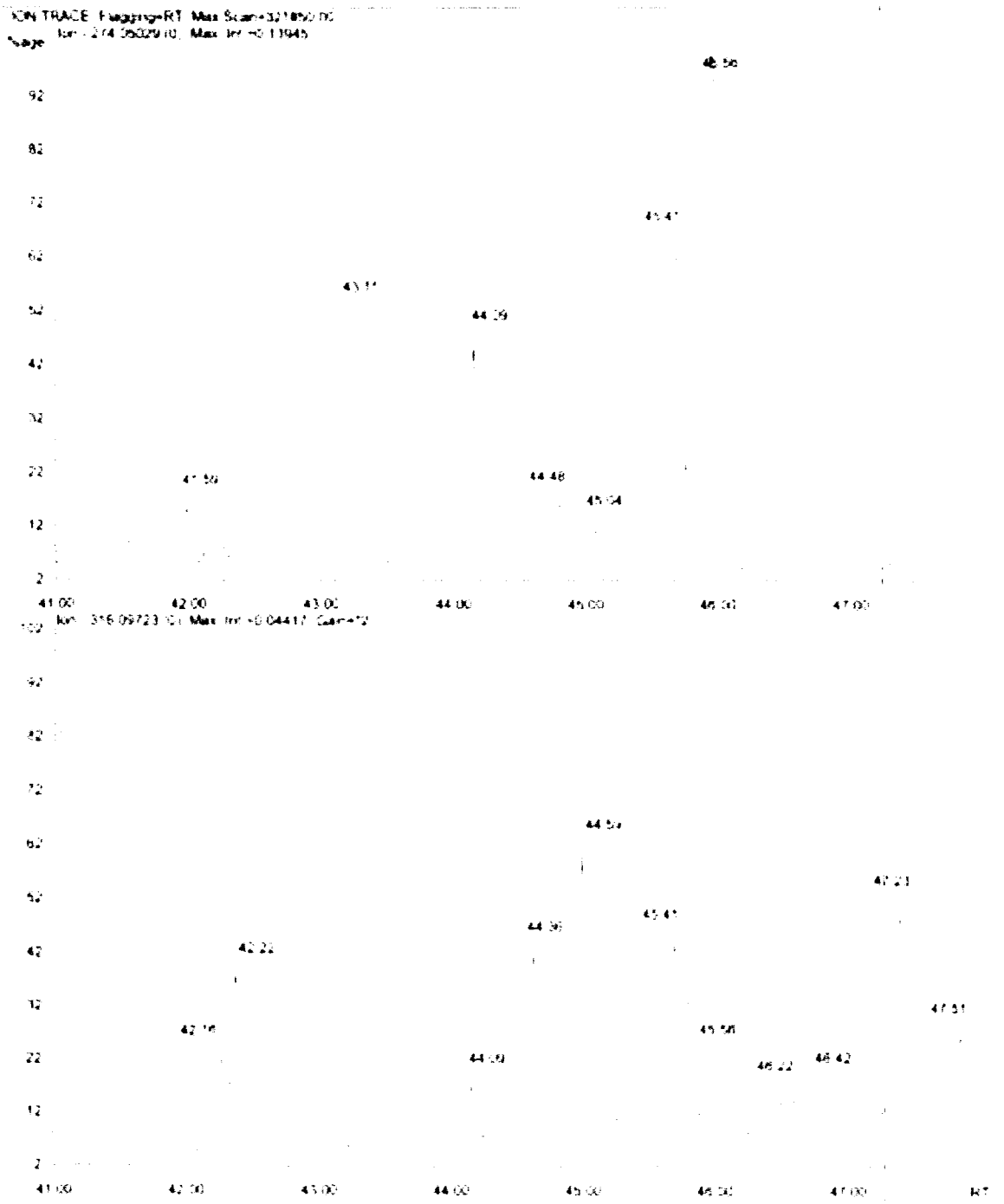

Figure 27. GC-MS trace of the derivatized crude plant extract from *Triticum aestivum* (wheat) with single ion selection for m/z = 274 (top) and m/z = 316 (bottom).

Reproduced with permission of the copyright owner. Further reproduction prohibited without permission.

3.3.3. Analysis of Crude Plant Sample by the Coupled Enzyme Assay

To verify the results of the GC-MS analysis, the crude plant extracts from *Arabidopsis thaliana* and *Brassica napus* can be analyzed by the coupled enzyme assay described by Wiseman and Nichols.[36] The crude plant extracts are obtained by crushing the plant material in liquid nitrogen with a mortar and pestle followed by addition of Tris buffer and centrifugation. The supernatant liquid is then concentrated and tested for DAP epimerase activity as described in the experimental section. The crude plant extract from *Arabidopsis thaliana* shows activity with LL-DAP (**2**) but no activity with DD-DAP (**3**) (Figure 28). This is expected since the purified DAP epimerase from *Arabidopsis thaliana* only shows activity towards LL-DAP (**2**). Furthermore, GC-MS analysis of the crude plant extract shows only the presence of LL-DAP (**2**) and *meso*-DAP (**1**). Analysis of the crude plant extract from *Brassica napus* shows activity towards both LL-DAP (**2**) and DD-DAP (**3**) (Figure 29). To determine if the observed activity is due to the conversion of LL-DAP and not another biochemical process, it was omitted from the assay in a control experiment. As expected during the control, no epimerase activity is detected. To determine if the DD-DAP (**3**) activity is from a PLP-dependant epimerase, 1 mM of hydroxylamine is added to the assay and activity is still shown towards **3**. This suggests that the activity is due to a PLP-independent epimerase but does not rule out glutamate racemase,[39, 40] aspartate racemase[41] or another PLP-independent racemase of being responsible for the activity. This would suggest that analysis of crude plant extracts with the coupled assay by Wiseman and Nichols[36] can determine which of the DAP isomers is present in the plant material.

Reproduced with permission of the copyright owner. Further reproduction prohibited without permission.

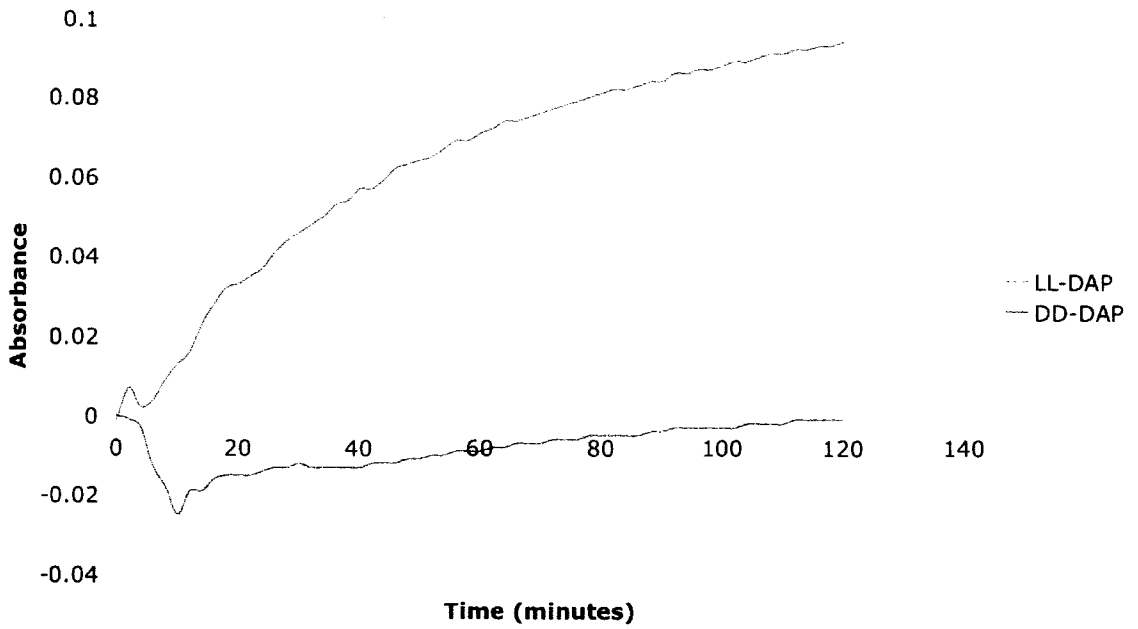

Figure 28. UV spectrum showing NADPH production of the coupled assay containing, 0.4 mM of DD- or LL-DAP, 0.3 mM $NADP^+$, 50 mU of DAP dehydrogenase and crude plant extract from *Arabidopsis thaliana* in a total volume of 1 mL Tris buffer.

Reproduced with permission of the copyright owner. Further reproduction prohibited without permission.

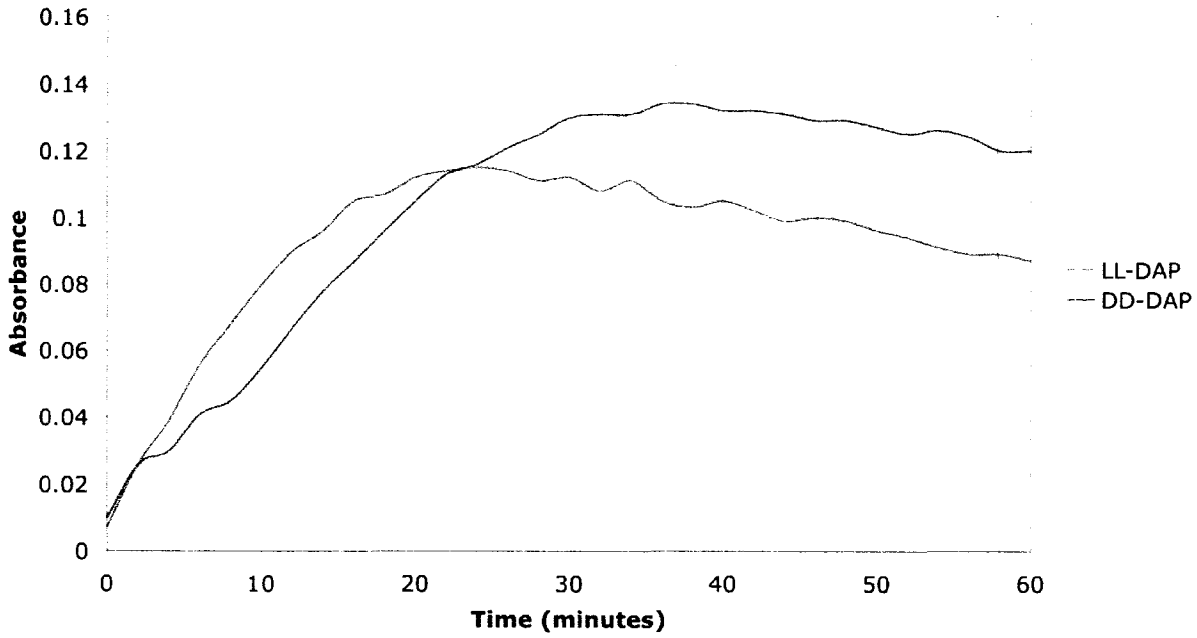

Figure 29. UV spectrum showing NADPH production of the coupled assay containing, 0.4 mM of DD- or LL-DAP, 0.3 mM $NADP^+$, 50 mU of DAP dehydrogenase and crude plant extract from *Brassica napus* in a total volume of 1 mL Tris buffer.

Reproduced with permission of the copyright owner. Further reproduction prohibited without permission.

3.4. Enzyme Substrate and Inhibition Studies with LL-DAP-AT

3.4.1. Characterization of LL-DAP-AT

The substrate specificity of the plant LL-DAP-AT can be analyzed by the assay described by Leustek and coworkers.[35] The assay at pH 7.6 employs the reverse reaction wherein 2-oxyglutarate (2-OG, **10**) along with LL-DAP-AT deaminates one of the L-amino acid centers of LL-DAP (**2**). The assay is followed spectrophotometrically by adding *o*-aminobenzaldehyde (OAB, **75**), which reacts with L-THDP (**7**) to form a dihydroquinazolinium adduct (**112**) that has an absorbance maximum at 440 nm (Scheme 39).[35, 115]

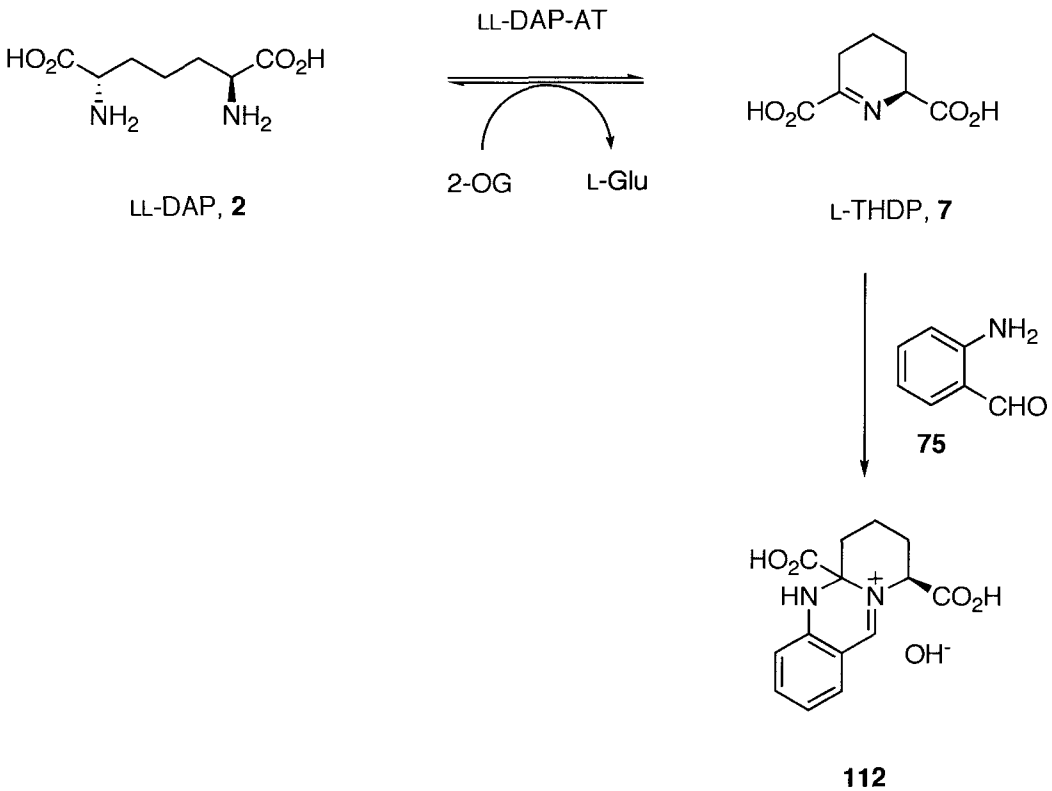

Scheme 39. Spectrophotometric assay for LL-DAP-AT activity.

Reproduced with permission of the copyright owner. Further reproduction prohibited without permission.

The LL-DAP aminotransferase used was isolated by Dr. Sandra Marcus from *E. coli* mutant M15[pREP4]. The mutant was transformed by Dr. Marco van Belkum with pQE60 plasmid containing LL-DAP-AT donated by Professor Mike Deyholos from *Arabidopsis thaliana*.[35]

The DAP isomers **1**-**3** can be tested as both substrates and inhibitors for LL-DAP aminotransferase. The enzyme is able to discriminate between the DAP isomers, showing activity towards LL-DAP (**2**) and no activity towards DD-DAP (**3**), or *meso*-DAP (**1**). Leustek and coworkers also reported that the LL-DAP-AT was able to discriminate between related keto acids including oxaloacetate, pyruvate and 2-oxyglutarate and showed that 2-oxyglutarate (2-OG, **10**) was the only one active.[35] The specificity for LL-DAP is made more evident by the observation that *meso*- or DD-DAP do not inhibit the use of LL-DAP by the aminotransferase.

To extend this study of the requirements for substrate recognition by the plant aminotransferase, L-lysine (**4**), L-aminoadipic acid (**15**), and L-aminopimelic acid (**18**) were also tested as inhibitors. Unfortunately, the amino acids **4**, **15**, and **18**, fail to inhibit the use of LL-DAP by the aminotransferase even in concentrations of 10 mM. This indicates that both carboxyl groups and the amino groups of DAP are needed for substrate recognition. The failure of **4** to inhibit the enzyme suggests that DAP epimerase is not involved in the regulatory mechanism of lysine biosynthesis.[32]

Leustek and coworkers found the purified aminotransferase enzyme to have a UV absorbance at 420 nm, typical of PLP-dependant aminotransferases.[35, 116] We chose to further investigate whether the aminotransferase is PLP-dependant by inhibiting the enzyme with hydrazine and hydroxylamine, as well as under reducing conditions with

Reproduced with permission of the copyright owner. Further reproduction prohibited without permission.

sodium borohydride. A number of PLP-dependant enzymes are irreversibly inhibited by *N*-hydroxy derivatives,[49] as they form stable nitrones by transamination with PLP (Figure 6).[49] Hydrazino derivatives are also potent competitive inhibitors of PLP-dependant enzymes through formation of hydrazone intermediates which are less susceptible to hydrolysis than the aldimine complex (Figure 6).[49] Treatment with sodium borohydride reduces the imine bond formed between the PLP and the enzyme to form a covalent bond.

At 2 mM, all three compounds show complete inhibition of the enzyme under the assay conditions. This is possibly due to inactivation of PLP, however, within the assay, 2-oxoglutarate (**10**) is also able to form nitrone or hydrazone species. LL-DAP (**2**) and **10** can also form imine complexes, which could be reduced with sodium borohydride, thereby providing the appearance of inhibition in the assay. Concentrations lower than 1 mM for hydroxylamine, semicarbazide and sodium borohydride, show incomplete inhibition, possibly due to side reactions described above. To remove the possibility of the side reactions interfering with the assay, LL-DAP-AT was incubated with either hydroxylamine or semicarbazide prior to the assay, followed by dialysis of the hydroxylamine-PLP or semicarbazide-PLP complexes from the enzyme, to prepare the PLP-free aminotransferase.[117, 118] Sodium borohydride is also incubated with the enzyme, followed by dialysis, to prepare the covalently bound PLP aminotransferase.[119] The inhibited LL-DAP-AT is then subjected to the assay conditions described above. A complete loss of activity is noticed for all three assays, suggesting that LL-DAP-AT is a PLP-dependant aminotransferase. Addition of PLP to the assay involving the

Reproduced with permission of the copyright owner. Further reproduction prohibited without permission.

hydroxylamine inhibited enzyme, shows a slight gain in activity further suggesting the enzyme is PLP-dependant. L-Glutamic acid (**79**) also shows inhibition of LL-DAP-AT in high concentrations (50 mM).

Control experiments ensured that the observed activity was due to the aminotransferase by methodically deleting one component of the assay at a time and as expected, no enzyme activity is detected in the absence of either enzyme, substrate or cofactor.

The conversion of L-THDP (**7**) to LL-DAP (**2**) requires the addition of an amino group through the use of LL-DAP-AT and glutamic acid and PLP as cofactors. One possible reaction mechanism that can be envisioned for this enzymatic transformation is given in Scheme 40. The first step in the mechanism involves the transamination of PLP (**21**) to PMP (**26**) by glutamic acid (**79**). This is followed by nucleophilic attack of **26** on the imine of L-THDP (**7**). Base abstraction, and subsequent opening of the ring then yields the aldimine **115**. Tautomerization of the aldimine **115**, to the ketimine **116**, gives the L-configuration. Hydrolysis of the imine bond then releases LL-DAP (**2**) and the PLP form of the enzyme **22**.

Reproduced with permission of the copyright owner. Further reproduction prohibited without permission.

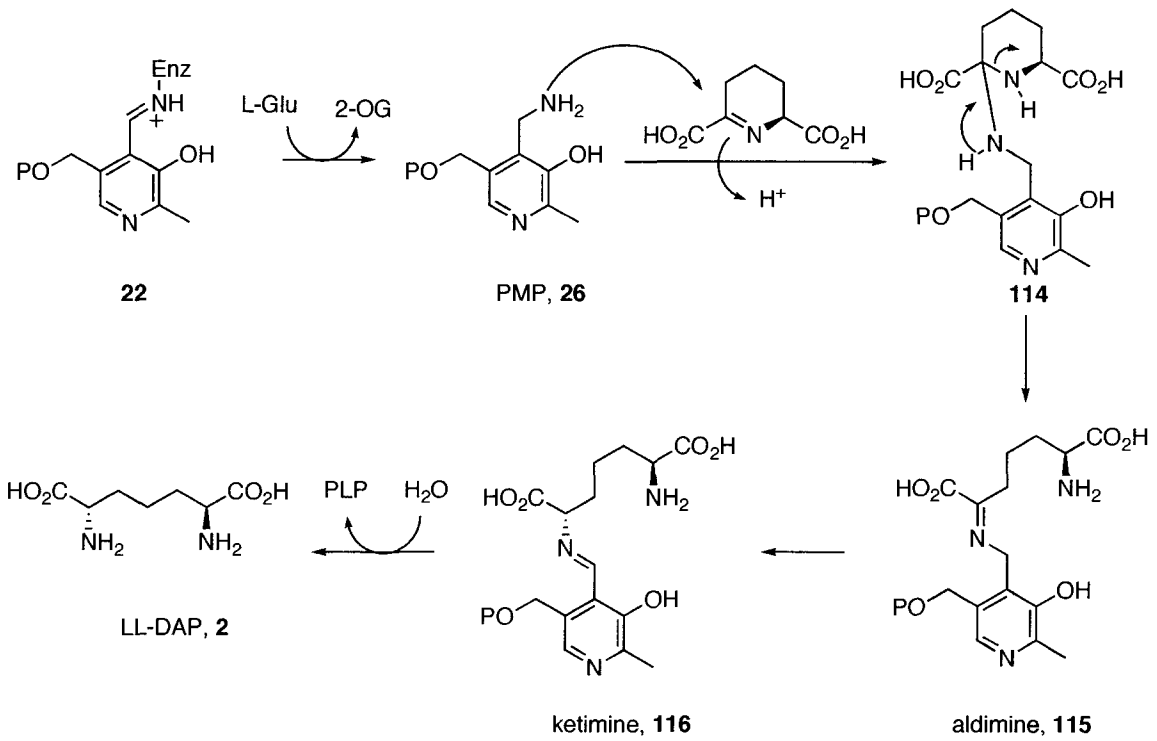

Scheme 40. Possible mechanism for the conversion of L-THDP (**7**) to LL-DAP (**2**) by LL-DAP-AT using PLP and glutamic acid as cofactors.

3.4.2. Synthesis of L-THDP Analog 89.

From a retrosynthetic perspective, cyclic derivative **89** in two racemic forms (carboxyls *cis* or *trans*), may be formed from hydrolysis of the hydantoin **117** formed *via* a classical Bucherer-Berg reaction of the corresponding ketoacid **118** (Scheme 41).[120-124] The construction of the ketone moiety involves cyanation of 2-cyclohexenone (**119**) and subsequent hydrolysis of the cyano group.[125]

Reproduced with permission of the copyright owner. Further reproduction prohibited without permission.

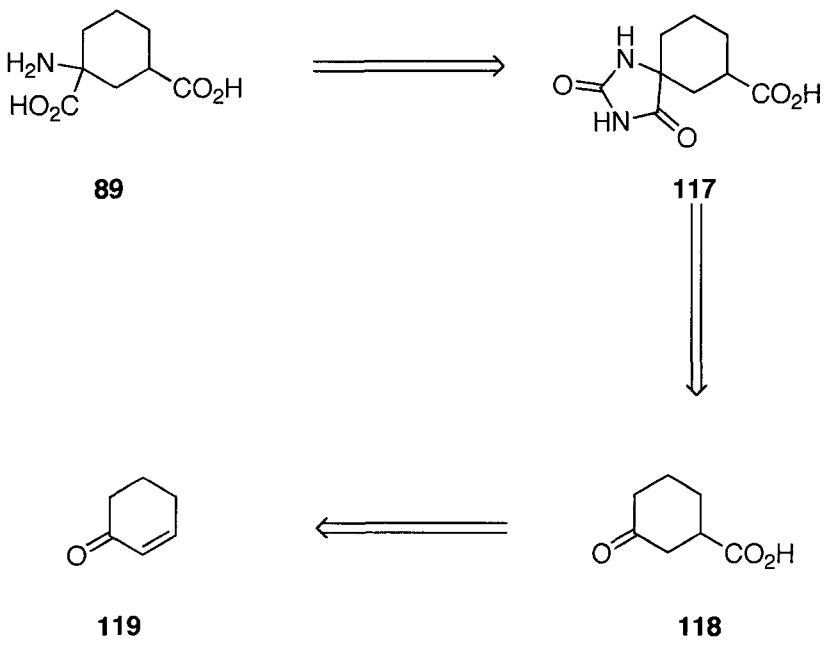

Scheme 41. Retrosynthetic analysis for the synthesis of racemic **89**.

The required ketoacid **118** can be synthesized as outlined in Scheme 42.[125] Treatment of 2-cyclohexenone (**119**) with potassium cyanide in the presence of triethylamine hydrochloride gives **120** in 87% yield. Hydrolysis of the cyano group is achieved with 6 M HCl to give **118** in 40% yield.

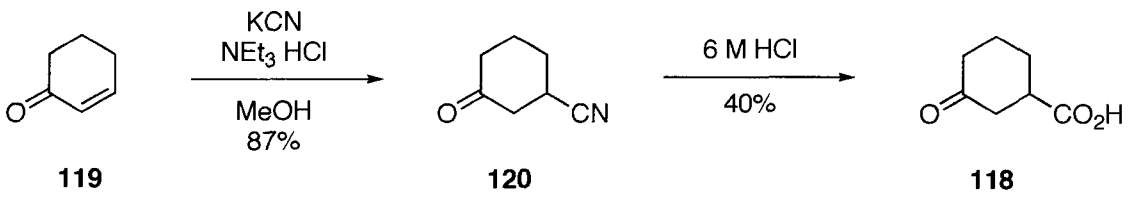

Scheme 42. Synthesis of ketoacid **118**.

Reproduced with permission of the copyright owner. Further reproduction prohibited without permission.

With the required ketone moiety in place, ketoacid **118** is transformed to the desired 1:1 diastereomeric mixture of hydantoin **117** in 40% yield using the classical Bucherer-Berg reaction conditions (Figure 43).[122] Purification by cation exchange chromatography or crystallization results in contamination with inorganic salts or the loss of product. This is most likely due to the tendency of the product to stay in the aqueous phase of the reaction upon crystallization or because it is not fully being absorbed onto the ion exchange resin to allow for the inorganic salts to elute through the column first. Attempts to separate the diastereomeric *cis* and *trans* hydantoins were also unsuccessful using fractional crystallization.[124]

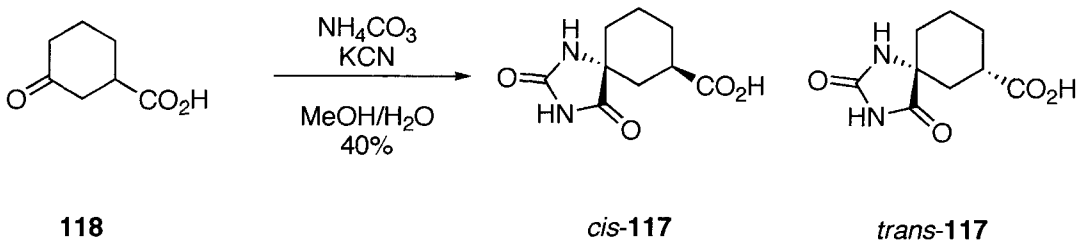

118 *cis*-**117** *trans*-**117**

Scheme 43. Synthesis of the racemic hydantoins **117**.

Esterification of the carboxylic acid leads to an easier purification of the hydantoins (Scheme 44). Esterification of the carboxylate to the isopropyl ester gives racemic ketoester **121** in 98% yield. Subjection of **121** to the Bucherer-Berg reaction conditions followed by silica gel chromatography gives the hydantoins **122** in 73% yield as a 1:1 mixture of diastereomers. Attempts to completely separate the diastereomers by silica gel chromatography or reverse phase High Pressure Liquid Chromatography (RP-HPLC) are unsuccessful. Hydrolysis of the hydantoin mixture with barium hydroxide

Reproduced with permission of the copyright owner. Further reproduction prohibited without permission.

hydrate yields the free cycloglutamic acid **89** in 91% yield as a mixture of four possible isomers.[126] Azerad and coworkers[120] suggested that the *cis* and *trans* isomers can be separated by anion exchange chromatography using BioRad AG 1 anion exchange resin in the acetate form. A gradient mobile phase from 0.25 M acetic acid to 0.5 M acetic acid was reported to separate the two diastereomers. Multiple attempts to separate the diastereomers using the procedure by Azerad and coworkers proved to be unsuccessful. Attempts to separate the diastereomers using RP-HPLC, monitoring at 214 nm were also unsuccessful.

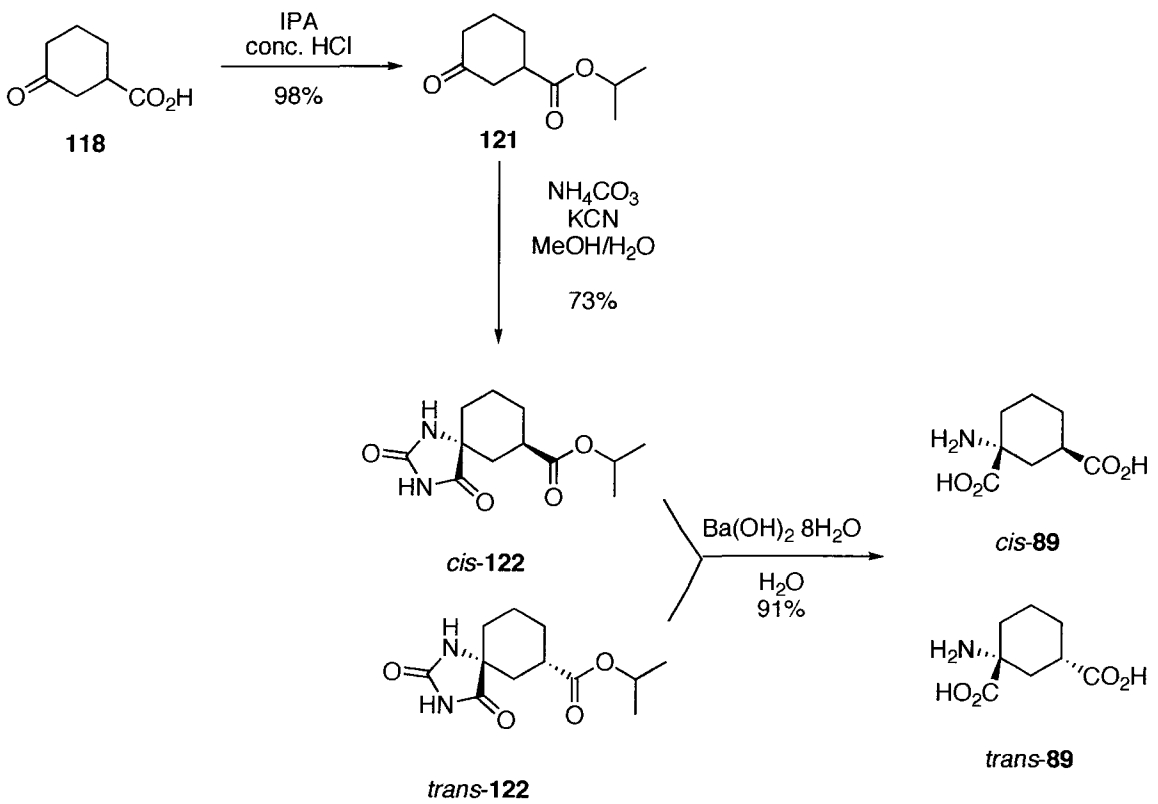

Scheme 44. Synthesis of cycloglutamic acid **89** as a mixture of 4 isomers.

Reproduced with permission of the copyright owner. Further reproduction prohibited without permission.

The *o*-phthalaldehyde (OPA) method previously described can be used to determine which isomer is eluting from the ion-exchange column as described by Azerad and coworkers (Figure 30).[120]

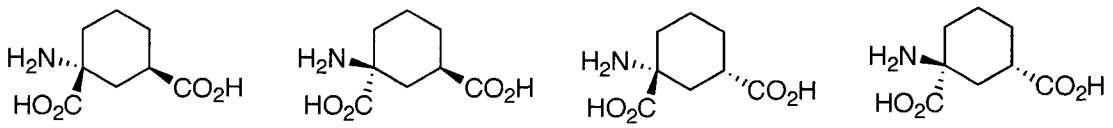

Figure 30. Structures of all possible isomers of **89**.

The OPA derivatives of racemic **89** are sufficiently separated using a C18 Phenomenex RP-HPLC column with a mobile phase of 20% methanol in phosphate buffer at a flow rate of 1 mLmin^{-1}. Assignment of the peaks is achieved by comparison with the results of Azerad and coworkers[120] to be 1*S-trans*-**89**: 1*S-cis*-**89**: 1*R-trans*-**89**: 1*R-cis*-**89** in a 1:1:1:1 ratio at retention times of 4.4, 5.1, 5.2, and 7.6 minutes, respectively (Figure 31).

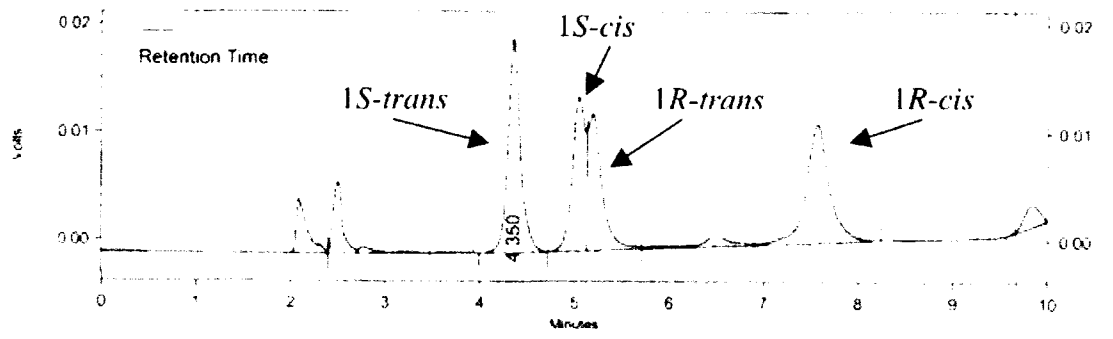

Figure 31. HPLC trace of separated **89** isomers after OPA derivatization.

Reproduced with permission of the copyright owner. Further reproduction prohibited without permission.

3.4.3. Attempted Synthesis of Chirally Pure L-THDP Derivative 1*R-cis*-89

The retrosynthetic path to target 1*R-cis*-**89**, presented in Scheme 45, employs a chirally pure intermediate (*R*)-**121** as the source of chirality for the cyclic glutamic acid skeleton. Once (*R*)-**121** is constructed, the Bucherer-Berg reaction followed by hydrolysis will provide 1*R*-**89** as a mixture of diastereomers.

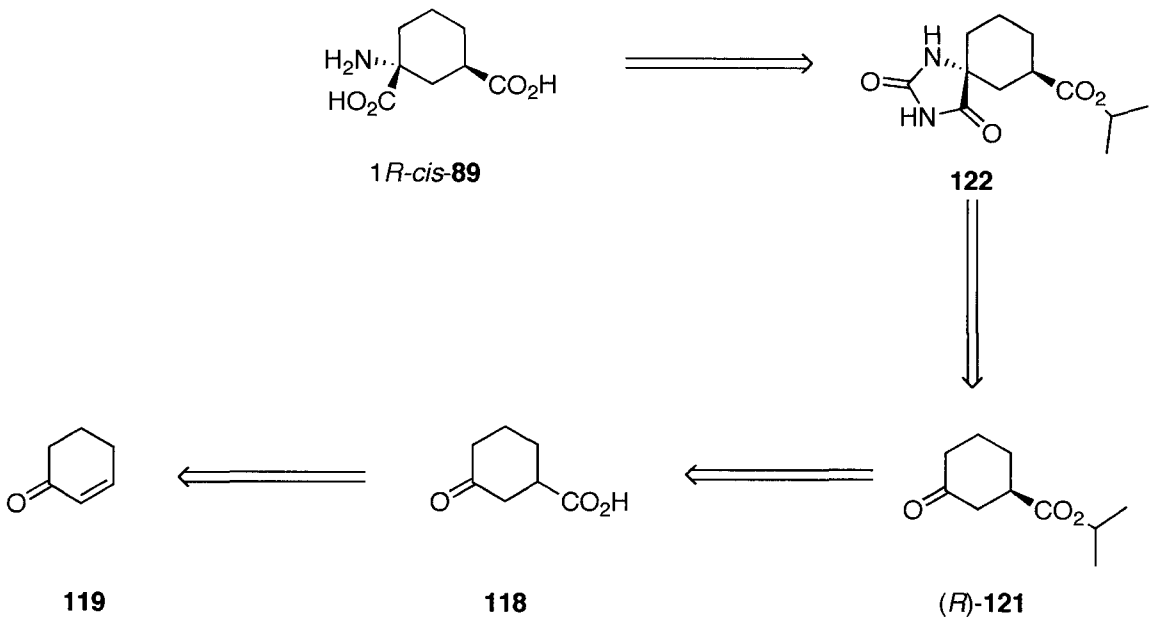

Scheme 45. Retrosynthetic scheme for the synthesis of 1*R-cis*-**89**.

The required chiral ketoester (*R*)-**121** can be synthesized as outlined in Scheme 46. The racemic isopropyl 3-oxocyclohexanecarboxylate (**121**) is readily generated using the method described in Schemes 42 and 44. Enzymatic resolution of racemic **121** is achieved using *Rhizopus arrhizus*, which selectively reduces the ketone to the (*S*)-alcohol.[120, 127] Silica gel chromatography results in the separation of the two

Reproduced with permission of the copyright owner. Further reproduction prohibited without permission.

diastereomers to give (1*S*,3*S*)-**123** and (1*R*,3*S*)-**123** in 5% and 15% yields, respectively. Ketoester **121** is generally recovered in 80% yield. Azerad and coworkers[120] reported the yields for the enzymatic resolution to be 60% with approximately the same ratio of *cis* and *trans* isomers. Unfortunately in our hands, repeated attempts at the resolution did not produce these yields even with an increased incubation time. With the desired isomer in hand, oxidation is required to furnish the ketone moiety. Thus, treatment of alcohols (1*S*,3*S*)-**123** and (1*R*,3*S*)-**123** with PDC gives the desired chiral ketones (*R*)-**121** and (*S*)-**121** in 76% and 82% yields, respectively. Azerad and coworkers reported that the hydroxy esters (1*S*,3*S*)-**123** and (1*R*,3*S*)-**123** were nearly optically pure (>98% *ee*) as shown by chiral GC so the synthesis was continued without determining the *ee* of the hydroxy esters **123**.[120, 128]

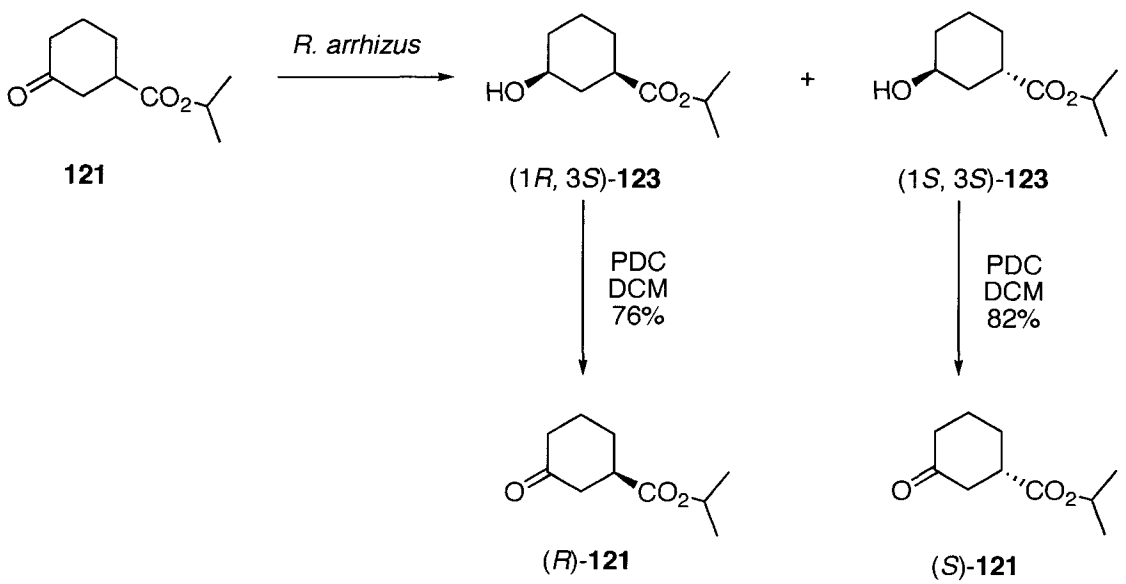

Scheme 46. Synthesis of chiral ketoesters (*R*)-**121** and (*S*)-**121**.

Reproduced with permission of the copyright owner. Further reproduction prohibited without permission.

With the chiral ketoester in hand, (*R*)-**121** is subjected to the classical Bucherer-Berg reaction conditions to give a 1:1 mixture of diastereomers of the hydantoin (3*R*)-**122** in 82% yield. Hydrolysis of the hydantoin mixture with barium hydroxide hydrate yields the free cycloglutamic acid (3*R*)-**89** in 91% yield as a mixture of diastereomers. Analysis of the diastereomeric mixture by derivatization to an *o*-phthalaldehyde adduct reveals an 82% enantiomeric excess.[120]

A noticed loss in chiral purity occurs between the resolution step reported by Azerad and coworkers[126] and **89**. To determine where the loss occurs, a number of techniques were attempted starting with the ketoester (*R*)-**121**. Since the GC column used by Azerad was not available to determine the *ee* of the hydroxyesters, another method for determining the *ee* had to be established. Chiral NMR shift reagents proved to be unsuccessful in determining the *ee* of the chiral ketoesters (*R*)-**121** and (*S*)-**121**. Chiral HPLC of the ketoesters (*R*)-**121** and (*S*)-**121** and the ketoacids (*R*)-**118** and (*S*)-**118** is also unsuccessful in resolving the two enantiomers.

During HPLC separations, the ketoester chromophore is found to have a very low absorptivity at 210 nm. Coupling of **118** to a strong chromophore like tryptophan and monitoring at 280 nm might allow for better detection as well as the separation of the resulting mixture of diastereomers. Synthesis of **124** as a mixture of (*RS*)- and (*SS*)-isomers is achieved by coupling **118** to L-tryptophan methyl ester (**125**) with PyBOP in 82% yield (Scheme 47).

Reproduced with permission of the copyright owner. Further reproduction prohibited without permission.

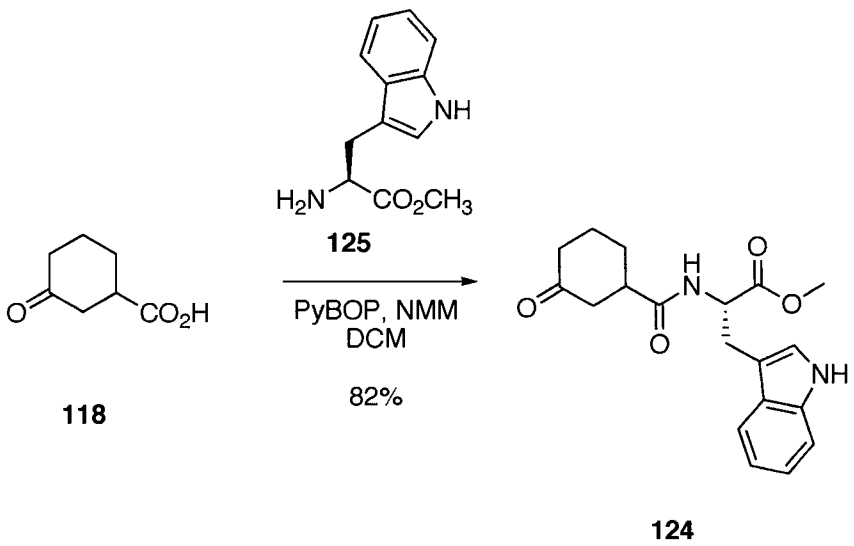

Scheme 47. Synthesis of **124**.

The separation of the isomers of **124** can be done by HPLC analysis on a ChiraDex column with a mobile phase of 10% methanol in water and a flow rate of 0.9 $mLmin^{-1}$. Although complete baseline separation is not achieved using an RP-HPLC column, it can be achieved with a chiral ChiraDex HPLC column. The separation shows two defined peaks in a 1:1 ratio (*SS*:*RS*) at retention times of 21.7 and 27.7 minutes each with a mass corresponding with **124** (Figure 32).

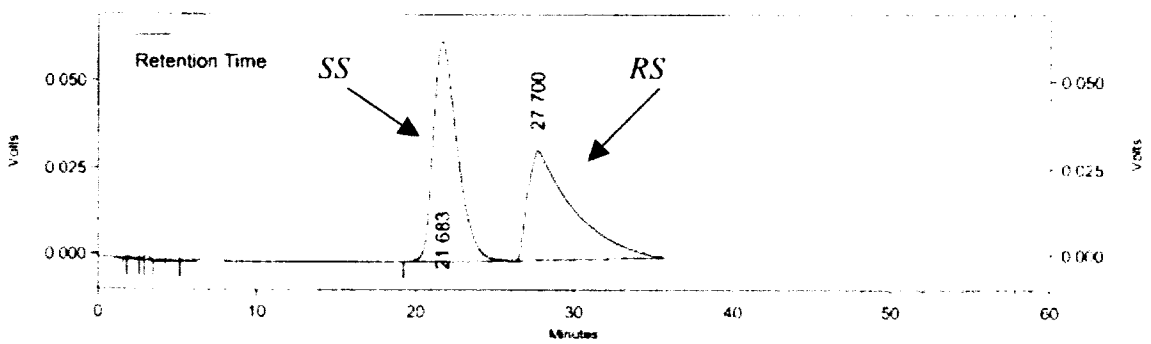

Figure 32. Chiral HPLC of the racemic **124** adduct.

Reproduced with permission of the copyright owner. Further reproduction prohibited without permission.

To determine the *ee* of the resolution, (*R*)-**121** is hydrolyzed with LiOH to yield (*R*)-**118** quantitatively, followed by PyBOP coupling with L-tryptophan methyl ester (**125**) to give (*R,S*)-**124** in 82% yield (Scheme 48).

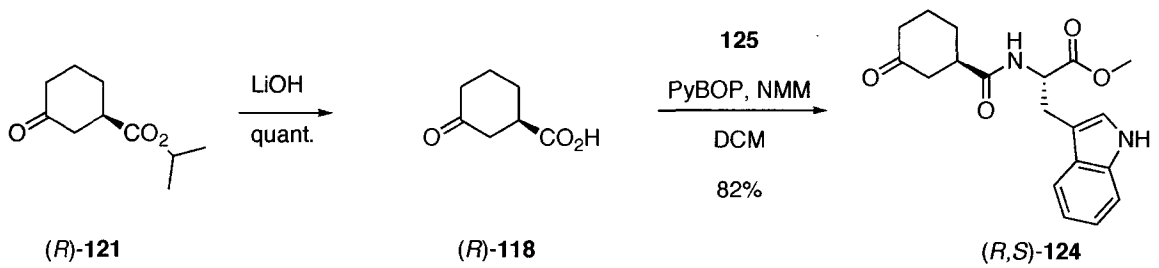

Scheme 48. Synthesis of (*R,S*)-**124**.

Separation of the isomers by chiral HPLC as described above shows an *ee* of 82%. A prolonged coupling time of 4 h produces the same result suggesting that racemization does not occur during derivatization. This result also suggests that no racemization occurs during the Bucherer-Berg reaction or barium hydroxide hydrolysis.

In summary, the synthesis of selected chiral adducts of **89** was achieved. Unfortunately, the enantiomeric excess of the reaction is far too low for crystallographic studies with the LL-DAP-AT.

Reproduced with permission of the copyright owner. Further reproduction prohibited without permission.

3.4.4. Inhibition Studies with LL-DAP Aminotransferase

Compound **89** (mixture of all possible isomers) is a poor reversible inhibitor of LL-DAP aminotransferase, with an IC_{50} value near 1 mM. This is a surprisingly weak binding given that this molecule possesses much of the functionality present in the substrates (L-THDP (**7**) and DAP) as well as the proposed intermediate **114**. The absence of the ring nitrogen at the center of **89** could generate unfavorable electronic interactions with the enzyme, causing the poor inhibition. This would suggest that the ring nitrogen is essential for effective binding with LL-DAP aminotransferase.

Reproduced with permission of the copyright owner. Further reproduction prohibited without permission.

3.5. Summary and Future Work

Three isomers of DAP have been synthesized and tested against key plant enzymes involved in the biosynthesis of lysine with the aim to gain additional knowledge concerning the enzymatic mechanism. The objectives were to determine the substrate specificity of DAP epimerase and LL-DAP-AT. The three DAP isomers (**1**-**3**) were synthesized *via* the diacyl peroxide procedure developed in our group.

The lack of substrate recognition by DAP epimerase observed for DD-DAP **3** suggests that an L-configuration at the distal site may be required in order to effectively inhibit this enzyme. Substrate recognition in LL-DAP-AT also shows a defined active site suggesting that an L-configuration in THDP (**7**) is required for recognition. The lack of potent inhibition against LL-DAP-AT and DAP epimerase observed for **4**, **15**, and **18** suggest that the substrate recognition is very specific, requiring all amine and carboxyl groups to be present in the substrates.

The L-THDP analog **89** was synthesized from ketoester **121** to investigate the inhibition mechanism of LL-DAP-AT. The inability to separate the diastereomers led to the testing of **89** as a mixture of all possible isomers. Inhibition studies revealed that cyclic analog **89** is not a potent inhibitor of LL-DAP-AT. It may be that the ring nitrogen present in L-THDP is essential for substrate recognition.

The analysis of plant material for DAP content by GC-MS and assay techniques was also described. GC-MS of the isopropyl *N*-pentafluoropropionic amides of DAP readily separated all three isomers to allow for the analysis of the crude plant mixtures. Crude extracts from *Arabidopsis thaliana* and *Brassica napus* showed the presence of

Reproduced with permission of the copyright owner. Further reproduction prohibited without permission.

meso-DAP and LL-DAP. *Brassica napus* was also found to contain DD-DAP. The crude plant mixtures were also analyzed by the coupled assay described by Wiseman and Nichols[36] to confirm the DAP content results.

Future work involves the synthesis of new DAP analogs based on the knowledge gained from this research. Synthesis of chirally pure isomers of cyclic **89** may provide a more detailed analysis of the mechanism of inhibition for the LL-DAP-AT. Selective protection of **89**, followed silica gel chromatography may allow for the separation of the diastereomers. In addition, synthesis of *N*-hydroxyglutamic acid could also lead to a novel irreversible inhibitor of LL-DAP-AT. Characterization of the plant DAP epimerase by irreversible inhibition with azi-DAP **19** and **20** is also ongoing. Isolation of the DAP epimerase from *Brassica napus* could also explain the structural requirements of the active site responsible for substrate recognition.

Reproduced with permission of the copyright owner. Further reproduction prohibited without permission.

Chapter 4: Experimental Procedures

4.1. General Methodologies

4.1.1. Reagents, Solvents and Solutions

All reactions involving air or moisture sensitive reactants and/or requiring anhydrous conditions were performed under a positive pressure of pre-purified argon using oven-dried glassware. All reagents and solvents utilized were of ACS grade or finer and were used without further purification unless otherwise mentioned. For anhydrous reactions, solvents were dried according to Perrin *et al.*[129] and Vogel.[130] Tetrahydrofuran (THF) and diethyl ether (Et_2O) were freshly distilled over sodium and benzophenone under an argon atmosphere whereas benzene and toluene were freshly distilled over sodium. Dichloromethane (DCM), carbon tetrachloride, acetonitrile, triethylamine (NEt_3), pyridine and methanol (MeOH) were freshly distilled over calcium hydride. Deionized water was obtained from a Milli-Q reagent water system (Millipore Co., Milford, MA). Removal of solvent *in vacuo* refers to evaporation under reduced pressure below 40 °C using a Büchi rotary evaporator, followed by evacuation (<0.1 mmHg) to a constant sample weight. Unless otherwise specified, solutions of NH_4Cl, $NaHCO_3$, HCl, NaOH, and KOH refer to aqueous solutions. Brine refers to a saturated aqueous solution of NaCl.

Reproduced with permission of the copyright owner. Further reproduction prohibited without permission.

4.1.2. Purification Techniques

All reactions and fractions from column chromatography were monitored by thin layer chromatography (TLC) using glass plates with a UV fluorescent indicator (normal SiO_2, Merck 60 F_{254}; reversed phase, Merck RP-8 or RP-18 F_{254}). One or more of the following methods were used for visualization: UV absorption by fluorescence quenching; iodine staining; phosphomolybdic acid/ceric sulfate/sulfuric acid/H_2O (10 g:1.25 g:12 mL:238 mL) spray; and Ninhydrin/methanol (1 g:100 mL) spray. Flash chromatography was performed according to the method of Still *et al.*[131] using Merck type 60, 230-400 mesh silica gel.

4.1.3. Instrumentation for Compound Characterization

Optical rotations were measured on a Perkin Elmer 241 polarimeter with a microcell (10 cm, 1 mL) at ambient temperature and are reported in units of 10^{-1} deg cm^2 g^{-1}. All optical rotations reported were referenced against air and were measured at the sodium D line and values quoted are valid within $\pm 1°$. Infrared spectra (IR) were recorded on a Nicolet Magna 750 or a 20SX FT-IR spectrometer. Mass spectra (MS) were recorded on a Kratos AEIMS-50 high resolution mass spectrometer (HRMS), electron impact ionization (EI) and Micromass Zabspec Hybrid Sector-TOF electrospray ionization instrument (ES) in either positive or negative mode (0.5% solution of formic acid in CH_3CN:H_2O/1:1).

Reproduced with permission of the copyright owner. Further reproduction prohibited without permission.

Nuclear magnetic resonance (NMR) spectra were obtained on Inova Varian 300, 400, 500, and 600 MHz spectrometers. ^{1}H NMR chemical shifts are reported in parts per million (ppm) using residual proton resonance of solvents as reference: $CDCl_3$, δ 7.24; CD_3OD, δ 3.30; $(CD_3)_2CO$, δ 2.04; CD_3CN, δ 1.93; D_2O, δ 4.79; C_6D_6, δ 7.16. The coupling constants reported are within an error range of ±0.5 Hz. ^{13}C NMR chemical shifts are reported relative to: $CDCl_3$, δ 77.0; CD_3OD, δ 49.0; $(CD_3)_2CO$, δ 29.8; CD_3CN, δ 1.3; C_6D_6, δ 128.1. ^{1}H NMR data are reported in the following order: multiplicity (s, singlet; d, doublet; t, triplet; q, quartet; dd, doublet of doublets; dq, doublet of quartets; app sextet, apparent sextet; sept, septet; app dt, apparent doublet of triplets; app sept of d, apparent septet of doublets; and m, multiplet), number of protons, coupling constant(s) (*J*) in Hertz (Hz), and assignment. For multiplets with large ranges (≥ 0.05 ppm), the range is provided. When appropriate, the multiplicity is preceded by br, indicating that the signal was broad. All literature compounds had IR, ^{1}H NMR and MS data consistent with the reported data.

4.1.4. First General Procedure for the Photodecarboxylation of Protected Amino Acids (Method A)

The carboxylic acid (1 eq.) was added to an aza aromatic compound (1 eq.) and the combined mixture (100-200 mg) was dissolved in a volatile solvent (2-5 mL), such as DCM, MeOH, or ethyl acetate, depending on solubility. The solution was then allowed to evaporate in a petri dish under an argon atmosphere to obtain a thin film of the substance

Reproduced with permission of the copyright owner. Further reproduction prohibited without permission.

on the bottom of the dish. The dish was then sealed with a quartz plate and was irradiated with a 0.9 A UV lamp directly from the top of the dish for 1-2 d at various temperatures (-78 °C – 80 °C) . The reaction mixture was then purified by flash chromatography on silica gel to obtain pure decarboxylated amino acids.

4.1.5. Second General Procedure for the Photo Decarboxylation of Protected Amino Acids (Method B)

The carboxylic acid (1 eq.) was added to an aza aromatic compound (1 eq.) and the combined mixture (100-200 mg) was dissolved in a volatile solvent (2-5 mL), such as DCM, MeOH, or ethyl acetate, depending on solubility. The solution was then allowed to evaporate in a petri dish under an argon atmosphere to obtain a thin film of the substance on the bottom of the dish. The dish was then sealed with a quartz plate and was irradiated with a 0.9 A UV lamp directly from the top of the dish at 4 °C. The film was re-dissolved in DCM or MeOH depending on solubility and allowed to evaporate under an argon atmosphere every 2 h to mix the thin film. The reaction mixture was then purified by flash chromatography on silica gel to obtain pure decarboxylated amino acids.

Reproduced with permission of the copyright owner. Further reproduction prohibited without permission.

4.1.6. General Procedure for the Preparation of 2-Methoxy-2-propyl Peresters

Prepared according to a modified literature procedure by Spantulescu *et al.*[98, 132] To a solution of 2-methoxyprop-2-yl hydroperoxide (**91**)[100] (2 mol eq.) in DCM (6 mL per mmol of protected amino acid) was added at –20 °C Cbz-Glu-OBn (1 mol eq.) followed by DCC (2 mol eq.) and DMAP (cat.). The suspension was slowly warmed to rt and stirred for an additional 1.5 h. The precipitated urea was filtered through Celite and the Celite was washed with DCM. The mixture was concentrated *in vacuo* and then purified by flash chromatography on silica gel (3/1 hexanes/ethyl acetate) to give the perester.

4.1.7. General Procedure for the Hydrolysis of 2-Methoxy-2-propyl Peresters to Peracids

Prepared according to a modified literature procedure by Spantulescu *et al.*[98, 132] To a solution of the appropriate protected perester (1 mol eq.) in $CHCl_3$ (3 mL per mmol perester) was added at rt 50% aqueous TFA (1 mL per mmol perester), and the resulting mixture was stirred for 15 min. The reaction was quenched by adding sat. $NaHCO_3$ and the organic were extracted with diethyl ether. The organic layer was washed with water, brine, dried ($MgSO_4$) and concentrated *in vacuo* to give the peracid.

Reproduced with permission of the copyright owner. Further reproduction prohibited without permission.

4.1.8. General Procedure for the Preparation of Unsymmetrical Diacyl Peroxides

Prepared according to a modified literature procedure by Spantulescu *et al.*[98, 132] To a solution of the appropriate peracid (1.3 mol eq.) in DCM (2 mL per mmol peracid) was added at 0 °C, DCC (1.3 mol eq.) and the appropriately protected amino acid (1 mol eq.). The suspension was slowly warmed to rt and stirred for an additional 2 h. The mixture was filtered through Celite, and the Celite was washed with DCM. The combined filtrates were concentrated *in vacuo* and then purified by flash chromatography on silica gel (3/1 hexanes/ethyl acetate) to give the peroxide.

4.1.9. General Procedure for the Photolysis of Diacyl Peroxides

Prepared according to a modified literature procedure by Spantulescu *et al.*[98, 132] The appropriate diacyl peroxide (50-250 mg) was dissolved in DCM and transferred to the photolysis vessel. The photolysis vessel has two side arms for introducing and evacuating argon and a sealing top window made of quartz, which is transparent to short-wavelength ultraviolet light. The solvent was evaporated under a stream of argon gas in order to obtain a thin film of the substance on the bottom of the vessel. The vessel was cooled to –78 °C (cryostat in acetone bath) and was irradiated with a 0.9 A UV lamp directly from the top of the vessel for 2-5 d. The mixture was then purified by flash chromatography on silica gel (4/1 hexanes/ethyl acetate) to give the protected DAP derivative.

Reproduced with permission of the copyright owner. Further reproduction prohibited without permission.

4.1.10. General Procedure for the Deprotection of Diaminopimelic Acid Derivatives

Prepared according to a modified literature procedure by Diaper *et al.*[47] A solution of the appropriate protected diaminopimelic acid derivative (50-200 mg) in diethyl ether (5 mL) was added to 6 M HCl (5 mL) and the mixture was heated to 90 °C for 2 h. The resulting aqueous solution was concentrated *in vacuo* and purified by ion-exchange chromatography (Biorad AG 50W-X8 hydrogen form resin), loading with distilled H_2O, flushing for 3 column lengths with de-ionized water and then eluting with 10% NH_4OH to give the DAP isomer after lyophilization.

4.1.11. General Procedure for the Resolution of Amino Acid Enantiomers by HPLC after Derivatization with a Chiral Adduct of *o*-Phthalaldehyde[106, 120]

To 10-20 μL of the amino acid solution (1 mg/mL) was added 10 μL of *o*-phthalaldehyde (OPA) solution (100 mg OPA in 3 mL of ethanol), 15 μL of *N*-acetyl-L-cysteine solution (30 mg in 10 mL of water) and 200 μL of 0.4 M sodium borate buffer (pH 10). After 3 min at rt, the mixture was diluted with water (1-2 mL). Twenty microlitre aliquots were analyzed on either a C18 Varian reverse phase column (Microsorb MV, 250 x 4.6 mm, 5μ column) or a C18 Phenomenex reverse phase column (Jupiter, 150 x 4.6 mm, 5μ column). The mobile phase was a phosphate buffer (made from 0.05 M potassium

Reproduced with permission of the copyright owner. Further reproduction prohibited without permission.

dihydrogenphosphate adjusted to pH 7.2 with sodium hydroxide) containing various amounts of methanol or acetonitrile. The column was operated at a constant flow rate of either 0.4 mL/min or 0.9 mL/min at rt. A Beckman Systems instrument was used with a System Gold model 126 pump and a System Gold model 166 detector monitoring at 340 nm.

4.1.12. General Procedure for the Analysis of Plant Material for DAP[113, 114]

Leaves from *Arabidopsis thaliana* donated by Prof. Mike Deyholos, were frozen with liquid nitrogen and crushed with a pestle and mortar. The crushed material (5 g) was placed in a sealed tube and 6 M HCl (10 mL) was added. The suspension was heated at 100 °C for 24 h. The remaining solids were removed by filtration and the pH was adjusted to pH 7 with sat. $NaHCO_3$. The solution was loaded onto BIORAD AG 50W-X8 resin (100–200 mesh). After flushing with H_2O (pH 7), material was eluted off using 4 M NH_4OH. The solvent was removed *in vacuo* and the residue was taken up into water (20 mL) and the pH adjusted to pH 7. The solution was again loaded onto BIORAD AG 50W-X8 resin (100 – 200 mesh) and the resin was washed with water and then with 1 M HCl and then 4 M HCl. The 4 M HCl washings were collected and lyophilized to dryness. Isopropyl alcohol (5 mL) and conc. HCl (5 drops) were added and the resulting mixture was heated at 100 °C for 16 h in a sealed tube and then concentrated *in vacuo*. The residue was dissolved in 6:1 CH_2Cl_2:PFPA (7 mL) and the mixture was then heated to 100 °C for 2 h in a sealed tube. The mixture was concentrated *in vacuo*. The crude

Reproduced with permission of the copyright owner. Further reproduction prohibited without permission.

mixture was then subjected to chiral GC-MS analysis, using the conditions described previously. Whole bundles from Canola (*Brassica napus*), Tobacco (*Nicotiana benthamiana*), Wheat (*Triticum aestivum*), and Flax (*Linum usitatissimum*) from Prof. Mike Deyholos were treated in an analogous fashion.

4.2. Experimental Data for Compounds

meso-2,6-Diaminopimelic acid (1)[9]

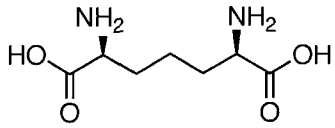

Prepared according to the procedure detailed in section 4.1.10. from **105** (White solid, 19.5 mg, 83%); Optical purity >99% *ee* determined by detailed procedure 4.1.11. Microsorb-MV, 15:85 MeCN:phosphate buffer (pH 7.2), 0.4 mL/min, 340 nm detection, t_R 21.4 min (*meso*-isomer); $[\alpha]_D = +0.4°$ (*c* 0.14, H_2O); IR (microscope) 3300-2300, 1594, 1494, 1458, 1437, 1394, 1314, 1094 cm^{-1}; ^1H NMR (D_2O, 500 MHz) δ 3.74 (dd, 2H, *J* = 6.9, 5.6 Hz, 2 × C<u>H</u>N), 1.83-1.97 (m, 4H, C<u>H</u>$_2$CH$_2$C<u>H</u>$_2$), 1.60-1.50 (m, 1H, CH$_2$C<u>H</u>HCH$_2$), 1.48-1.41 (m, 1H, CH$_2$CH<u>H</u>CH$_2$); ^{13}C NMR (D_2O, 100 MHz) δ 174.8, 54.8, 30.4, 21.0; HRMS (ES) Calcd for $C_7H_{13}N_2O_4$ 189.0869, found 189.0867.

Reproduced with permission of the copyright owner. Further reproduction prohibited without permission.

LL-2,6-Diaminopimelic acid (2)[9]

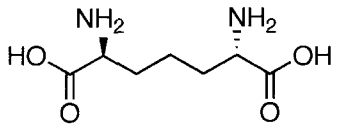

Prepared according to the procedure detailed in section 4.1.10. from **106** (White solid, 0.0446 g, 90%); Optical purity >99% *ee* determined by detailed procedure 4.1.11. Microsorb-MV, 15:85 MeCN:phosphate buffer (pH 7.2), 0.4 mL/min, 340 nm detection, t_R 17.3 min (LL-isomer); $[\alpha]_D$ = +2.5° (*c* 0.12, H_2O); IR (microscope) 3396, 3300-2300, 2937, 1581, 1465, 1436, 1412, 1349, 1326, 1103 cm^{-1}; ^1H NMR (D_2O, 500 MHz) δ 3.75 (t, 2H, *J* = 6.0 Hz, 2 × C<u>H</u>N), 1.86-1.93 (m, 4H, C<u>H</u>$_2$CH_2C<u>H</u>$_2$), 1.42-1.48 (m, 2H, CH_2C<u>H</u>$_2$CH_2); ^{13}C NMR (D_2O, 125 MHz) δ 175.4, 55.2, 30.9, 20.9; HRMS (ES) Calcd for $C_7H_{13}N_2O_4$ 189.0869, found 189.0868.

DD-2,6-Diaminopimelic acid (3)[9]

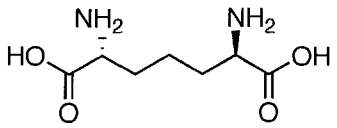

Prepared according to the procedure detailed in section 4.1.10. from **107** (White solid, 9.2 mg, 52%); Optical purity >99% *ee* determined by detailed procedure 4.1.11. Microsorb-MV, 15:85 MeCN:phosphate buffer (pH 7.2), 0.4 mL/min, 340 nm detection, t_R 19.8 min (DD-isomer); $[\alpha]_D$ = -14.2° (*c* 0.10, H_2O); IR (microscope) 3300-2300, 2925, 1573, 1464, 1436, 1410, 1346, 1325, 1099 cm^{-1}; ^1H NMR (D_2O, 500 MHz) δ 3.75 (t, 2H, *J* = 6.0 Hz, 2 × C<u>H</u>N), 1.86-1.93 (m, 4H, C<u>H</u>$_2$CH_2C<u>H</u>$_2$), 1.42-1.48 (m, 2H, CH_2C<u>H</u>$_2$CH_2); ^{13}C NMR

Reproduced with permission of the copyright owner. Further reproduction prohibited without permission.

(D_2O, 100 MHz) δ 175.2, 55.1, 30.7, 20.7; HRMS (ES) Calcd for $C_7H_{13}N_2O_4$ 189.0869, found 189.0868.

Benzyl phenethylcarbamate (31)[133]

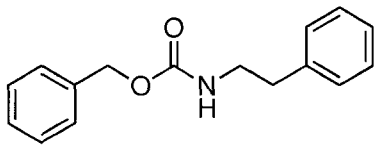

Prepared according to the procedure detailed in section 4.1.5. using **29** and **30** in the thin film (Colorless oil, 27 mg, 32%, Rf 0.59 in 3/2 hexanes/ethyl acetate); IR (microscope) 3323, 3087, 3062, 3029, 2973, 1680, 1540, 1454 cm^{-1}; ^1H NMR ($CDCl_3$, 400 MHz) δ 7.40–7.13 (m, 10H, ArH), 5.11 (s, 2H, $ArCH_2$), 4.84 (br s, 1H, NH), 3.47 (q, 2H, J = 6.8 Hz, NCH_2), 2.82 (t, 2H, J = 6.8 Hz, $PhCH_2$); ^{13}C NMR ($CDCl_3$, 100 MHz) δ 156.3, 138.7, 136.6, 128.8, 128.6, 128.5, 128.1, 126.5, 66.6, 42.2, 36.1; HRMS (ES) Calcd for $C_{16}H_{17}NO_2Na$ 278.1152, found 278.1149.

***N*-Phenethylacetamide (43a)**[134]

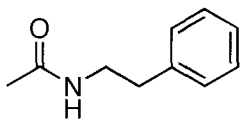

Prepared according to the procedure detailed in section 4.1.5. using **43** and **30** in the thin film (Colorless oil, 21 mg, 27%, Rf 0.59 in 3/2 hexanes/ethyl acetate); IR (microscope) 3290, 3086, 1635, 1548, 1453, 1426 cm^{-1}; ^1H NMR ($CDCl_3$, 300 MHz) δ 7.38–7.17 (m, 5H, ArH), 5.62 (br s, 1H, NH), 3.52 (q, 2H, J = 4.0 Hz, NCH_2), 2.82 (t, 2H, J = 4.0 Hz,

Reproduced with permission of the copyright owner. Further reproduction prohibited without permission.

PhC$\underline{H}_2$), 1.95 (s, 3H, C$\underline{H}_3$); ^{13}C NMR ($CDCl_3$, 125 MHz) δ 170.6, 138.8, 128.7, 128.6, 126.5, 40.7, 35.5, 23.2; HRMS (EI) Calcd for $C_{10}H_{13}NO$ 163.0997, found 163.0999.

(*S*)-2-Benzylamino-3-phenylpropionic acid (44) [68, 135]

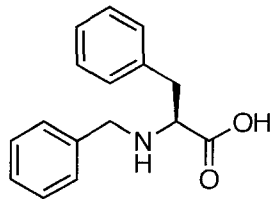

Prepared according to a literature procedure by Verardo *et al.*[68] L-Phenylalanine (2.64 g, 16 mmol) was suspended in methanol (30 mL) and sodium hydroxide (0.68 g, 17 mmol) and benzaldehyde (2.3 ml, 22 mmol) were added. After 10 min of stirring at rt, the solution was cooled to 0 °C and sodium borohydride (0.79 g, 21 mmol) was added. The reaction mixture was then stirred at 0 °C for 2 h. The mixture was then neutralized with conc. HCl and concentrated *in vacuo*. The residue was triturated with acetone and filtered to obtain the desired product as a white solid (3.69 g, 90%). $[\alpha]_D$ = +33.91 (*c* 1.0, AcOH); IR ($CHCl_3$ cast) 3355, 3033, 2322, 1612 cm^{-1}; ^{1}H NMR ($CHCl_3$, 500 MHz) δ 7.43-7.19 (m, 10H, Ar$\underline{H}$), 3.74 (d, 1H, *J* = 12.5 Hz, NCH$\underline{H}$), 3.56 (d, 1H, *J* = 12.5 Hz, NC$\underline{H}$H), 3.34 (dd, 1H, *J* = 7.6, 6.1 Hz, NC$\underline{H}$), 2.90 (dd, 1H, *J* = 13.3, 6.1 Hz, PhC$\underline{H}$HCH), 2.85 (dd, 1H, *J* = 13.3, 7.6 Hz, PhCH$\underline{H}$CH); ^{13}C NMR ($CHCl_3$, 125 MHz) δ 182.0, 139.8, 139.0, 130.2, 129.5, 129.4, 128.2, 127.5, 65.4, 51.9, 39.9; HRMS (ES) Calcd for $C_{16}H_{18}NO_2$ 256.1332, found 256.1332.

Reproduced with permission of the copyright owner. Further reproduction prohibited without permission.

(*S*)-2-Dibenzylamino-3-phenylpropionic acid (45)[136]

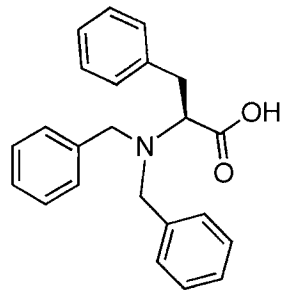

N,N-Dibenzyl phenylalanine benzyl ester **47** (4.52 g, 10.3 mmol) was dissolved in a mixture of dioxane (90 ml), methanol (15 ml) and 2 N KOH (45 mL) and stirred at rt for 16 h. The reaction mixture was then extracted with diethyl ether (3 x 100 mL). The organic fraction was then washed with water (2 x 100 mL), dried (Na_2SO_4), and concentrated *in vacuo*. Purification by flash column chromatography, eluting with 20% ethyl acetate in hexanes gave the title compound as a colorless oil (3.10 g, 88%). $[\alpha]_D = -53.2$ (*c* 5.5, $CHCl_3$); IR ($CHCl_3$ cast) 3085, 3062, 3028, 1706, 1603, 1495, 1454 cm^{-1}; ^1H NMR ($CHCl_3$, 500 MHz) δ 7.39-7.35 (m, 2H, ArH), 7.33-7.23 (m, 7H, ArH), 7.22-7.17 (m, 4H, ArH), 7.16-7.11 (m, 2H, ArH), 3.86-3.70 (m, 5H, 2 x NCH_2 + NCH), 3.31 (dd, 1H, *J* = 14.8, 6.4 Hz, PhCHHCH), 3.07 (dd, 1H, *J* = 14.8, 8.8 Hz, PhCHHCH); ^{13}C NMR ($CHCl_3$, 125 MHz) δ 175.6, 138.1, 137.8, 129.3, 128.8, 128.5, 128.4, 128.3, 127.6, 126.9, 126.4, 65.2, 62.6, 54.4, 34.1; HRMS (ES) Calcd for $C_{23}H_{24}NO_2$ 346.1802, found 346.1800.

Reproduced with permission of the copyright owner. Further reproduction prohibited without permission.

(*S*)-2-Dibenzylamino-3-phenylpropioic acid benzyl ester (47)[67]

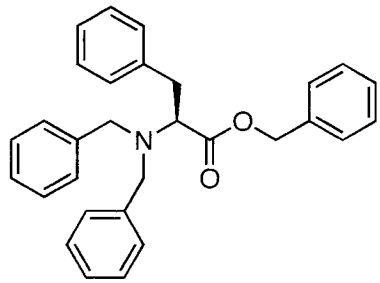

Prepared according to a modified literature procedure by Stuk *et al.*[67] L-Phenylalanine (2.81 g, 17 mmol) was suspended in a 10:2 mixture of ethanol:water (120 mL) and sodium carbonate (7.21 g, 68 mmol) was added at rt. Benzyl bromide (8.08 mL, 68 mmol) was then added drop wise over a period of 10 min. The suspension was then stirred at reflux for 16 h. The reaction mixture was then cooled to rt and concentrated *in vacuo*. The resulting residue was dissolved in water (50 mL) and extracted with ethyl acetate (3 x 100 mL). The organic fractions were combined, dried (Na_2SO_4), and concentrated *in vacuo*. Purification by flash column chromatography, eluting with 10% ethyl acetate in hexanes gave the title compound as a colorless oil (7.02 g, 95%). $[\alpha]_D = -55.5$ (*c* 4.5, $CHCl_3$); IR ($CHCl_3$ cast) 3085, 3028, 1706, 1603, 1495, 1454, 1373 cm^{-1}; ^1H NMR ($CHCl_3$, 500MHz) δ 7.44-7.35 (m, 7H, ArH), 7.27-7.20 (m, 7H, ArH), 7.19-7.13 (m, 4H, ArH), 7.07-7.01 (m, 2H, ArH), 5.26 (d, 1H, *J* = 12.5 Hz, OCHH), 5.15 (d, 1H, *J* = 12.5 Hz, OCHH), 3.96 (d, 2H, *J* = 15.0 Hz, NCHH), 3.79-3.72 (m, 2H, NCHH), 3.61-3.52 (m, 1H, NCH), 3.17 (dd, 1H, *J* = 14.0, 7.5 Hz, PhCHHCH), 3.04 (dd, 1H, *J* = 14.0, 8.5 Hz, PhCHHCH); ^{13}C NMR ($CHCl_3$, 125 MHz) δ 172.3, 139.4, 138.2, 136.1, 129.6, 128.8, 128.7, 128.6, 128.3, 128.2, 127.8, 127.0, 126.4, 66.2, 62.5, 54.5, 35.8; HRMS (ES) Calcd for $C_{30}H_{30}NO_2$ 436.2271, found 436.2271.

Reproduced with permission of the copyright owner. Further reproduction prohibited without permission.

Benzyl benzylcarbamate (49)[137]

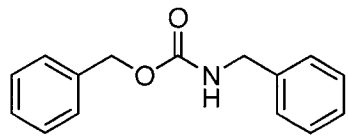

Prepared according to the procedure detailed in section 4.1.5. using **48** and **30** in the thin film (Colorless oil, 9 mg, 11%, R_f 0.58 in 3/2 hexanes/ethyl acetate); IR (DCM cast) 3330, 3087, 3065, 3033, 2958, 1706, 1535, 1454, 1245, 1141, 1046 cm^{-1}; ^1H NMR ($CDCl_3$, 400 MHz) δ 7.42-7.20 (m, 10H, ArH), 5.16 (s, 2H, $PhCH_2O$), 5.05 (br s, 1H, NH), 4.41 (d, J = 6.0 Hz, 2H, $NHCH_2Ph$); ^{13}C NMR ($CDCl_3$, 125 MHz) δ 156.4, 138.4, 136.5, 128.7, 128.5, 128.1, 127.5, 66.9, 45.2; HRMS (EI) Calcd for $C_{15}H_{15}NO_2$ 241.1103, found 241.1099.

Benzyl 1-phenylpropan-2-ylcarbamate (51)

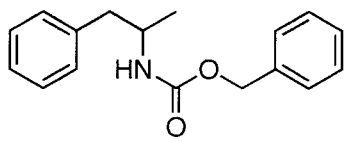

Prepared according to the procedure detailed in section 4.1.5. using **50** and **30** in the thin film (Colorless oil, 13 mg, 15%, Rf 0.59 in 3/2 hexanes/ethyl acetate); IR (DCM cast) 3328, 3086, 3028, 2930, 1697, 1530, 1250, 1062 cm^{-1}; ^1H NMR ($CDCl_3$, 300 MHz) δ 7.43–7.12 (m, 10H, ArH), 5.10 (s, 2H, $ArCH_2$), 4.66 (br s, 1H, NH), 4.02 (sept, 1H, J = 7.0 Hz, NCH), 2.87 (dd, 1H, J = 13.5, 7.0 Hz, PhCHH), 2.71 (dd, 1H, J = 13.5, 7.0 Hz, PhCHH), 1.14 (d, 3H, J = 7.0 Hz, CH_3); ^{13}C NMR ($CDCl_3$, 125 MHz) δ 156.7, 136.7, 135.2, 129.5, 128.7, 128.6, 128.5, 128.4, 128.3, 128.1, 126.4, 66.5, 48.0, 42.8, 20.2;

Reproduced with permission of the copyright owner. Further reproduction prohibited without permission.

HRMS (EI) Calcd for $C_{17}H_{19}NO_2$ 269.1416, found 269.1417.

tert-Butyl phenethylcarbamate d_5,α,β,β-d_8 (53)

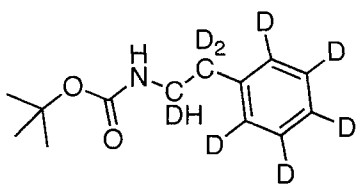

Prepared according to the procedure detailed in section 4.1.5. using **52** and **30** in the thin film (Clear colorless oil, 32 mg, 31%, Rf 0.58 in 3/2 hexanes/ethyl acetate); IR (DCM cast) 3290, 3087, 1635, 1548, 1453, 1426 cm^{-1}; ^1H NMR ($CDCl_3$, 500 MHz) δ 4.53 (br s, 1H, N<u>H</u>), 3.36 (br s, 1H, C<u>H</u>DCD_2), 1.44 (s, 9H, C(C<u>H_3</u>)$_3$); ^{13}C NMR ($CDCl_3$, 125 MHz) δ 155.9, 138.73, 128.5, 128.3, 128.2, 128.1, 128.0, 127.8, 125.9, 125.7, 79.2, 28.4; HRMS (ES) Calcd for $C_{13}H_{11}D_8NO_2Na$ 252.1810, found 252.1809.

(*S*)-2-Methoxy-*N*-phenethyl-2-phenyl-2-(trifluoromethoxy)acetamide (56)

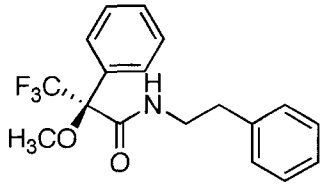

Prepared according to a modified literature procedure by Kusumi *et al.*[138] To a solution of phenethylamine (0.050 mL, 0.37 mmol) in DCM (4 mL) was added pyridine (0.29 mL, 3.9 mmol) and (*S*)-MTPA (0.15 mL, 0.79 mmol). The mixture was then stirred at rt for 1 h and then concentrated *in vacuo*. Purification by flash column chromatography, eluting with 25% ethyl acetate in hexanes, gave the title compound as a white solid (114 mg,

Reproduced with permission of the copyright owner. Further reproduction prohibited without permission.

89%, Rf 0.65 in 3/1 hexanes/ethyl acetate); $[\alpha]_D$= -16.8° (*c* 1.16, $CHCl_3$); IR ($CHCl_3$ cast) 3337, 3062, 3028, 2948, 2846, 1688, 1680, 1518, 1460, 1269, 1105 cm^{-1}; ^1H NMR (CD_3CN, 500 MHz) δ 7.57-7.48 (m, 5H, ArH), 7.41-7.35 (m, 2H, ArH), 7.34-7.27 (m, 3H, ArH), 3.66 (dt, *J* = 19.9, 7.0 Hz, 1H, NHCHH), 3.56 (dt, *J* = 19.9, 7.0 Hz, 1H, NHCHH), 3.42 (s, 3H, OCH_3), 2.92 (t, *J* = 7.0 Hz, 2H, CH_2Ph); ^{13}C NMR (CD_3CN, 100 MHz) δ 166.9, 140.2, 134.1, 130.4, 129.8, 129.4, 128.6, 127.3, 126.6, 123.7, 84.8 (q, *J* = 25.2 Hz), 55.6, 41.2, 35.8; HRMS (EI) Calcd for $C_{18}H_{18}N_2O_2F_3$ 337.1290, found 337.1283.

(*S*)-2-Methoxy-*N*-phenethyl-2-phenyl-2-(trifluoromethoxy)acetamide $d_5,\alpha,\beta,\beta\text{-}d_8$ (58)

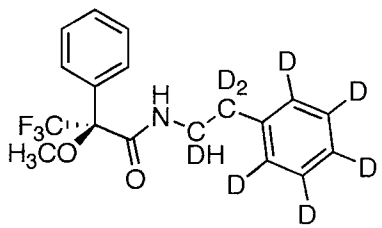

Prepared according to a modified literature procedure by Kusumi *et al.*[138] *tert*-Butyl phenethyl carbamate $d_5,\alpha,\beta,\beta\text{-}d_8$ **53** (5 mg, 0.02 mmol) was dissolved in a 1:1 DCM : TFA (10 mL) solution, stirred for 30 min and the mixture was concentrated *in vacuo*. 1 M HCl (5 mL) was then added to the resulting residue and washed with ethyl acetate (2 x 10 mL). The aqueous layer was then concentrated *in vacuo*. The resulting residue was dissolved in freshly distilled pyridine (0.1 mL) and (*S*)-MTPA chloride (0.08 mL, 0.40 mmol) was added. The mixture was then stirred for 30 min and then concentrated *in*

Reproduced with permission of the copyright owner. Further reproduction prohibited without permission.

vacuo. Purification by preparative thin layer chromatography, eluting with 40% ethyl acetate in hexanes gave the title compound as an inseparable mixture of diastereomers (6.8:1.4 *SS*:*SR* – ^{1}H NMR) as a colorless oil (5 mg, 65%); $[\alpha]_D$= -18.1° (*c* 0.10, $CHCl_3$); IR ($CHCl_3$ cast) 3330, 3061, 3028, 2940, 2846, 1688, 1680, 1518, 1460, 1269, 1105 cm^{-1}; ^{1}H NMR (CD_3CN, 500 MHz) δ (*SS* isomer, major diastereomer) 7.46-7.37 (m, 5H, Ar<u>H</u>), 7.26 (br s, 1H, N<u>H</u>), 3.52 (d, *J* = 5.9 Hz, 1H, NHC<u>H</u>DCD_2), 3.30 (s, 3H, O$C\underline{H}_3$); ^{1}H NMR (CD_3CN, 500 MHz) δ (*SR* isomer, minor diastereomer) 7.46-7.37 (m, 5H, Ar<u>H</u>), 7.26 (br s, 1H, N<u>H</u>), 3.43 (d, *J* = 5.9 Hz, 1H, NHCD<u>H</u>CD_2), 3.30 (s, 3H, O$C\underline{H}_3$); ^{13}C NMR (CD_3CN, 100 MHz) δ (both diastereomers) 166.9, 134.1, 129.8, 129.4, 127.3, 123.7, 84.8 (q, *J* = 25.2 Hz), 55.6; HRMS (ES) Calcd for $C_{18}H_{10}D_8NO_2F_3Na$ 368.1684, found 368.1684.

4,7-Dichloro-1,10-phenanthroline (59)[75]

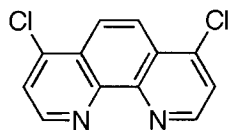

Prepared according to a literature procedure by Snyder *et al.*[75] Phosphorous pentachloride (1.96 g, 9.4 mmol) and $POCl_3$ (1.94 ml, 21.2 mmol) were combined and stirred at 90 °C for 10 min. To this mixture was quickly added 4,7-dihydroxy-1,10-phenanthroline **69** (1.06 g, 5.0 mmol). The reaction mixture was then stirred at 130 °C for 90 min. The excess $POCl_3$ was removed by distillation and the resulting brown residue was poured onto ice. After the residue dissolved, the resulting brown solution was treated with charcoal and filtered. The filtrate was then made basic with a 15% NaOH solution and the

Reproduced with permission of the copyright owner. Further reproduction prohibited without permission.

precipitate product was collected by filtration. Recrystallization from a methanol / water solution yielded the desired product as a white solid (0.062 g, 0.05%). m.p. 251-252 °C (lit.[75] 249-250 °C); IR (DCM cast) 3048, 3939, 1573, 1434, 1096, 876, 722 cm^{-1}; ^1H NMR ($CDCl_3$, 500 MHz) δ 7.76 (d, 2H, J = 4.8 Hz, 3-H), 8.35 (s, 2H, 5-H), 9.08 (d, 2H, J = 4.8 Hz, 2-H); ^{13}C NMR ($CDCl_3$, 125 MHz) δ 150.3, 147.0, 142.9, 126.9, 123.9, 123.3; HRMS (EI) Calcd for $C_{12}H_6N_2Cl_2$ 247.9908, found 247.9903.

4,7-Dichloro-1,10-phenanthroline (59)[76]

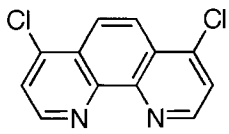

Prepared according to a literature procedure by Graf *et al.*[76] 1,2-Bis[(2,2-dimethyl-4,6-dioxo-1,3-dioxan-5-ylidenemethyl)amino]benzene **71** (11.1 g, 26 mmol) was added to Ph_2O (150 mL) and stirred at 270 °C for 30 min. The mixture was allowed to cool to room temperature and hexane was added to precipitate the dione. The precipitate was filtered, washed with hexanes and dried. Phosphorous oxychloride (90 mL) was then added to the dione and stirred under argon at 130 °C for 30 min. The excess $POCl_3$ was removed by distillation and the resulting brown residue was poured onto ice. After the residue dissolved, the resulting brown solution was treated with charcoal and filtered. The filtrate was then made basic with a 15% NaOH solution and extracted with dichloromethane (3 x 100 mL). The organic layers were combined, dried (Na_2SO_4) and concentrated *in vacuo*. Purification by flash column chromatography, eluting with 10%

Reproduced with permission of the copyright owner. Further reproduction prohibited without permission.

methanol in ethyl acetate with 1% NEt_3 gave the title compound as a slightly yellow solid (3.88 g, 58%). m.p. 251-253 °C (lit.[75] 249-250 °C); IR (DCM cast) 3048, 3939, 1573, 1434, 1096, 876, 722 cm^{-1}; ^1H NMR ($CDCl_3$, 500 MHz) δ 9.08 (d, 2H, J = 4.8 Hz, 2-H), 8.35 (s, 2H, 5-H), 7.76 (d, 2H, J = 4.8 Hz, 3-H); ^{13}C NMR ($CDCl_3$, 125 MHz) δ 150.3, 147.0, 142.9, 126.9, 123.9, 123.3; HRMS (EI) Calcd for $C_{12}H_6N_2Cl_2$ 247.9908, found 247.9903.

4,7-Dimethoxy-1,10-phenanthroline (60)[77]

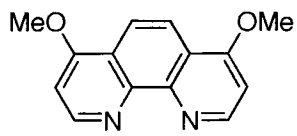

Prepared according to a literature procedure by Wehman *et al.*[77] 4,7-Dichloro-1,10-phenanthroline **59** (1.01 g, 4 mmol) was added to a freshly prepared solution of sodium methoxide (1.09 g, 20 mmol in 60 mL methanol). The reaction mixture was then stirred at reflux for 48 h. The reaction was allowed to cool to rt and concentrated *in vacuo*. Recrystallization from a methanol / water solution yielded the desired product as a brown solid (0.778 g, 80%). m.p. 206-208 °C (lit.[77] 207-208 °C); IR (DCM cast) 2980, 2843, 1635, 1615, 1517, 1506, 1312, 1028 cm^{-1}; ^1H NMR ($CDCl_3$, 500 MHz) δ 9.01 (d, 2H, J = 5.5 Hz, 2-H), 8.18 (s, 2H, 5-H), 7.00 (d, 2H, J = 5.5 Hz, 3-H), 4.10 (s, 6H, 2 x $C\underline{H}_3$); ^{13}C NMR ($CDCl_3$, 125 MHz) δ 162.3, 151.2, 146.9, 120.9, 119.0, 102.7, 55.8; HRMS (EI) Calcd for $C_{14}H_{12}N_2O_2$ 240.0899, found 240.0898.

Reproduced with permission of the copyright owner. Further reproduction prohibited without permission.

9-Methoxyacridine (65)[139]

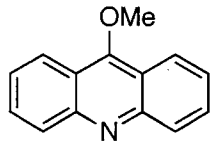

Prepared according to a modified literature procedure by Wehman *et al.*[77] 9-Chloroacridine **73** (0.21 g, 1 mmol) was added to a freshly prepared solution of sodium methoxide (0.53 g, 10 mmol in 40 mL methanol). The reaction mixture was then stirred at reflux for 24 h. The reaction was allowed to cool to rt and concentrated *in vacuo*. Recrystallization from a methanol / water solution yielded the desired product as a brown solid (0.207 g, 100%). m.p. 135-138 °C; IR (DCM cast) 3270, 2944, 1626, 1559, 1515, 799 cm^{-1}; ^1H NMR (DMSO-d_6, 500 MHz) δ 8.31 (d, 2H, J = 9.0 Hz, 4-H), 8.15 (d, 2H, J = 9.0 Hz, 1-H), 7.85 (ddd, 2H, J = 9.0, 7.0, 1.6 Hz, 3-H), 7.62 (ddd, 2H, J = 9.0, 7.0, 1.6 Hz, 2-H), 4.24 (s, 3H, $C\underline{H}_3$); ^{13}C NMR (DMSO-d_6, 125 MHz) δ 161.1, 149.8, 130.5, 129.2, 125.4, 122.3, 119.4, 64.2; HRMS (EI) Calcd for $C_{14}H_{11}NO$ 209.0841, found 209.0836.

Bis(benzo[2,3:9,8]-1,10-phenanthroline) (68)[79]

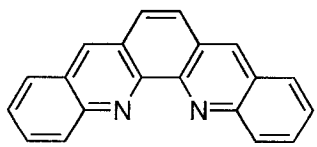

Prepared according to a modified literature procedure by Wu *et al.*[79] A mixture of 3,3'-dimethylene-2,2'-biquinoline **76** (1.1 g, 4 mmol), 10% Pd/C (0.68 g) and nitrobenzene (30 mL) was stirred at 210 °C for 6 d. The mixture was then cooled to rt, filtered through

Reproduced with permission of the copyright owner. Further reproduction prohibited without permission.

a pad of celite and the celite was washed with dichloromethane (3 x 20 mL). The filtrate and washings were combined, dried (Na_2SO_4) and concentrated *in vacuo* to give a brown solid. Purification by alumina flash column chromatography, a gradient eluent system (100% hexanes to 100% dichloromethane) gave the title compound as a brown yellow solid (0.519 g, 47%). m.p. 290-293 °C (lit.[79] 292-294 °C); IR (microscope) 3053, 3010, 1488, 744 cm^{-1}; ^1H NMR ($CDCl_3$, 500 MHz) δ 8.72 (d, 2H, J = 8.5 Hz, 1-H), 8.71 (s, 2H, 5-H), 8.08 (d, 2H, J = 8.0 Hz, 4-H), 7.89 (dd, 2H, J = 8.5, 7.0 Hz, 2-H), 7.77 (s, 2H, 6-H), 7.69 (dd, 2H, J = 8.0, 7.0 Hz, 3-H); ^{13}C NMR ($CDCl_3$, 125 MHz) δ 148.1, 147.8, 135.5, 131.4, 129.9, 127.8, 127.5, 127.4, 127.2, 126.6; HRMS (EI) Calcd for $C_{20}H_{12}N_2$ 280.1000, found 280.1000.

1,2-Bis-[(2,2-dimethyl-4,6-dioxo-1,3-dioxan-5-ylidenemethyl)amino]benzene (71)[76]

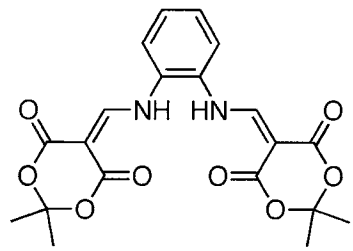

Prepared according to a literature procedure by Graf *et al.*[76] Meldrum's acid (10.1 g, 70 mmol) was dissolved in trimethyl orthoformate (100 mL) and stirred at 110 °C for 2 h. 1,2-Phenylenediamine (3.27 g, 30 mmol) was then added and the resulting mixture was stirred at 110 °C for an additional hour. The solution was then cooled to room temperature and concentrated *in vacuo*. Recrystallization from ethanol yielded the desired product as a slightly yellow solid (11.1 g, 88%). m.p. >210 °C (lit.[76] >209 °C); IR ($CHCl_3$

Reproduced with permission of the copyright owner. Further reproduction prohibited without permission.

cast) 3208, 3059, 2995, 1732, 1685, 1634 cm^{-1}; ^1H NMR ($CDCl_3$, 500 MHz) δ 11.33 (br d, 2H, *J* = 13.5 Hz, 2 x NH), 8.51 (d, 2H, *J* = 13.5 Hz, 2 x NCH), 7.41 (m, 4H, ArH), 1.76 (s, 12H, 4 x CH_3); ^{13}C NMR ($CDCl_3$, 125 MHz) δ 165.4, 163.0, 154.9, 131.0, 128.5, 121.3, 105.5, 89.5, 27.2; HRMS (ES) Calcd for $C_{20}H_{20}N_2O_8Na$ 439.1112, found 439.1109.

3,3'-Dimethylene-2,2'-biquinoline (76)[79]

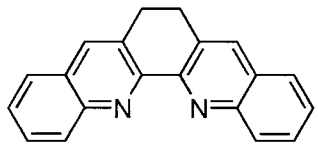

Prepared according to a literature procedure by Wu *et al.*[79] A mixture of 2-aminobenzaldehyde **75** (0.94 g, 8 mmol), 1,1-cyclohexadione **74** (0.44 g, 4 mmol) and saturated ethanolic potassium hydroxide (1 mL) in absolute ethanol (40 mL) was refluxed for 48 h. The mixture was then cooled to rt, water (50 mL) was added and the organics were extracted with dichloromethane (3 x 50 mL). The organic fractions were combined, dried (Na_2SO_4) and concentrated *in vacuo*. The residue was then washed with hexanes to yield the desired product as a brown solid (1.10 g, 100%). m.p. 186-189 °C (lit.[79] 188-190 °C); IR ($CHCl_3$ cast) 3032, 2944, 2835, 1494 cm^{-1}; ^1H NMR ($CDCl_3$, 500 MHz) δ 8.46 (d, 2H, *J* = 8.5 Hz, 1-H), 8.05 (s, 2H, 5-H), 7.79 (d, 2H, *J* = 8.0 Hz, 4-H), 7.71 (app t, 2H, *J* = 7.0 Hz, 2-H), 7.54 (dd, 2H, *J* = 8.0, 7.0 Hz, 3-H), 3.24 (s, 4H, 2 x CH_2); ^{13}C NMR ($CDCl_3$, 125 MHz) δ 152.3, 148.2, 134.6, 132.6, 131.0, 128.9, 128.4, 127.2, 126.8, 28.6; HRMS (EI) Calcd for $C_{20}H_{14}N_2$ 282.1157, found 282.1158.

Reproduced with permission of the copyright owner. Further reproduction prohibited without permission.

Methyl (2*S*,5*E*)-*N*-benzyloxycarbonyl-2-aminohept-5-ene-dioate (77)[140]

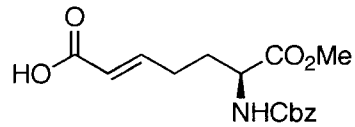

Methyl (2*S*,6*E*)-2-aminohept-5-ene-dioate **83** (0.438 g, 1.9 mmol) was dissolved in a 1:1 mixture of dioxane:water (80 mL) at 0 °C. Sodium carbonate (0.31 g, 3 mmol) was then added followed by benzyl chloroformate (0.32 ml, 2 mmol) over a 10 min period. The solution was then stirred for 12 h at rt. The reaction mixture was then acidified with conc. HCl to pH 1.5 and extracted with diethyl ether (3 x 80 mL). The organic layers were combined, dried (Na_2SO_4) and concentrated *in vacuo*. Purification by flash column chromatography, eluting with 4% methanol in chloroform gave the title compound as a gummy colorless oil (0.484 g, 77%). $[\alpha]_D$ +16.1 (*c* 1.0, $CHCl_3$); IR ($CHCl_3$ cast) 3500-2500, 3328, 2954, 1698, 1652, 1529, 1454 cm^{-1}; ^1H NMR ($CDCl_3$, 300 MHz) δ 7.43-7.32 (m, 5H, ArH), 7.03 (dt, 1H, *J* = 20.0, 10.0 Hz, CH_2CH=), 5.85 (d, 1H, *J* = 20.0 Hz, =$CHCO_2H$), 5.39 (br d, 1H, *J* = 10.5 Hz, NH), 5.12 (s, 2H, $PhCH_2$), 4.49-4.38 (m, 1H, NCH), 3.76 (s, 3H, OCH_3), 2.31 (m, 2H, =$CHCH_2$), 2.12-2.00 (m, 1H, CHCHH), 1.90-1.78 (m, 1H, CHCHH); ^{13}C NMR ($CDCl_3$, 75 MHz) δ 172.4, 171.0, 155.8, 149.6, 136.1, 128.6, 128.3, 128.1, 121.6, 67.2, 53.3, 52.6, 31.0, 28.0; HRMS (ES) Calcd for $C_{16}H_{19}NO_6Na$ 344.1105, found 344.1105.

Reproduced with permission of the copyright owner. Further reproduction prohibited without permission.

2-(*N*-Benzyloxycarbonylamino)-2-cyclopropylacetic acid (78)[141]

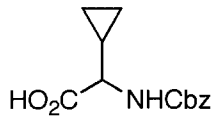

2-Amino-2-cyclopropylacetic acid **88** (0.075 g, 0.65 mmol) was dissolved in a 2:1 solution of 10% $NaHCO_3$:dioxane at 0 °C and added benzyl chloroformate (0.11 ml, 0.95 mmol) over a 10 min period. The solution was then stirred for 90 min at 0 °C, adjusting the pH to 9 with 10% $NaHCO_3$ if necessary. The solution was then warmed to rt and washed with diethyl ether (2 x 60 mL). The aqueous layer was then acidified to pH 1.5 with conc. HCl and extracted with diethyl ether (3 x 60 mL). The organic fractions were combined, dried (Na_2SO_4) and concentrated *in vacuo*. Purification by flash column chromatography, using a gradient eluent system (100% chloroform to 10% methanol in chloroform) gave the title compound as a gummy colorless solid (0.109 g, 67%). IR ($CHCl_3$ cast) 3500-2500, 3011, 1716, 1521 cm^{-1}; ^1H NMR (D_2O, 500 MHz) δ 7.40-7.26 (m, 5H, ArH), 5.38 (br d, J = 7.0 Hz, NH), 5.15-5.09 (m, 2H, $PhCH_2$), 3.93-3.80 (m, 1H, NCH), 1.18-1.09 (m, 1H, NCHCH), 0.75-0.58 (m, 4H, 2 x $CHCH_2$); ^{13}C NMR (D_2O, 125 MHz) δ 176.8, 156.1, 136.1, 128.5, 128.2, 128.3, 67.2, 57.4, 13.7, 3.1; HRMS (ES) Calcd for $C_{13}H_{15}NO_4Na$ 272.0893, found 272.0891.

Reproduced with permission of the copyright owner. Further reproduction prohibited without permission.

Dimethyl (2*S*)-*N*-*tert*-butoxycarbonylamino-pentanodioate (79)[82]

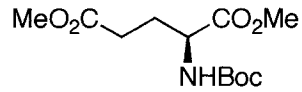

Prepared according to a literature procedure by Padron *et al.*[82] L-Glutamic acid (7.0 g, 47 mmol) was suspended in methanol (100 mL) and cooled to 0 °C. Chlorotrimethylsilane (27 mL, 207 mmol) was added drop wise over a period of 10 min. The reaction mixture was warmed to rt after 30 min and left stirring for 12 h. Triethylamine (28.7 ml, 207 mmol) was then added along with Boc_2O (11.3 g, 52 mmol). After 3 h, the reaction mixture was concentrated *in vacuo*. The resulting residue was dissolved in diethyl ether (200 mL) and filtered to remove the resulting white precipitate. The filtrate was concentrated *in vacuo*. Purification by flash column chromatography, eluting with 35% ethyl acetate in hexane gave the title compound as a colorless oil (13.2 g, 99%). $[\alpha]_D$ = +12.6 (*c* 5.18, $CHCl_3$); IR ($CHCl_3$ cast) 3368, 2977, 1741, 1716, 1517 cm^{-1}; ^1H NMR ($CDCl_3$, 500 MHz) δ 5.12 (br d, 1H, *J* = 7.0 Hz, NH), 4.36-4.24 (m, 1H, NCH), 3.73 (s, 3H, OCH_3), 3.66 (s, 3H, OCH_3), 2.48-2.29 (m, 2H, CH_2CO_2), 2.21-2.10 (m, 1H, CHCHH), 1.95-1.88 (m, 1H, CHCHH), 1.41 (s, 9H, $OC(CH_3)_3$); ^{13}C NMR ($CDCl_3$, 100 MHz) δ 173.1, 172.6, 155.3, 79.9, 52.8, 52.3, 51.7, 30.0, 28.2, 27.7; HRMS (ES) Calcd for $C_{12}H_{21}NO_6Na$ 298.1261, found 298.1263.

Reproduced with permission of the copyright owner. Further reproduction prohibited without permission.

Dimethyl (2*S*)-*N*,*N*-di-*tert*-butoxycarbonylamino-pentanedioate (80)[82]

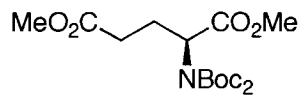

Prepared according to a literature procedure by Padron *et al.*[82] Dimethyl (*S*)-*N*-*tert*-butoxycarbonyl-2-amino-pentanodioate **79** (10.4 g, 37 mmol) was dissolved in acetonitrile (130 mL) under an argon atmosphere. DMAP (1.0 g, 8 mmol) was added along with a solution of Boc_2O (9.6 g, 44 mmol) in acetonitrile (40 mL) and the reaction was stirred for 12 h. An additional amount of Boc_2O (4.8 g, 22 mmol) in acetonitrile (20 mL) was then added and the reaction was stirred for 3 h. The reaction mixture was then concentrated *in vacuo*. Purification by flash column chromatography, eluting with 20% ethyl acetate in hexane gave the title compound as a white solid (11.9 g, 84%). $[\alpha]_D$ –47.6 (*c* 0.2, $CHCl_3$); IR ($CHCl_3$ cast) 2980, 2953, 1795, 1746, 1702, 1436 cm^{-1}; ^1H NMR ($CDCl_3$, 500 MHz) δ 4.93 (dd, 1H, *J* = 9.5, 4.3 Hz, NC<u>H</u>), 3.72 (s, 3H, OC<u>H</u>$_3$), 3.68 (s, 3H, OC<u>H</u>$_3$), 2.53-2.35 (m, 3H, CHCH<u>H</u> and C<u>H</u>$_2$CO$_2$), 2.23-2.10 (m, 1H, CHC<u>H</u>H), 1.50 (s, 18H, 2 x OC(C<u>H</u>$_3$)$_3$); ^{13}C NMR ($CDCl_3$, 125 MHz) δ 173.1, 170.8, 151.9, 83.3, 57.4, 52.2, 51.6, 30.6, 28.0, 25.2; HRMS (ES) Calcd for $C_{17}H_{29}NO_8Na$ 398.1785, found 398.1783.

Reproduced with permission of the copyright owner. Further reproduction prohibited without permission.

Methyl (2*S*)-*N*,*N*-di-*tert*-butoxycarbonylamino-5-oxopentanoate (81)[82]

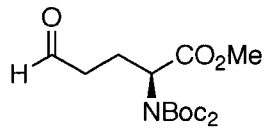

Prepared according to a literature procedure by Padron *et al.*[82] Dimethyl (*S*)-*N*,*N*-Di-*tert*-butoxycarbonyl-2-amino-pentanedioate **80** (1.21 g, 3 mmol) was dissolved in diethyl ether (40 mL) and cooled to –78 °C. Neat diisobutylaluminum hydride (0.8 ml, 4.5 mmol, 1.0 M) was then added drop wise. After 15 min a saturated solution of NH_4Cl (20 mL) was added and the reaction mixture was warmed to rt. The reaction mixture was filtered through a pad of Celite to remove the precipitate. The filtrate was concentrated *in vacuo* to give a viscous oil. Purification by flash column chromatography, eluting with 25% ethyl acetate in hexane gave the desired compound as a viscous colorless oil (0.86 g, 83%). $[\alpha]_D$ –38.3 (*c* 1.0, $CHCl_3$); IR ($CHCl_3$ cast) 2980, 2975, 1791, 1748, 1456 cm^{-1}; ^1H NMR ($CDCl_3$, 500 MHz) δ 9.74 (t, 1H, J = 0.65 Hz, C<u>H</u>O), 4.88 (dd, 1H, J = 9.7, 4.2 Hz, NC<u>H</u>), 3.72 (s, 3H, OC<u>H</u>$_3$), 2.63-2.20 (m, 3H, CHC<u>H</u>H and CHOC<u>H</u>$_2$), 2.19-2.09 (m, 1H, CHCH<u>H</u>), 1.49 (s, 18H, 2 x OC(C<u>H</u>$_3$)$_3$); ^{13}C NMR ($CDCl_3$, 125 MHz) δ 200.9, 170.7, 152.0, 83.4, 57.3, 52.2, 40.5, 28.0, 22.5; HRMS (ES) Calcd for $C_{16}H_{27}NO_7Na$ 368.1680, found 368.1677.

Reproduced with permission of the copyright owner. Further reproduction prohibited without permission.

(2*S*,5*E*)-7-*tert*-Butyl-1-methyl-*N*,*N*-Di-*tert*-Butoxycarbonyl-2-aminohept-5-ene-dioate (82)[83]

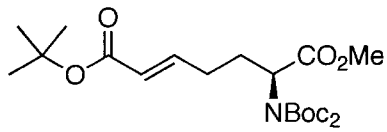

Prepared according to a literature procedure by Bycroft *et al.*[83] Methyl (2*S*)-*N*,*N*-Di-*tert*-Butoxycarbonyl-2-amino-5-oxopentanoate **81** (0.72 g, 2 mmol) was dissolved in toluene (50 mL) and (*tert*-butoxycarbonylmethylene)triphenyl phosphorane (0.946 g, 2.5 mmol) was added and stirred at to 120 °C for 12 h. The reaction mixture was then concentrated *in vacuo*. Purification by flash column chromatography, eluting with 20% ethyl acetate in hexane gave the title compound as a colorless oil (0.77 g, 87%). $[\alpha]_D$ –24.7 (*c* 6.5, $CHCl_3$); IR ($CHCl_3$ cast) 2979, 2934, 1795, 1749, 1713, 1653, 1478, 1367 cm^{-1}; ^1H NMR ($CDCl_3$, 500 MHz) δ 6.84 (dt, 1H, *J* = 16.0, 7.0 Hz, $CH_2CH_2C\underline{H}$=), 5.77 (d, 1H, *J* = 16.0 Hz, =$C\underline{H}CO_2H$), 4.94-4.80 (m, 1H, NC$\underline{H}$), 3.72 (s, 3H, $OC\underline{H}_3$), 2.31-2.26 (m, 3H, CHC$\underline{H}$H and $CHCH_2C\underline{H}_2$), 2.17-2.01 (m, 1H, CHCH$\underline{H}$), 1.50 (s, 18H, 2 x $OC(C\underline{H}_3)_3$), 1.48 (s, 9H, $OC(C\underline{H}_3)_3$); ^{13}C NMR ($CDCl_3$, 125 MHz) δ 170.9, 165.7, 152.0, 148.2, 123.8, 83.2, 80.1, 57.6, 52.2, 28.7, 28.5, 28.1, 28.0; HRMS (ES) Calcd for $C_{22}H_{37}NO_8Na$ 466.2411, found 466.2411.

Reproduced with permission of the copyright owner. Further reproduction prohibited without permission.

5-Carboxy-1-methoxycarbonylpent-4-enylammonium chloride (83)

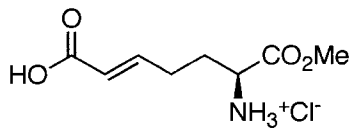

tert-Butyl (2*S*,5*E*)-*N*,*N*-di-*tert*-Butoxycarbonyl-2-aminohept-5-ene-dioate **82** (0.49 g, 1 mmol) was dissolved in DCM (10 mL) and added a solution of TFA (10 mL) and DCM (2 mL). After 30 min the reaction was concentrated *in vacuo*. The resulting oil was then dissolved in 1 M HCl (30 mL) and washed with ethyl acetate (3 x 30 mL). The aqueous layer was then concentrated *in vacuo* to yield the desired compound as a colorless oil (0.248 g, 99%). $[\alpha]_D$ +26.8 (*c* 2.5, H_2O); IR (microscope) 3500-2500, 2958, 1746, 1702, 1655, 1511 cm^{-1}; ^1H NMR (D_2O, 500 MHz) δ 6.98 (dt, 1H, *J* = 16.0, 7.0 Hz, CH_2CH=), 5.95 (dt, 1H, *J* = 16.0, 1.8 Hz, =$CHCO_2H$), 4.14 (t, 1H, *J* = 6.5 Hz, NC<u>H</u>), 3.84 (s, 3H, OCH_3), 2.54-2.40 (m, 2H, CH_2CH=), 2.21-2.13 (m, 2H, $CHCH_2$); ^{13}C NMR (D_2O, 125 MHz) δ 171.2, 171.1, 149.4, 122.7, 54.5, 53.0, 28.9, 27.8; HRMS (ES) Calcd for $C_8H_{14}NO_4$ 188.0917, found 188.0917.

2-(*N*-Benzylamino)-2-cyclopropylacetonitrile (86)[84]

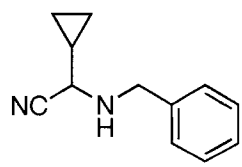

Prepared according to a patent procedure by Bayston *et al.*[84] Cyclopropylcarboxaldehyde **85** (2.0 ml, 26 mmol) was dissolved in water (200 mL) and added benzylamine (3.1 ml, 28 mmol) drop wise over 10 min. The reaction was then stirred for 3 h at rt. Potassium

Reproduced with permission of the copyright owner. Further reproduction prohibited without permission.

cyanide (1.83 g, 28 mmol) was added and the solution was stirred for an additional 2 h at rt. The solution was then adjusted to pH 10 by the addition of conc. HCl and extracted with ethyl acetate (3 x 100 mL). The organic fractions were combined, washed with brine (200 mL), dried (Na_2SO_4), and concentrated *in vacuo*. Purification by flash column chromatography, eluting with 20% ethyl acetate in hexanes gave the title compound as a colorless oil (3.69 g, 74%). IR ($CHCl_3$ cast) 3323, 3085, 3028, 3007, 2843, 2225, 1027 cm^{-1}; ^1H NMR ($CDCl_3$, 500 MHz) δ 7.40-7.23 (m, 5H, ArH), 4.09 (d, 1H, J = 13.5 Hz, PhCHH), 3.84 (d, 1H, J = 13.5 Hz, PhCHH), 3.41 (d, 1H, J = 6.5 Hz, NCH), 1.69 (br s, 1H, NH), 1.24 (dtt, 1H, J = 9.0, 6.5, 5.0 Hz, NCHCH), 0.70-0.62 (m, 2H, 2 x CHCHH), 0.52–0.46 (m, 2H, 2 x CHCHH); ^{13}C NMR ($CDCl_3$, 125 MHz) δ 138.4, 128.6, 128.3, 127.6, 118.5, 53.5, 51.6, 13.6, 3.4, 2.4; HRMS (ES) Calcd for $C_{12}H_{15}N_2$ 187.1230, found 187.1227.

2-(*N*-Benzylamino)-2-cyclopropylacetic acid (87)[84]

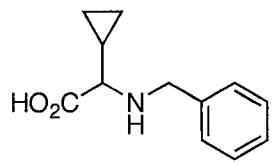

Prepared according to a modified patent procedure by Bayston *et al.*[84] 2-(*N*-Benzylamino)-2-cyclopropylacetonitrile **86** was dissolved in conc. HCl (30 mL) and stirred at 100 °C for 3 h. The solution was then cooled to rt and adjusted to pH 3-4 *via* the addition of 2 N NaOH and washed with ethyl acetate (2 x 50 ml). The solution was then neutralized with 2 N NaOH and concentrated *in vacuo*. Purification by flash column

Reproduced with permission of the copyright owner. Further reproduction prohibited without permission.

chromatography, eluting with 10% methanol in chloroform gave the title compound as a white solid (2.09 g, 63%). IR ($CHCl_3$ cast) 3200-2000, 3035, 2654, 1593 cm^{-1}; ^1H NMR (D_2O, 500 MHz) δ 7.41-7.32 (m, 5H, ArH), 3.72 (d, 1H, J = 13.5 Hz, PhCHH), 3.54 (d, 1H, J = 13.5 Hz, PhCHH), 2.35 (d, 1H, J = 9.5 Hz, NCH), 0.85 (dtt, 1H, J = 8.5, 8.5, 5.0 Hz, NCHCH), 0.56-0.48 (m, 1H, CHCHH), 0.46-0.38 (m, 1H, CHCHH), 0.25 (app sextet, 1H, J = 5 Hz, CHCHH), 0.16 (app sextet, 1H, J = 6 Hz, CHCHH); ^{13}C NMR ($CDCl_3$, 125 MHz) δ 182.6, 139.9, 129.6, 129.5, 128.2, 68.3, 52.0, 14.7, 5.1, 2.6; HRMS (ES) Calcd for $C_{12}H_{15}NO_2Na$ 228.0995, found 228.0993.

2-Amino-2-cyclopropylacetic acid (88)[84]

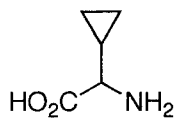

Prepared according to a patent procedure by Bayston *et al.*[84] 2-(*N*-Benzylamino)cycloproylacetic acid **87** (0.508 g, 2.5 mmol) was suspended in methanol (30 mL) and added 10% Pd/C (0.05 g). The reaction was then stirred under a hydrogen atmosphere (1 atm) for 24 h. The reaction mixture was filtered through a pad of Celite to remove the catalyst and concentrated *in vacuo* to give a white solid. The filtered catalyst was then slurried in water (50 ml) and stirred at 100 °C for 2 h. The reaction mixture was filtered through a pad of Celite to remove the catalyst and combined with the previous filtrate. The combined filtrates were then lyophilized to give the desired compound as a white solid (0.302 g, 100%). IR (microscope) 3500-2500, 1575, 1470 cm^{-1}; ^1H NMR (D_2O, 500 MHz) δ 3.10 (d, 1H, J = 10.2 Hz, NCH), 1.13 (dtt, 1H, J = 10.2, 8.0, 4.8 Hz,

Reproduced with permission of the copyright owner. Further reproduction prohibited without permission.

NCHCH), 0.80-0.66 (m, 2H, $CHCH_2$), 0.60 (app sextet, 1H, J = 5.0 Hz, CHCHH), 0.43 (app sextet, 1H, J = 4.8 Hz, CHCHH); ^{13}C NMR (D_2O, 125 MHz) δ 175.2, 60.5, 12.9, 4.8, 4.1; HRMS (ES) Calcd for $C_5H_9NO_2Na$ 138.0526, found 138.0525.

(±)-1-Aminocyclohexane-1,3-dicarboxylic acid (89)[120-122, 126, 142]

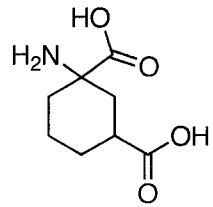

Prepared according to a modified literature procedure by Azerad *et al.*[122, 126] To a suspension of isopropyl 3-cyclohexanecarboxylate-1-spiro-5'hydantoin (**122**) (0.25 g, 1 mmol) in water (25 mL) was added $Ba(OH)_2 \cdot 8H_2O$ (1.56 g, 4.9 mmol). The mixture was then heated to 140 °C for 1 h in a sealed tube reaction vessel. The mixture was cooled to rt and then the pH was adjusted to 4.0 with 4 N H_2SO_4 and filtered. The resulting filtrate was concentrated *in vacuo* and purified by ion-exchange chromatography (Biorad AG 1 X4 AcO^- form resin), loading at pH 9.0, flushing for 3 column lengths with de-ionized water and then eluting with 0.5 M AcOH to give the desired compound after lyophilization as a mixture of diastereomers (1:1 *cis*:*trans* – ^1H NMR) as a white solid (0.17 g, 91%); IR (microscope) 3401, 3325, 3200-2500, 1749, 1714, 1697, 1536, 1470, 1413, 1197, 1143 cm^{-1}; ^1H NMR (D_2O, 500 MHz) δ (*cis* isomer) 2.72-2.63 (m, 1H, CO_2CH), 2.32-2.22 (m, 3H, $CO_2CHCH_2CCO_2$ and $CHCHHCH_2$), 2.18-1.92 (m, 3H, CH_2CHHCH_2 and CCH_2CH_2), 1.64-1.42 (m, 2H, $CHCHHCH_2$ and CH_2CHHCH_2); ^1H NMR (D_2O, 500 MHz) δ (*trans* isomer) 3.09-3.00 (m, 1H, $CHCO_2$),

Reproduced with permission of the copyright owner. Further reproduction prohibited without permission.

2.47 (d, 1H, J = 14.0 Hz, $CO_2CHC\underline{H}HCCO_2$), 2.32-2.20 (m, 1H, $CC\underline{H}HCH_2$), 2.18-1.92 (m, 2H, $CO_2CHC\underline{H}HCH_2$ and $CH_2C\underline{H}HCH_2$), 1.84-1.66 (m, 3H, $CO_2CHCH\underline{H}CCO_2$ and $CH_2CH\underline{H}CH_2$ and $CCH\underline{H}CH_2$), 1.64-1.42 (m, 1H, $CO_2CHCH\underline{H}CH_2$); ^{13}C NMR (D_2O, 125 MHz,) δ 179.6, 178.9, 175.6, 174.3, 61.0, 59.6, 39.4, 37.7, 33.3, 33.0, 32.1, 30.7, 27.3, 27.2, 20.9, 19.5; HRMS (ES) Calcd for $C_8H_{12}NO_4$ 186.0761, found 186.0762.

(3*R*)-(±)- 1-Aminocyclohexane-1,3-dicarboxylic acid ((3*R*)-89)[120, 126, 142, 143]

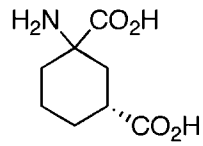

Prepared according to a modified literature procedure by Azerad *et al.*[122, 126] To a suspension of (*R*)-isopropyl 3-oxo-1-cyclohexanecarboxylate-1-spiro-5'hydantoin (**(3*R*)-122**) (56 mg, 0.22 mmol) in water (5 mL) was added $Ba(OH)_2 \cdot 8H_2O$ (0.28 g, 0.88 mmol). The mixture was then heated to 140 °C for 1 h in a sealed tube reaction vessel. The mixture was cooled to rt and then the pH was adjusted to 4.0 with 4 N H_2SO_4 and filtered. The resulting filtrate was concentrated *in vacuo* and purified by ion-exchange chromatography (Biorad AG 1-X4 AcO^- form resin), loading at pH 9.0, flushing for 3 column lengths with de-ionized water and then eluting with 0.5 M AcOH to give the desired compound after lyophilization as a mixture of diastereomers (1:1 *cis:trans* – ^1H NMR) as a white solid (39 mg, 94%); IR (microscope) 3401, 3325, 3200-2500, 1749, 1714, 1697, 1536, 1470, 1413, 1197, 1143 cm^{-1}; ^1H NMR (D_2O, 500 MHz) δ (*cis* isomer) 2.72-2.63 (m, 1H, $CO_2C\underline{H}$), 2.32-2.22 (m, 3H, $CO_2CHC\underline{H}_2CCO_2$ and $CHC\underline{H}HCH_2$), 2.18-

Reproduced with permission of the copyright owner. Further reproduction prohibited without permission.

1.92 (m, 3H, $CH_2C\underline{H}HCH_2$ and $CC\underline{H}_2CH_2$), 1.64-1.42 (m, 2H, $CHCH\underline{H}CH_2$ and $CH_2CH\underline{H}CH_2$); ^{1}H NMR (D_2O, 500 MHz) δ (*trans* isomer) 3.09-3.00 (m, 1H, $C\underline{H}CO_2$), 2.47 (d, 1H, J = 14.0 Hz, $CO_2CHC\underline{H}HCCO_2$), 2.32-2.20 (m, 1H, $CC\underline{H}HCH_2$), 2.18-1.92 (m, 2H, $CO_2CHC\underline{H}HCH_2$ and $CH_2C\underline{H}HCH_2$), 1.84-1.66 (m, 3H, $CO_2CHCH\underline{H}CCO_2$ and $CH_2CH\underline{H}CH_2$ and $CCH\underline{H}CH_2$), 1.64-1.42 (m, 1H, $CO_2CHCH\underline{H}CH_2$); ^{13}C NMR ($D_2O$, 125 MHz,) δ 179.6, 178.9, 175.6, 174.3, 61.0, 59.6, 39.4, 37.7, 33.3, 33.0, 32.1, 30.7, 27.3, 27.2, 20.9, 19.5; HRMS (ES) Calcd for $C_8H_{12}NO_4$ 186.0761, found 186.0762.

2-Hyroperoxy-2-methoxypropane (91)[100, 132]

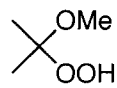

Prepared according to a literature procedure by Dussault *et al.*[100] 2,3-Dimethyl-2-butene (4.0 mL, 33 mmol) was dissolved in 1:1 DCM:MeOH (40 mL) and was added $NaHCO_3$ (cat.). The mixture was cooled to -78 °C and a 2.0 Lpm stream of ozone was bubbled through the solution until an intense blue color persisted. The solution was then purged with oxygen for 20 min and concentrated *in vacuo* to give the desired product as a colorless oil. (2.09 g, 59%); IR (DCM cast) 3416, 3000, 2947, 1464, 1370, 1200, 1171, 1053 cm^{-1}; ^{1}H NMR ($CDCl_3$, 400 MHz) δ 3.16 (s, 3H, $OC\underline{H}_3$), 1.24 (s, 6H, $C(C\underline{H}_3)_2$); ^{13}C NMR ($CDCl_3$, 100 MHz) δ 104.9, 48.9, 21.9; HRMS (EI) Calcd for $C_4H_{10}O_3$ 106.0630, found 106.0627.

Reproduced with permission of the copyright owner. Further reproduction prohibited without permission.

(2*R*)-Benzyl-2-(*N*-benzyloxycarbonylamino)-5-(2-methoxy-2-proplyperoxy)-5-oxopentanoate (97)

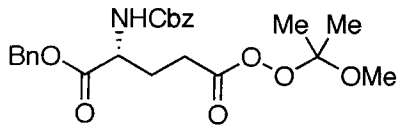

Prepared according to the procedure detailed in section 4.1.6. from acid **96** and **91** (Colorless oil, 0.247 g, 89%, R_f 0.56 in 2/1 hexanes/ethyl acetate); $[\alpha]_D$ = -2.3° (*c* 1.29, DCM); IR (DCM cast) 3350, 3033, 2995, 1775, 1724, 1523, 1454, 1215, 1064 cm^{-1}; ^1H NMR ($CDCl_3$, 500 MHz) δ 7.39-7.28 (m, 10H, ArH), 5.56 (d, 1H, *J* = 7.5 Hz, NH), 5.12 (s, 2H, $PhCH_2$), 5.07 (s, 2H, $PhCH_2$), 4.44-4.41 (m, 1H, NCH), 3.29 (s, 3H, OCH_3), 2.41-2.28 (m, 2H, CH_2CH_2CO), 2.25-2.21 (m, 1H, CHCHH), 2.02-1.97 (m, 1H, CHCHH), 1.40 (s, 6H, 2 x CH_3); ^{13}C NMR ($CDCl_3$, 100 MHz) δ 171.2, 169.5, 155.8, 135.9, 134.9, 128.6, 128.5, 128.4, 128.2, 128.1, 128.1, 128.0, 106.9, 67.4, 67.0, 53.2, 49.7, 27.5, 27.0, 22.4; HRMS (ES) Calcd for $C_{24}H_{29}NO_8Na$ 482.1785, found 482.1788.

(4*R*)-5-Benzyloxy-4-(*N*-benzyloxycarbonylamino)-5-oxoperpentanoic acid (98)

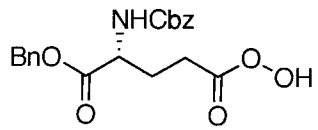

Prepared according to the procedure detailed in section 4.1.7. from perester **97** (Colorless oil, 0.440 g, 90%, Rf 0.20 in 2/1 hexanes/ethyl acetate); $[\alpha]_D$ = -3.4° (*c* 1.26, DCM); IR (DCM cast) 3329, 3066, 3034, 2954, 1720, 1528, 1454, 1388, 1263, 1214, 1056 cm^{-1}; ^1H NMR ($CDCl_3$, 400 MHz) δ 7.34-7.27 (m, 10H, ArH), 5.59 (d, 1H, *J* = 7.6 Hz, NH), 5.14 (s, 2H, $PhCH_2$), 5.08 (s, 2H, $PhCH_2$), 4.48-4.42 (m, 1H, NCH), 2.48-2.32 (m, 2H,

Reproduced with permission of the copyright owner. Further reproduction prohibited without permission.

$CH_2C\underline{H}_2Ph$), 2.30-2.21 (m, 1H, CHC$\underline{H}$H), 2.05-1.95 (m, 1H, CHCH$\underline{H}$); ^{13}C NMR ($CDCl_3$, 100 MHz) δ 173.1, 171.0, 155.8, 135.8, 134.7, 128.7, 128.6, 128.5, 128.4, 128.3, 128.2, 128.1, 128.0, 67.6, 67.2, 58.4, 53.0, 27.2, 26.4, 18.2; HRMS (ES) Calcd for $C_{20}H_{21}NO_7Na$ 410.1210, found 410.1210.

(4*R*)-5-Benzyloxy-4-(*N*-benzyloxycarbonylamino)-5-oxopentanoic (3*R*)-4-*tert*-butoxy-3-(*N*-*tert*-butoxycarbonylamino)-4-oxobutanoic peroxyanhydride (100)

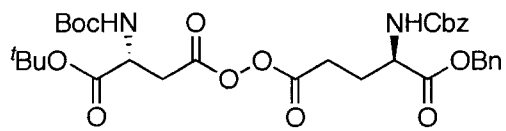

Prepared according to the procedure detailed in section 4.1.8. from peracid **98** and acid **99** (Colorless gum, 0.521 g, 93%, Rf 0.39 in 2/1 hexanes/ethyl acetate); $[\alpha]_D$ = -21.3° (*c* 1.02, DCM); IR (DCM cast) 3352, 3034, 2978, 2935, 1812, 1782, 1721, 1499, 1500, 1368, 1254, 1155, 1059 cm^{-1}; ^1H NMR ($CDCl_3$, 500 MHz) δ 7.38-7.24 (m, 10H, Ar$\underline{H}$), 5.60 (d, 1H, *J* = 8.0 Hz, N$\underline{H}$), 5.48 (d, 1H, *J* = 7.5 Hz, N$\underline{H}$), 5.13 (s, 2H, PhC$\underline{H}_2$), 5.06 (s, 2H, PhC$\underline{H}_2$), 4.50-4.46 (m, 1H, NC$\underline{H}$), 4.44-4.41 (m, 1H, NC$\underline{H}$), 2.99 (dd, 1H, *J* = 16.5 Hz, 4.0 Hz, CHC$\underline{H}$HCO), 2.91 (dd, 1H, *J* = 16.5 Hz, 5.0 Hz, CHCH$\underline{H}$CO), 2.51-2.36 (m, 2H, $CH_2C\underline{H}_2CO$), 2.30-2.24 (m, 1H, CHC$\underline{H}$HCH_2), 2.06-1.99 (m, 1H, CHCH$\underline{H}CH_2$), 1.42 (s, 9H, C($C\underline{H}_3$)$_3$), 1.41 (s, 9H, C($C\underline{H}_3$)$_3$); ^{13}C NMR ($CDCl_3$, 125 MHz) δ 171.1, 168.8, 167.9, 166.6, 155.9, 155.1, 136.0, 135.1, 128.6, 128.5, 128.3 128.1, 128.0, 83.0, 80.1, 67.6, 67.1, 53.1, 50.2, 33.0, 28.2, 27.7, 27.3, 26.0; HRMS (ES) Calcd for $C_{33}H_{42}N_2O_{12}Na$ 681.2630, found 681.2630.

Reproduced with permission of the copyright owner. Further reproduction prohibited without permission.

(2*S*)-Benzyl-2-(*N*-benzyloxycarbonylamino)-5-(2-methoxy-2-proplyperoxy)-5-oxopentanoate (102)[98, 132]

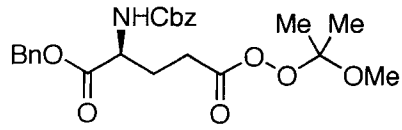

Prepared according to the procedure detailed in section 4.1.6. from acid **101** and **91** (Colorless oil, 0.812 g, 94%, Rf 0.56 in 2/1 hexanes/ethyl acetate); $[\alpha]_D = +1.5°$ (*c* 1.07, DCM); IR (DCM cast) 3343, 3033, 2994, 2944, 1775, 1724, 1521, 1454, 1215, 1064 cm^{-1}; ^1H NMR ($CDCl_3$, 500 MHz) δ 7.38-7.28 (m, 10H, ArH), 5.57 (d, 1H, *J* = 7.5 Hz, NH), 5.12 (s, 2H, $PhCH_2$), 5.04 (s, 2H, $PhCH_2$), 4.45-4.41 (m, 1H, NCH), 3.29 (s, 3H, OCH_3), 2.41-2.28 (m, 2H, CH_2CH_2CO), 2.24-2.21 (m, 1H, CHCHH), 2.02-1.97 (m, 1H, CHCHH), 1.40 (s, 6H, $C(CH_3)_2$); ^{13}C NMR ($CDCl_3$, 100 MHz) δ 171.2, 169.5, 155.8, 135.9, 134.9, 128.6, 128.5, 128.4, 128.2, 128.1, 128.1, 128.0, 106.9, 67.4, 67.0, 53.2, 49.7, 27.5, 27.0, 22.4; HRMS (ES) Calcd for $C_{24}H_{29}NO_8Na$ 482.1785, found 482.1787.

(4*S*)-5-Benzyloxy-4-(*N*-benzyloxycarbonylamino)-5-oxoperpentanoic acid (103)[98, 132]

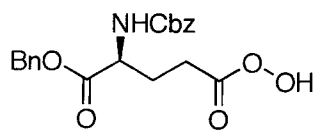

Prepared according to the procedure detailed in section 4.1.7. from perester **102** (Colorless oil, 0.359 g, 82%, Rf 0.20 in 2/1 hexanes/ethyl acetate); $[\alpha]_D = +4.1°$ (*c* 1.87, DCM); IR (DCM cast) 3330, 3065, 3034, 2952, 1733, 1717, 1586, 1521, 1498, 1455, 1213, 1058 cm^{-1}; ^1H NMR ($CDCl_3$, 400 MHz) δ 7.34-7.27 (m, 10H, ArH), 5.59 (d, 1H, *J*

Reproduced with permission of the copyright owner. Further reproduction prohibited without permission.

= 7.6 Hz, NH), 5.14 (s, 2H, $PhCH_2$), 5.08 (s, 2H, $PhCH_2$), 4.48-4.42 (m, 1H, NCH), 2.48-2.32 (m, 2H, CH_2CH_2Ph), 2.30-2.21 (m, 1H, CHCHH), 2.05-1.95 (m, 1H, CHCHH); ^{13}C NMR ($CDCl_3$, 100 MHz) δ 173.1, 171.0, 155.8, 135.8, 134.7, 128.7, 128.6, 128.5, 128.4, 128.3, 128.2, 128.1, 128.0, 67.6, 67.2, 58.4, 53.0, 27.2, 26.4, 18.2; HRMS (ES) Calcd for $C_{20}H_{21}NO_7Na$ 410.1210, found 410.1210.

(4*R*)-5-Benzyloxy-4-(*N*-benzyloxycarbonylamino)-5-oxopentanoic (3*S*)-4-*tert*-butoxy-3-(*N*-tert-butoxycarbonylamino)-4-oxobutanoic peroxyanhydride (104)

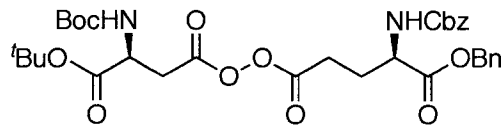

Prepared according to the procedure detailed in section 4.1.8. from peracid **103** and acid **99** (Colorless gum, 0.303 g, 65%, Rf 0.37 in 2/1 hexanes/ethyl acetate); $[\alpha]_D$= -14.0° (*c* 1.26, DCM); IR ($CHCl_3$ cast) 3349, 2978, 2934, 1812, 1782, 1721, 1500, 1455, 1368, 1253, 1155, 1057 cm^{-1}; ^1H NMR ($CDCl_3$, 500 MHz) δ 7.40-7.28 (m, 10H, ArH), 5.44 (br s, 1H, 2 x NH), 5.18 (s, 2H, $PhCH_2$), 5.06 (s, 2H, $PhCH_2$), 4.55-4.40 (m, 2H, 2 x NCH), 3.04 (dd, 1H, *J* = 16.5, 4.0 Hz, CHCHHCO), 2.94 (dd, 1H *J* = 16.5, 5.0 Hz, CHCHHCO), 2.59-2.39 (m, 2H, CH_2CH_2CO), 2.37-2.28 (m, 1H, $CHCHHCH_2$), 2.12-2.00 (m, 1H, $CHCHHCH_2$), 1.46 (s, 9H, $C(CH_3)_3$), 1.45 (s, 9H, $C(CH_3)_3$); ^{13}C NMR ($CDCl_3$, 125 MHz) δ 171.1, 168.8, 167.9, 166.7, 155.9, 155.2, 136.0, 134.9, 128.7, 128.6, 128.5, 128.4, 128.2, 128.1, 83.1, 80.2, 67.6, 67.2, 53.1, 50.4, 33.1, 28.3, 27.8, 27.7, 26.0; HRMS (ES) Calcd for $C_{33}H_{42}N_2O_{12}Na$ 681.2630, found 681.2630.

Reproduced with permission of the copyright owner. Further reproduction prohibited without permission.

(2*R*,6*S*)-1-Benzyl 7-*tert*-butyl 2-(*N*-benzylcarbonylamino)-6-(*N*-*tert*-butoxycarbonyl-amino)heptanedioate (105)

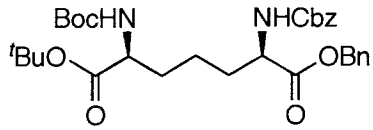

Prepared according to the procedure detailed in section 4.1.9. from diacyl peroxide **104** (Colorless gum, 0.0761 g, 49%, Rf 0.57 in 2/1 hexanes/ethyl acetate); $[\alpha]_D$ = -3.3° (*c* 0.87, DCM); IR (DCM cast) 3347, 2976, 2932, 1715, 1500, 1455, 1366, 1250, 1154 cm^{-1}; ^1H NMR ($CDCl_3$, 500 MHz) δ 7.45-7.22 (m, 10H, ArH), 5.42 (d, 1H, *J* = 5.0 Hz, NH), 5.17 (s, 2H, CH_2Ph), 5.10 (s, 2H, CH_2Ph), 5.01 (d, 1H, *J* = 5.0 Hz, NH), 4.43-4.38 (m, 1H, NHCH), 4.15-4.10 (m, 1H, NHCH), 1.92-1.83 (m, 1H, $NCHCHHCH_2$), 1.80-1.62 (m, 3H, $NCHCHHCH_2$ and $NCHCH_2CH_2CH_2$), 1.60-1.50 (m, 1H, CH_2CHHCH_2), 1.44 (s, 9H, $C(CH_3)_3$), 1.43 (s, 9H, $C(CH_3)_3$), 1.38-1.26 (m, 1H, CH_2CHHCH_2); ^{13}C NMR ($CDCl_3$, 125 MHz) δ 172.1, 171.7, 155.9, 155.5, 136.3, 135.3, 128.7, 128.5, 128.3, 128.2, 128.1, 81.9, 79.7, 67.2, 67.0, 53.8, 53.5, 32.6, 32.0, 28.4, 28.3, 28.0, 20.9; HRMS (ES) Calcd for $C_{31}H_{42}N_2O_8Na$ 593.2833, found 593.2832.

Reproduced with permission of the copyright owner. Further reproduction prohibited without permission.

(2*S*,6*S*)-7-*tert*-butyl 1-Methyl 2-(*N*-benzylcarbonylamino)-6-(*N*-*tert*-butoxycarbonyl-amino)heptanedioate (106)[98, 132]

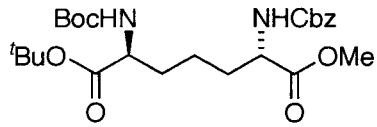

Prepared according to the procedure detailed in section 4.1.9. from diacyl peroxide **95** (Colorless gum, 0.0761 g, 49%, Rf 0.54 in 2/1 hexanes/ethyl acetate); $[\alpha]_D$ = +2.3° (*c* 0.96, DCM); IR (DCM cast) 3349, 2976, 1712, 1513, 1453, 1366, 1251, 1154 cm^{-1}; ^1H NMR ($CDCl_3$, 400 MHz) δ 7.33-7.23 (m, 5H, ArH), 5.44 (d, 1H, *J* = 7.2 Hz, NH), 5.09-5.06 (m, 3H, NH + $PhCH_2$), 4.31-4.27 (m, 1H, NCH), 4.12-4.07 (m, 1H, NCH), 3.70 (s, 3H, OCH_3), 1.84-1.53 (m, 4H, $CH_2CH_2CH_2$), 1.43-1.35 (m, 20H, $CH_2CH_2CH_2$ and 2 x $C(CH_3)_3$); ^{13}C NMR ($CDCl_3$, 125 MHz) δ 172.8, 171.7, 156.0, 155.6, 136.2, 128.5, 128.1, 81.9, 79.7, 67.0, 53.7, 53.3, 52.3, 32.6, 31.8, 28.3, 27.9, 21.1; HRMS (ES) Calcd for $C_{25}H_{38}N_2O_8Na$ 517.2520, found 517.2521.

(2*R*,6*R*)-1-Benzyl 7-*tert*-butyl 2-(*N*-benzylcarbonylamino)-6-(*N*-*tert*-butoxycarbonyl-amino)heptanedioate (107)

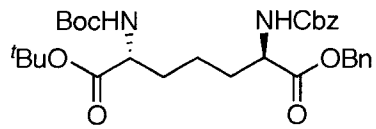

Prepared according to the procedure detailed in section 4.1.9. from diacyl peroxide **100** (Clear colorless gum, 0.0552 g, 30%, Rf 0.61 in 2/1 hexanes/ethyl acetate); $[\alpha]_D$ = -5.4° (*c* 0.98, DCM); IR (DCM cast) 3347, 2974, 1717, 1514, 1455, 1363, 1250, 1154 cm^{-1}; ^1H

Reproduced with permission of the copyright owner. Further reproduction prohibited without permission.

NMR ($CDCl_3$, 500 MHz) δ 7.34-7.27 (m, 10H, ArH), 5.46 (d, 1H, J = 7.0 Hz, NH) 5.15-5.06 (m, 5H, NH and 2 x CH_2Ph), 4.38-4.33 (m, 1H, NCH), 4.12-4.07 (m, 1H, NCH), 1.88-1.80 (m, 1H, $NCHCHHCH_2$), 1.75-1.66 (m, 2H, $NCHCHHCH_2$ and $CHCH_2CH_2CHH$), 1.62-1.54 (m, 1H, $CHCH_2CH_2CHH$), 1.45-1.38 (m, 20H, $CH_2CH_2CH_2$ and 2 x $C(CH_3)_3$); ^{13}C NMR ($CDCl_3$, 125 MHz) δ 172.1, 171.7, 155.9, 155.4, 136.0, 135.2, 128.5, 128.4, 128.3, 128.1, 128.0, 81.7, 79.6, 67.1, 66.7, 53.6, 53.2, 32.4, 31.8, 28.2, 27.8, 21.1; HRMS (ES) Calcd for $C_{31}H_{42}N_2O_8Na$ 593.2833, found 593.2831.

Diisopropyl 2,6-bis(2,2,3,3,3-pentafluoropropanamido)-heptanedioate (111)[114]

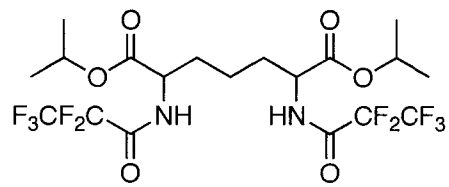

Prepared according to a modified literature procedure by Schieber *et al.*[114] Concentrated HCl (10 drops) was added to commercial DAP containing all isomers (75 mg, 0.39 mmol) and IPA (10 mL) in a sealed tube reaction vessel. The mixture was then heated at 100 °C for 16 h. The resulting mixture was concentrated *in vacuo*. The residue was dissolved in 6:1 DCM:PFPA (7 mL) and the mixture was then heated to 100 °C for 2 h in a sealed tube. The mixture was concentrated *in vacuo* and then purified by flash chromatography, eluting with 100% DCM to give the desired compound as a mixture of all possible isomers as a white solid (93 mg, 42%, R_f 0.35 in DCM); Chiral GC-MS (Alltech Heliflex Chirasil-Val Capillary column (48 m), 70 °C (5 m) → 100 °C (2.5 °C/m) → 190 °C (3.5 °C/m) showed 1:1:2, LL:DD:*meso*; t_R's 46.0, 46.1, 46.2 min

Reproduced with permission of the copyright owner. Further reproduction prohibited without permission.

respectively. IR (DCM cast) 3314, 3085, 2986, 1738, 1702, 1551, 1207 cm^{-1}; ^1H NMR ($CDCl_3$, 400 MHz) δ (all isomers) 7.11-7.07 (m, 2H, NH), 5.09-5.04 (m, 2H, $CHCH_3$), 4.56-4.50 (m, 2H, 2 x CHN), 2.00-1.94 (m, 2H, 2 x CHNCHH), 1.85-1.76 (m, 2H, 2 x CHNCHH), 1.40-1.33 (m, 2H, 2 x $CHNCH_2CHH$), 1.30-1.24 (m, 16H, 4 x $CHCH_3$ and 2 x $CHHCH_2CHH$); ^{13}C NMR ($CDCl_3$, 125 MHz) δ 170.0, 169.9, 157.6 (dt, J = 26.3, 26.3 Hz), 117.8 (qt, J = 286.7, 34.7 Hz), 106.7 (tq, J = 266.1, 39.7 Hz), 70.6, 70.5, 52.6, 52.5, 31.5, 31.3, 21.6, 21.5, 21.4, 20.6, 20.5; HRMS (EI) Calcd for $C_{19}H_{24}N_2O_6F_{10}$ 566.1475, found 566.1471.

3-Cyclohexanecarboxylate-1-spiro-5'-hydantoin (117)[126]

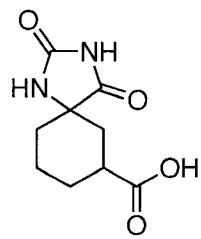

Prepared according to a modified literature procedure by Azerad *et al.*[121, 122, 126] To a solution of 3-oxo-1-cylohexanecarboxylic acid (**118**) (99 mg, 0.7 mmol) in EtOH (3 mL) and water (1 mL) was added $(NH_4)_2CO_3$ (0.32 g, 4.2 mmol) in small portions until the evolution of carbon dioxide gas ceased. To this mixture was then added potassium cyanide (46 mg, 0.7 mmol) along with additional $(NH_4)_2CO_3$. The mixture was then heated at 58 °C for 5 h followed by 1 h at 90 °C. The mixture was then acidified while still hot with conc. HCl to pH 1. The resulting aqueous solution was concentrated *in vacuo* and purified by ion-exchange chromatography (Biorad AG 1-X8 OH^- form resin),

Reproduced with permission of the copyright owner. Further reproduction prohibited without permission.

loading with distilled H_2O, flushing for 3 column lengths with de-ionized water and then eluting with 2 M HCl to give the desired compound after lyophilization as a white solid (59 mg, 40%); IR (microscope) 3500-2500, 3062, 2947, 2866, 1772, 1408, 1380, 1105 cm^{-1}; ^1H NMR (500 MHz, $CDCl_3$) δ 2.41-2.31 (m, 1H, C<u>H</u>CO_2), 1.99-1.38 (m, 8H, 4 x C<u>H_2</u>); ^{13}C NMR (125 MHz, $CDCl_3$) δ (both isomers) 193.8, 185.4, 171.0, 170.9, 158.9, 158.2, 66.1, 63.8, 43.7, 42.5, 37.1, 36.8, 34.2, 33.4, 29.4, 28.9, 22.4, 21.3; HRMS (ES) Calcd for $C_9H_{11}N_2O_4$ 211.0713, found 211.0713.

3-Oxo-1-cylohexanecarboxylic acid (118)[144]

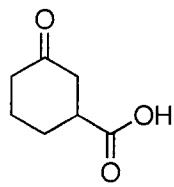

To a solution of 3-oxo-1-cyclohexanecarbonitrile (**120**) (8.98 g, 73 mmol) in diethyl ether (30 mL) was added 6 M HCl (150 mL) and the mixture was then heated at 100 °C for 15 h. The mixture was then cooled to rt and extracted with DCM (5 x 100 mL). The organic fractions were combined, dried (Na_2SO_4) and concentrated *in vacuo*. Purification by flash column chromatography, eluting with 40% ethyl acetate in hexanes gave the desired compound as a colorless oil (3.99 g, 40%, Rf 0.17 in 3/2 ethyl acetate/hexanes); IR (DCM cast) 3500-2500, 2956, 1710, 1421, 1264, 1225, 1179, 931 cm^{-1}; ^1H NMR ($CDCl_3$, 500 MHz) δ 10.6 (br s, 1H, CO_2<u>H</u>), 2.90-2.82 (m, 1H, C<u>H</u>CO_2H), 2.60-2.54 (m, 2H, CH_2COC<u>H_2</u>CH), 2.44-2.30 (m, 2H, C<u>H_2</u>$COCH_2CH$), 2.20-2.13 (m, 1H, CHC<u>H</u>HCH_2), 2.04-2.13 (m, 1H, $CHCH_2C$<u>H</u>H), 1.94-1.83 (m, 1H, $CHCH$<u>H</u>CH_2), 1.83-1.70 (m, 1H,

Reproduced with permission of the copyright owner. Further reproduction prohibited without permission.

$CHCH_2CH\underline{H}$); ^{13}C NMR ($CDCl_3$, 125 MHz) δ 209.2, 179.5, 42.9, 42.7, 40.8, 27.5, 24.3; HRMS (EI) Calcd for $C_7H_{10}O_3$ 142.0630, found 142.0627.

(*R*)-3-Oxo-1-cyclohexanecarboxylic acid ((*R*)-118)[144]

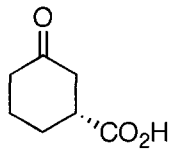

A solution of (*R*)-isopropyl 3-oxo-1-cyclohexanecarboxylate ((***R*)-121**) (0.030 g, 0.16 mmol) in a 1:1 mixture of 1 M LiOH:MeOH (5 mL) was stirred for 48 h. The mixture was then acidified with conc. HCl to pH 2 and extracted repeatedly with DCM. The organic fractions were combined, dried (Na_2SO_4) and concentrated *in vacuo* to give the desired compound as a colorless oil (0.023 g, 100%); $[\alpha]_D$ = -6.3° (*c* 1.70, $CHCl_3$); IR (DCM cast) 3500-2500, 2956, 1710, 1421, 1264, 1225, 1179, 931 cm^{-1}; ^1H NMR ($CDCl_3$, 500 MHz) δ 10.6 (br s, 1H, CO_2H), 2.90-2.82 (m, 1H, $C\underline{H}CO_2H$), 2.60-2.54 (m, 2H, $CH_2COC\underline{H}_2CH$), 2.44-2.30 (m, 2H, $C\underline{H}_2COCH_2CH$), 2.20-2.13 (m, 1H, $CHC\underline{H}HCH_2$), 2.04-2.13 (m, 1H, $CHCH_2C\underline{H}H$), 1.94-1.83 (m, 1H, $CHCH\underline{H}CH_2$), 1.83-1.70 (m, 1H, $CHCH_2CH\underline{H}$); ^{13}C NMR ($CDCl_3$, 125 MHz) δ 209.2, 179.5, 42.9, 42.7, 40.8, 27.5, 24.3; HRMS (EI) Calcd for $C_7H_{10}O_3$ 142.0630, found 142.0627.

Reproduced with permission of the copyright owner. Further reproduction prohibited without permission.

3-Oxo-1-cyclohexanecarbonitrile (120)[125]

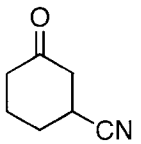

Prepared according to a literature procedure by Sekiyama *et al.*[125] To a solution of 2-cyclohexenone (**119**) (10 mL, 75 mmol) in MeOH (200 mL) was added 1 M HCl (112 mL), NEt_3 (15.7 mL, 112 mmol) and KCN (5.84 g, 90 mmol) and the mixture was then heated at 70 °C for 16 h. To the reaction mixture was then added sat. $NaHCO_3$ (100mL) and the aqueous was extracted with $CHCl_3$ (3 x 200mL). The organic fractions were combined, dried (Na_2SO_4) and concentrated *in vacuo*. Purification by flash column chromatography, eluting with 25% ethyl acetate in hexanes gave the desired compound as a colorless oil (11.12 g, 87%, R_f 0.36 in 3/2 hexanes/ethyl acetate); IR (DCM cast) 3416, 2957, 2873, 2241, 1716, 1451, 1420, 1224, 1102 cm^{-1}; ^1H NMR ($CDCl_3$, 500 MHz) δ 3.12-2.93 (m, 1H, C<u>H</u>CN), 2.64 (dd, J = 14.8, 5.2 Hz, 1H, CHC<u>H</u>HCO), 2.55 (dd, 1H, J = 14.8, 9.1 Hz, CHCH<u>H</u>CO), 2.37 (dd, 2H, J = 6.1, 1.0 Hz, C<u>H</u>$_2$COCH$_2$CH), 2.20-2.05 (m, 2H, CHC<u>H</u>HCH$_2$ and CHCH$_2$C<u>H</u>H), 2.04-1.93 (m, 1H, CHCH<u>H</u>CH$_2$), 1.89-1.75 (m, 1H, CHCH$_2$CH<u>H</u>); ^{13}C NMR ($CDCl_3$, 100 MHz) δ 205.4, 120.2, 43.1, 40.6, 28.5, 27.9, 23.6; HRMS (EI) Calcd for C_7H_9NO 123.0684, found 123.0684.

Reproduced with permission of the copyright owner. Further reproduction prohibited without permission.

Isopropyl 3-oxocyclohexanecarboxylate (121)[126, 145]

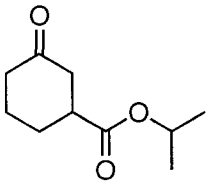

3-Oxo-1-cylohexanecarboxylic acid (**118**) (1.04 g, 7.3 mmol) was dissolved in IPA (80 mL) and added conc. HCl (10 drops). The mixture was then heated at 85 °C for 15 h. The solution was then concentrated *in vacuo* and purified by flash column chromatography, eluting with 20% ethyl acetate in hexanes to give the desired compound as a colorless oil (1.31 g, 98%, Rf 0.35 in 1/4 ethyl acetate/hexanes); IR (microscope) 2981, 2942, 2872, 1726, 1375, 1305, 1180, 1110 cm^{-1}; ^1H NMR ($CDCl_3$, 400 MHz) δ 5.00 (sept, 1H, J = 6.4 Hz, C<u>H</u>$(CH_3)_2$), 2.80-2.70 (m, 2H, C<u>H</u>CO_2), 2.56-2.50 (m, 2H, C<u>H</u>$_2$CO), 2.41-2.26 (m, 2H, C<u>H</u>$_2$$COCH_2CH$), 2.14-2.00 (m, 2H, CHC<u>H</u>HCH_2 and $CHCH_2C$<u>H</u>H), 1.89-1.66 (m, 2H, $CHCH$<u>H</u>CH_2 and $CHCH_2CH$<u>H</u>), 1.23 (d, 6H J = 6.4 Hz, $CH(C$<u>H</u>$_3)_2$); ^{13}C NMR ($CDCl_3$, 125 MHz) δ 209.3, 173.2, 68.2, 43.4, 43.1, 40.9, 27.7, 24.4, 21.7; HRMS (EI) Calcd for $C_{10}H_{16}O_3$ 184.1099, found 184.1099.

(*R*)-Isopropyl 3-oxo-1-cyclohexanecarboxylate ((*R*)-121)[126]

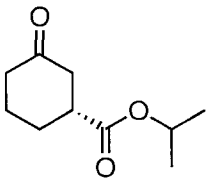

To a solution of (1*R*,3*S*)-isopropyl-3-hydroxycyclohexane-1-carboxylate ((**1*R*,3*S*)-123**) (0.472 g, 2.5 mmol) in DCM (40 mL) was added PDC (2.02 g, 5.4 mmol) and the

Reproduced with permission of the copyright owner. Further reproduction prohibited without permission.

mixture was then stirred at rt for 15 h. The suspension was then filtered through Celite and the Celite was washed with DCM. The filtrates were combined, dried (Na_2SO_4) and concentrated *in vacuo*. Purification by flash column chromatography, eluting with 25% ethyl acetate in hexanes gave the desired compound as a colorless oil (0.35 g, 76%, R_f 0.67 in 2/3 ethyl acetate/hexanes); $[\alpha]_D$ = -4.5° (*c* 1.00, MeOH); IR (microscope) 2981, 2942, 2872, 1726, 1375, 1305, 1180, 1110 cm^{-1}; ^1H NMR ($CDCl_3$, 400 MHz) δ 5.00 (sept, 1H, *J* = 6.4 Hz, C<u>H</u>$(CH_3)_2$), 2.80-2.70 (m, 1H, C<u>H</u>CO_2), 2.56-2.50 (m, 2H, C<u>H</u>$_2$CO), 2.41-2.26 (m, 2H, C<u>H</u>$_2$COCH_2CH), 2.14-2.00 (m, 2H, CHC<u>H</u>HCH_2 and CHCH_2C<u>H</u>H), 1.89-1.66 (m, 2H, CHCH<u>H</u>CH_2 and CHCH_2CH<u>H</u>), 1.23 (d, 6H, *J* = 6.4 Hz, CH(C<u>H</u>$_3$)$_2$); ^{13}C NMR ($CDCl_3$, 125 MHz) δ 209.3, 173.2, 68.2, 43.4, 43.1, 40.9, 27.7, 24.4, 21.7; HRMS (EI) Calcd for $C_{10}H_{16}O_3$ 184.1099, found 184.1099.

(*S*)-Isopropyl 3-oxocyclohexanecarboxylate ((*S*)-121)[126]

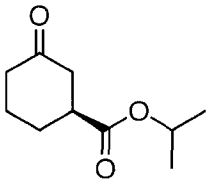

To a solution of (1*S*,3*S*)-isopropyl-3-hydroxycyclohexane-1-carboxylate (**(1*S*,3*S*)-123**) (0.160 g, 0.9 mmol) in DCM (40 mL) was added PDC (0.64 g, 1.7 mmol) and the mixture was then stirred at rt for 15 h. The suspension was then filtered through Celite and the Celite was washed with DCM. The filtrates were combined, dried (Na_2SO_4) and concentrated *in vacuo*. Purification by flash column chromatography, eluting with 25% ethyl acetate in hexanes gave the desired compound as a colorless oil (0.13 g, 82%, R_f

Reproduced with permission of the copyright owner. Further reproduction prohibited without permission.

0.67 in 2/3 ethyl acetate/hexanes); $[\alpha]_D = +10.3°$ (*c* 1.41, MeOH); IR (microscope) 2981, 2942, 2872, 1726, 1375, 1305, 1180, 1110 cm^{-1}; ^1H NMR ($CDCl_3$, 400 MHz) δ 5.00 (sept, 1H, *J* = 6.4 Hz, C<u>H</u>$(CH_3)_2$), 2.80-2.70 (m, 1H, C<u>H</u>CO_2), 2.56-2.50 (m, 2H, C<u>H</u>$_2$CO), 2.41-2.26 (m, 2H, C<u>H</u>$_2$COCH_2CH), 2.14-2.00 (m, 2H, CHC<u>H</u>HCH_2 and CHCH_2C<u>H</u>H), 1.89-1.66 (m, 2H, CHC<u>H</u>HCH_2 and CHCH_2C<u>H</u>H), 1.23 (d, 6H, *J* = 6.4 Hz, CH(C<u>H</u>$_3$)$_2$); ^{13}C NMR ($CDCl_3$, 125 MHz) δ 209.3, 173.2, 68.2, 43.4, 43.1, 40.9, 27.7, 24.4, 21.7; HRMS (EI) Calcd for $C_{10}H_{16}O_3$ 184.1099, found 184.1099.

Isopropyl 3-cyclohexanecarboxylate-1-spiro-5'hydantoin (122)[126]

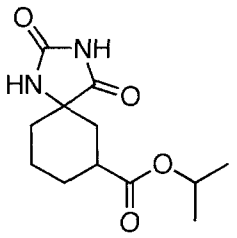

Prepared according to a modified literature procedure by Azerad *et al.*[121, 122, 126] To a solution of isopropyl 3-oxocyclohexanecarboxylate (**121**) (0.65 g, 3.5 mmol) in EtOH (5 mL) and water (5 mL) was then added $(NH_4)_2CO_3$ (0.34 g, 3.5 mmol). To this mixture was then added KCN (0.23 g, 3.5 mmol) along with additional $(NH_4)_2CO_3$ (1.70 g, 17.5 mmol). The mixture was then heated at 58 °C for 15 h followed by 1 h at 90 °C. The mixture was then acidified with conc. HCl to pH 1 and extracted with DCM (4 x 40 mL). The organic fractions were combined, dried (Na_2SO_4) and concentrated *in vacuo* to give the desired compound as a mixture of diastereomers (1:1 *cis:trans* – ^1H NMR) as a white solid (0.64 g, 73%, Rf 0.45 in 3/2 ethyl acetate/hexanes); IR (microscope) 3401, 3165,

Reproduced with permission of the copyright owner. Further reproduction prohibited without permission.

3114, 3062, 2947, 2866, 1772, 1724, 1405, 1382, 1192, 1105 cm^{-1}; ^1H NMR ($CDCl_3$, 600 MHz) δ (*cis* isomer) 8.89 (br s, 1H, NH), 7.60 (br s, 1H, NH), 5.00 (sept, 1H, J = 6.0 Hz, $CH(CH_3)_2$), 2.45-2.41 (m, 1H, CO_2CH, TROESY correlation to δ 7.60), 2.15-2.06 (m, 1H, $CO_2CHHHCCO_2$), 2.00-1.40 (m, 7H, 3 x CH_2 and $CO_2CHHHCCO_2$), 1.24-1.21 (m, 6H, $CH(CH_3)_2$); ^1H NMR ($CDCl_3$, 600 MHz) δ (*trans* isomer) 8.83 (br s, 1H, NH), 6.75 (br s, 1H, NH), 5.00 (sept, 1H, J = 6.0 Hz, $CH(CH_3)_2$), 3.02 (app sept, 1H, J = 3.6 Hz, CO_2CH), 2.16 (dd, 1H, J = 13.8, 4.8 Hz, $CO_2CHCHHHCCO_2$), 2.00-1.50 (m, 7H, 3 x CH_2 and $CO_2CHCHHHCCO_2$), 1.24-1.21 (m, 6H, $CH(CH_3)_2$); ^{13}C NMR ($CDCl_3$, 125 MHz) δ (both diastereomers) 177.4, 177.2, 175.3, 173.7, 157.4, 156.6, 68.2, 68.1, 63.5, 61.5, 61.4, 39.2, 38.1, 35.2, 34.1, 32.5, 27.3, 27.0, 21.7, 21.0, 19.4; HRMS (EI) Calcd for $C_{12}H_{18}N_2O_4$ 254.1267, found 254.1265.

(*R*)-Isopropyl 3-oxo-1-cyclohexanecarboxylate-1-spiro-5'hydantoin ((*3R*)-122)[126]

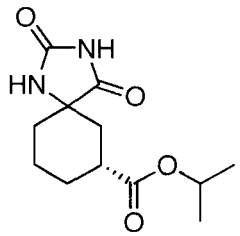

Prepared according to a modified literature procedure by Azerad *et al.*[121, 122, 126] To a solution of (*R*)-isopropyl 3-oxo-1-cyclohexanecarboxylate ((***R*)-121**) (0.12 g, 0.66 mmol) in a 1:1 mixture of EtOH:water (2 mL) was added $(NH_4)_2CO_3$ (63 mg, 0.66 mmol). To this mixture was then added KCN (43 mg, 0.66 mmol) along with additional $(NH_4)_2CO_3$ (315 mg, 5 eq). The mixture was then heated at 58 °C for 15 h followed by 1 h at 90 °C.

Reproduced with permission of the copyright owner. Further reproduction prohibited without permission.

The mixture was then acidified with conc. HCl to pH 1 and extracted with DCM (4 x 40 mL). The organic fractions were combined, dried (Na_2SO_4) and concentrated *in vacuo* to give the title compound as a inseparable mixture of diastereomers (1:1 *cis:trans* – ^1H NMR) as a white solid (0.138 g, 82%, R_f 0.45 in 3/2 ethyl acetate/hexanes); IR (microscope) 3401, 3165, 3114, 3062, 2947, 2866, 1772, 1724, 1405, 1382, 1192, 1105 cm^{-1}; ^1H NMR ($CDCl_3$, 600 MHz) δ (*cis* isomer) 8.89 (br s, 1H, NH), 7.60 (br s, 1H, NH), 5.00 (sept, 1H, J = 6.0 Hz, CH(CH_3)$_2$), 2.45-2.41 (m, 1H, CO_2CH, TROESY correlation to δ 7.60), 2.15-2.06 (m, 1H, $CO_2CHHCCO_2$), 2.00-1.40 (m, 7H, 3 x CH_2 and $CO_2CHHCCO_2$), 1.24-1.21 (m, 6H, CH(CH_3)$_2$); ^1H NMR ($CDCl_3$, 600 MHz) δ (*trans* isomer) 8.83 (br s, 1H, NH), 6.75 (br s, 1H, NH), 5.00 (sept, 1H, J = 6.0 Hz, CH(CH_3)$_2$), 3.02 (app sept, 1H, J = 3.6 Hz, CO_2CH), 2.16 (dd, 1H, J = 13.8, 4.8 Hz, $CO_2CHCHHCCO_2$), 2.00-1.50 (m, 7H, 3 x CH_2 and $CO_2CHCHHCCO_2$), 1.24-1.21 (m, 6H, CH(CH_3)$_2$); ^{13}C NMR ($CDCl_3$, 125 MHz) δ (both diastereomers) 177.4, 177.2, 175.3, 173.7, 157.4, 156.6, 68.2, 68.1, 63.5, 61.5, 61.4, 39.2, 38.1, 35.2, 34.1, 32.5, 27.3, 27.0, 21.7, 21.0, 19.4; HRMS (EI) Calcd for $C_{12}H_{18}O_4N_2$ 254.1267, found 254.1265.

(1*S*,3*S*)- and (1*R*,3*S*)-Isopropyl-3-hydroxycyclohexane-1-carboxylate (123)[126, 145]

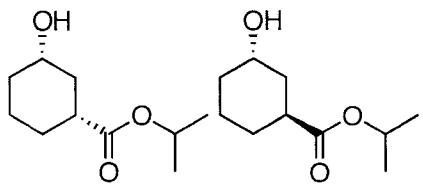

Prepared according to a modified literature procedure by Azerad *et al.*[126, 127] *Rhizopus arrhizus* ATCC 11145 was grown for 48 h in 1 L of a standard medium (24 g potato

Reproduced with permission of the copyright owner. Further reproduction prohibited without permission.

dextrose broth in 1 L water). The fungus was filtered through microcloth and re-suspended in water (0.5 L). Isopropyl 3-oxocyclohexanecarboxylate (**121**) (3.74 g, 20.3 mmol) in IPA (10 mL) was then added to the re-suspended *R. arrhizus* in water (0.5 L) and incubated at 27 °C with gentle shaking for 4 d. Complete reduction was not observed. The suspension was then filtered and the filtrate was saturated with sodium chloride, then filtered through Celite and extracted with DCM (3 x 200 mL). The organic fractions were combined, dried (Na_2SO_4) and concentrated *in vacuo*. The diastereomeric products were purified by flash column chromatography, eluting with 25% ethyl acetate in hexanes gave starting material **121** (3.08 g, 82%, R_f 0.67 in 2/3 ethyl acetate/hexanes), (1S,3S)-**123** (0.20 g, 5%, R_f 0.46 in 2/3 ethyl acetate/hexanes) and (1R,3S)-**123** (0.57 g, 15%, R_f 0.40 in 2/3 ethyl acetate/hexanes);

(1*S*,3*S*)-**123**: $[\alpha]_D$ = +12.0° (*c* 1.67, MeOH); IR (microscope) 3428, 2980, 2937, 2864, 1726, 1452, 1375, 1177, 1100 cm^{-1}; ^1H NMR ($CDCl_3$, 500 MHz) δ 4.97 (sept, 1H, *J* = 6.2 Hz, C<u>H</u>$(CH_3)_2$), 4.06 (app pent, 1H, *J* = 4.3 Hz, C<u>H</u>OH), 2.75-2.68 (m, 1H, C<u>H</u>CO_2), 1.85-1.75 (m, 3H, CHC<u>H</u>$_2$CHOH and CH_2C<u>H</u>HCHOH), 1.75-1.65 (m, 1H, CH_2C<u>H</u>HCHCO_2), 1.61-1.48 (m, 4H, CH_2CH<u>H</u>CHCO_2 and CH_2CH<u>H</u>CHOH and CH_2C<u>H</u>$_2$CH_2), 1.21 (d, 6H, *J* = 6.2 Hz, CH(C<u>H</u>$_3$)$_2$); ^{13}C NMR ($CDCl_3$, 125 MHz) δ 175.3, 67.3, 66.2, 38.1, 35.5, 32.9, 28.1, 21.8, 19.8; HRMS (EI) Calcd for $C_{10}H_{18}O_3$ 186.1256, found 186.1259.

Reproduced with permission of the copyright owner. Further reproduction prohibited without permission.

(1*R*,3*S*)-**123**: $[\alpha]_D$ = -4.0° (*c* 1.41, MeOH); IR (microscope) 3402, 2980, 2862, 1729, 1452, 1375, 1259, 1179, 1110 cm^{-1}; ^1H NMR ($CDCl_3$, 500 MHz) δ 4.96 (sept, 1H *J* = 6.2 Hz, C<u>H</u>$(CH_3)_2$), 3.58 (app pent, 1H, *J* = 4.2 Hz, C<u>H</u>OH), 2.34-2.26 (m, 1H, C<u>H</u>CO_2), 2.20-2.13 (m, 1H, CHC<u>H</u>HCHOH), 2.00-1.90 (m, 2H, CH_2C<u>H</u>HCHOH and CH_2C<u>H</u>HCH_2), 1.88-1.78 (m, 2H, CHC<u>H</u>HCH_2 and CH_2CH<u>H</u>CH_2), 1.44-1.34 (m, 1H, CHCH<u>H</u>CHOH), 1.33-1.26 (m, 2H, CH_2CH<u>H</u>CH and CH_2CH<u>H</u>CHOH), 1.20 (d, 6H, *J* = 6.2 Hz, CH(C<u>H</u>$_3)_2$); ^{13}C NMR ($CDCl_3$, 125 MHz) δ 174.7, 69.7, 67.5, 42.0, 37.6, 34.9, 27.9, 23.1, 21.7; HRMS (EI) Calcd for $C_{10}H_{18}O_3$ 186.1256, found 186.1258.

(2*S*)-Methyl 3-(1*H*-indol-3-yl)-2-(3-oxocyclohexanecarboxamido)propanoate (124)

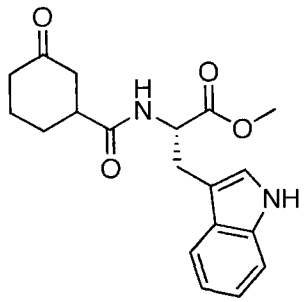

To a solution of 3-oxo-1-cyclohexanecarboxylic acid (**118**) (94.3 mg, 0.66 mmol) in DCM (5 mL) was added PyBOP (0.327 g, 0.63 mmol) and NMM (0.36 mL, 33 mmol). The solution was then stirred at rt for 10 min. L-Tryptophan methyl ester HCl salt (**125**) (0.201 g, 0.79 mmol) was then added and the mixture was stirred at rt for 2 h. The mixture was then concentrated *in vacuo* and purified by flash column chromatography, eluting with 25% hexanes in ethyl acetate to give the desired compound as a mixture diastereomers (1:1 *RS*:*SS* - ^1H NMR) as a colorless oil (0.186 g, 82%, Rf 0.26 in 3/2 ethyl

Reproduced with permission of the copyright owner. Further reproduction prohibited without permission.

acetate/hexanes); Optical purity 0% *ee* determined by chiral HPLC. LiChroCART ChiraDex, 90:10 MeOH:H_2O, 0.9mL/min, 280 nm detection, t_R = 21.7 min (*SS*-diastereomer), t_R = 27.7 min (*RS*-diastereomer); IR (microscope) 3408, 2951, 2866, 2475, 1736, 1709, 1648, 1454, 1334, 1225, 1009 cm^{-1}; ^1H NMR (CD_3OD, 500 MHz) δ (both diastereomers) 7.50 (d, 1H, *J* = 9.0 Hz, Ar 4-H), 7.32 (d, 1H, *J* = 9.0 Hz, Ar 7-H), 7.10-7.04 (m, 2H, Ar 1-H and Ar 6-H), 7.00 (t, 1H, *J* = 7.5 Hz, Ar 5-H), 4.77-4.68 (m, 1H, NC<u>H</u>), 3.66 (m, 3H, OC<u>H</u>$_3$), 3.34 (br s, 1H, N<u>H</u>), 3.33-3.26 (m, 1H, NCHC<u>H</u>H), 3.18-3.08 (m, 1H, NCHCH<u>H</u>), 2.73-2.64 (m, 1H, C<u>H</u>CON), 2.50-2.36 (m, 1H, CHC<u>H</u>HCO), 2.33-2.14 (m, 2H, CHCH<u>H</u>CO and C<u>H</u>HCOCH$_2$CH), 2.05-1.48 (m, 5H, 2 x CH_2 and CH<u>H</u>COCH$_2$CH); ^{13}C NMR (125 MHz, $CDCl_3$) δ (both diastereomers) 212.8, 176.2, 176.1, 174.0, 173.9, 138.0, 128.8, 128.7, 124.5, 124.4, 122.5, 122.4, 119.9, 119.8, 119.2, 119.1, 112.4, 112.3, 110.9, 110.8, 110.7, 54.8, 54.7, 52.7, 45.4, 45.3, 44.1, 44.0, 41.6, 41.5, 29.2, 28.6, 28.5, 25.4, 25.2; HRMS (ES) Calcd for $C_{19}H_{22}O_4N_2Na$ 365.1472, found 365.1471.

Reproduced with permission of the copyright owner. Further reproduction prohibited without permission.

(*S*)-Methyl-3-(1*H*-indol-3-yl)-2-((*R*)-3-oxocyclohexanecarboxamido)propanoate ((*RS*)-124)

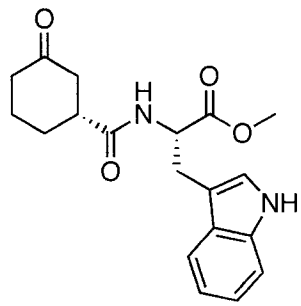

To a solution of (*R*)-3-oxocyclohexanecarboxylic acid ((***R*)-118**) (21 mg, 0.15 mmol) in DCM (5 mL) was added PyBOP (73 mg, 0.14 mmol) and NMM (82 μL, 0.75 mmol) and was then stirred at rt for 10 min. L-Tryptophan methyl ester HCl salt (46 mg, 0.18 mmol) was then added and the mixture was stirred at rt for 2 h. The mixture was then concentrated *in vacuo* and purified by flash column chromatography, eluting with 25% hexanes in ethyl acetate to give the desired compound as a mixture of diastereomers (9:1 *RS:SS* - HPLC) as a colorless oil (40 mg, 65%, R_f 0.26 in 3/2 ethyl acetate/hexanes); Optical purity 70% *ee* determined by chiral HPLC. LiChroCART ChiraDex, 90:10 MeOH:H_2O, 0.9mL/min, 280 nm detection, t_R = 21.7 min (*SS*-diastereomer), t_R = 27.7 min (*RS*-diastereomer); IR (microscope) 3408, 2951, 2866, 2475, 1736, 1709, 1648, 1454, 1334, 1225, 1009 cm^{-1}; ^1H NMR (CD_3OD, 500 MHz) δ (major diastereomer) 7.50 (d, 1H, *J* = 6.0 Hz, Ar 4-H), 7.31 (d, 1H, *J* = 6.0 Hz, Ar 7-H), 7.08 (t, 1H, *J* = 6.0 Hz, Ar 6-H), 7.05 (s, 1H, Ar 1-H), 7.00 (t, 1H, *J* = 6.0 Hz, Ar 5-H), 4.72-4.68 (m, 1H, NC<u>H</u>), 3.67 (m, 3H, C<u>H</u>$_3$), 3.33 (br s, 1H, N<u>H</u>), 3.33-3.26 (m, 1H, NCHC<u>H</u>H), 3.18-3.08 (m, 1H, NCHCH<u>H</u>), 2.73-2.64 (m, 1H, C<u>H</u>CON), 2.50-2.36 (m, 1H, CHC<u>H</u>HCO), 2.33-2.14 (m,

Reproduced with permission of the copyright owner. Further reproduction prohibited without permission.

2H, CHCH<u>H</u>CO and C<u>H</u>HCOCH$_2$CH), 2.05-1.48 (m, 5H, 2 x CH$_2$ and CH<u>H</u>COCH$_2$CH); ^{13}C NMR ($CDCl_3$, 125 MHz) δ (both diastereomers) 212.8, 176.2, 176.1, 174.0, 173.9, 138.0, 128.8, 128.7, 124.5, 124.4, 122.5, 122.4, 119.9, 119.8, 119.2, 119.1, 112.4, 112.3, 110.9, 110.8, 110.7, 54.8, 54.7, 52.7, 45.4, 45.3, 44.1, 44.0, 41.6, 41.5, 29.2, 28.6, 28.5, 25.4, 25.2; HRMS (ES positive) Calcd for $C_{19}H_{22}O_4N_2Na$ 365.1472, found 365.1471.

4.3. Enzyme Assays

4.3.1. Coupled Enzyme Assay for Plant DAP Epimerase Activity[36]

DAP epimerase activity was monitored using a coupled assay with DAP dehydrogenase which detects the production of NADPH at 340 nm. The assay was performed in a 1 mL plastic cuvette filled with buffer solution (0.1 M Tris-HCl, 1 mM EDTA, 1 mM DTT, pH 7.8), 0.4 mM LL-DAP, 0.3 mM $NADP^+$ and 0.06 units of DAP dehydrogenase. For inhibition studies, the assay buffer contained varying concentrations of the inhibitor, 0.4 mM LL-DAP, 0.3 mM $NADP^+$, 50 mU of DAP dehydrogenase and 32 μg of DAP epimerase. These results were compared against a control performed simultaneously, where the Tris-HCl buffer replaced the inhibitor. The plant DAP epimerase used was isolated by Dr. Sandra Marcus from *Escherichia coli* M15[pREP4].[108] The *E. coli* strain was transformed by Dr. Marco van Belkum with pQE60 plasmid[32] containing plant DAP epimerase DNA donated by Professor Thomas Leustek (Rutgers University) from *Arabidopsis thaliana*. The first 51 amino acids of the epimerase precursor were removed

Reproduced with permission of the copyright owner. Further reproduction prohibited without permission.

by amplifying the mature part of the epimerase with PCR and the PCR product was cloned into pQE60. *meso*-DAP dehydrogenase was purified by previous members of the Vederas group from *Bacillus spaericus* IFO 3525 as previously reported.[107]

4.3.2. Test of Analogs as Substrates for Plant DAP Epimerase

Compounds were tested as substrates for the epimerase by incubating 20 μL (1.6 mg/mL solution) of active epimerase in the presence of the substrate (4.0 mM, 0.04 mmol) in deuterated buffer (0.1 M Tris, 1 mM DTT, 1 mM EDTA, pD 7.8, total volume 10.00 mL) at rt for 3 d. The incubations were quenched by freezing in a dry ice / IPA bath. The mixtures were then thawed and loaded onto ion exchange columns (5 mL, Biorad AG 50W-X8 hydrogen form resin, 100-200 mesh). The column was washed with water (2 x 5 mL), 1 M HCl (1 x 5 mL) and eluted with 4 M HCl (10 mL). The 4 M HCl eluents were combined and lyophilized to dryness. The sample was then dissolved in D_2O and the proton NMR spectrum was acquired.

4.3.3. DAP Epimerase Activity in Crude Plant Extracts

Leaves from *Arabidopsis thaliana* donated by Prof. Mike Deyholos, were frozen with liquid nitrogen and crushed with a pestle and mortar. The crushed material (5 g) was added 0.1 M Tris buffer (20 mL) and was followed by centrifugation. The supernatant

Reproduced with permission of the copyright owner. Further reproduction prohibited without permission.

liquid was then concentrated using a Millipore 10,000 MWCO filter. The crude extracts were then used in the DAP epimerase assay as previously described in section 4.3.1.

4.3.4. LL-DAP Aminotransferase Activity[35]

The LL-DAP aminotransferase (LL-DAP-AT) activity was monitored using an assay to measure the production of L-THDP using *o*-aminobenzaldehyde (OAB), a compound that yields a dihydrodoquinazolinium adduct that has an absorbance maximum at 440 nm.[115] The assay was preformed in a 1 mL cuvette filled with buffer solution (0.1 M HEPESKOH, pH 7.6), 0.5 mM LL-DAP, 2 mM 2-oxyglutarate (2-OG), 1.25 mg OAB, and 0.3 μg LL-DAP-AT. Reactions were incubated at rt and monitored continuously at 440 nm. For inhibition studies, the assay buffer contained varying concentrations of the inhibitor, 0.5 mM LL-DAP, 2 mM 2-OG, 1.25 mg OAB, and 0.3 μg LL-DAP-AT. These results were compared against a control performed simultaneously, where the HEPESKOH buffer replaced the inhibitor. The LL-DAP aminotransferase used was isolated by Dr. Sandra Marcus from *Escherichia coli* mutant M15[pREP4]. The mutant was transformed by Dr. Marco van Belkum with pQE60 plasmid containing LL-DAP-AT donated by Dr. Mike Deyholos.[35]

Reproduced with permission of the copyright owner. Further reproduction prohibited without permission.

4.3.5. Preparation of PLP-bound and PLP-free LL-DAP-AT[117, 118]

PLP–free enzyme was prepared by incubating 20 μL (1.6 mg/mL solution) of active aminotransferase with 10 mM of either hydroxylamine or semicarbazide for 1 h at 4 °C, followed by concentration using a Millipore 10,000 MWCO filter. The PLP-bound enzyme was prepared by incubating 20 μL (1.6 mg/mL solution) of active aminotransferase with 5 mM of sodium borohydride for 30 min at 4 °C, followed by concentration using a Millipore 10,000 MWCO filter. The PLP-free and PLP-bound enzymes were then used in the LL-DAP aminotransferase assay as previously described in section 4.3.4.

Reproduced with permission of the copyright owner. Further reproduction prohibited without permission.

References

1. Greenstein, J. P.; Winitz, S. *Chemistry of Amino Acids*. Krieger Publishing Co.: Malabar, **1984**; *Vol. 3*, p 2511-2522.
2. Schleifer, K. H.; Kandler, O. Peptidoglycan types of bacterial cell walls and their taxonomic implications. *Bacteriol. Rev.* **1972**, *36*, 407-477.
3. Gale, E. F.; Cundliffe, E.; Reynolds, P. E.; Richmond, M. H.; Waring, M. J. *The Molecular Basis of Antibiotic Action*. 2nd ed.; Wiley-Interscience: New York, **1981**.
4. Dezelee, P.; Bricas, E. Structure of peptidoglycan in *Escherichia coli* B and *Bacillus megaterium* KM. Stereospecific synthesis of two *meso*-diaminopimelic acid peptides with the tetrapeptide subunit of bacterial cell wall peptidoglycan. *Biochemistry* **1970**, *9*, 823-831.
5. Hoare, D. S.; Work, E. Stereoisomers of α,ε-diaminopimelic acid: Their distribution in the bacterial order actinomycetales and in certain eubacteriales. *Biochem. J.* **1957**, *65*, 441-447.
6. Ghuysen, J. M. Use of bacteriolytic enzymes in determination of wall structure and their role in cell metabolism. *Bact. Rev.* **1968**, *32*, 425-464.
7. Strominger, J. L.; Blumberg, P. M.; Suginaka, H.; Umbreit, J.; Wickus, G. G. How penicillin kills bacteria: Progress and problems. *Proc. Roy. Soc. London, Ser. B* **1971**, *179*, 369-383.

Reproduced with permission of the copyright owner. Further reproduction prohibited without permission.

8. Van Heijenoort, J. Formation of the glycan chains in the synthesis of bacterial peptidoglycan. *Glycobiology* **2001**, *11*, 25R-36R.

9. van Heijenoort, J.; Bricas, E. A study of α,α'-diaminopimelic acid isomers. *Bull. Chim. Soc. Fr.* **1968**, 2828-2831.

10. Walsh, C. *In Antibiotics, actions, origins, resistance*. American Society for Microbiology Press: Washington, D.C., **2003**.

11. Bright, S. W. J.; Shewry, P. R. Improvement of protein-quality in cereals. *CRC Crit. Rev. Plant Sci.* **1983**, *1*, 49-93.

12. Gilvarg, C. Biosynthesis of diaminopimelic acid. *Fed. Proc.* **1960**, *19*, 948-952.

13. Shedlarski, J. G.; Gilvarg, C. J. Pyruvate-aspartate semialdehyde condensing enzyme of *Escherichia coli*. *J. Biol. Chem* **1970**, *245*, 1362-1373.

14. Schrumpf, B.; Schwarzer, A.; Kalinowski, J.; Puhler, A.; Eggeling, L.; Sahm, H. A functionally split pathway for lysine synthesis in *Corynebacterium glutamicum*. *J. Bacteriol.* **1991**, *173*, 4510-4516.

15. Bartlett, A. T. M.; White, P. J. Species of bacillus that make a vegetative peptidoglycan containing lysine lack diaminopimelate epimerase but have diaminopimelate dehydrogenase. *J. Gen. Microbiol.* **1985**, *131*, 2145-2152.

16. Peterkofsky, B. *N*-Succinyl-L-diaminopimelic glutamic transaminase. *Meth. Enzym.* **1962**, *5*, 853-858.

17. Pillai, B.; Cherney, M. M.; Diaper, C. M.; Sutherland, A.; Blanchard, J. S.; Vederas, J. C. Structural insights into stereochemical inversion by

Reproduced with permission of the copyright owner. Further reproduction prohibited without permission.

diaminopimelate epimerase: An antibacterial drug target. *Proc. Natl. Acad. Sci.* **2006**, *103*, 8668-8673.

18. Work, E. Diaminopimelic decarboxylase. *Method. Enzymol.* **1962**, *5*, 864-870.

19. Ishino, S.; Yamaguchi, K.; Shirahata, K.; Araki, K. Involvement of *meso*-diaminopimelate dehydrogenase in lysine biosynthesis in *Corynebacterium glutamicum*. *Agric. Biol. Chem.* **1984**, *48*, 2557-2560.

20. Sonntag, K.; Eggeling, L.; De Graff, A. A.; Sahm, H. Flux partitioning in the split pathway of lysine synthesis in *Corynebacterium glutamicum* quantification by C-13 NMR and H-1 NMR spectroscopy. *Eur. J. Biochem.* **1993**, *213*, 1325-1331.

21. Zabriskie, T. M.; Jackson, M. D. Lysine biosynthesis and metabolism in fungi. *Nat. Prod. Rep.* **2000**, *17*, 85-97.

22. Banuelos, O.; Casqueiro, J.; Fierro, F.; Hijarrubia, M. J.; Gutierrez, S.; Martin, J. F. Characterization and lysine control of expression of the *lys*1 gene of *Penicillium chrysogenum* homocitrate synthase. *Gene* **1999**, *226*, 51-59.

23. Culotta, V. C.; Klomp, L. W.; Strain, J.; Casareno, R. L.; Krems, B.; Gitlin, J. D. The copper chaperone for superoxide dismutase. *J. Biol. Chem.* **1997**, *272*, 23469-23472.

24. Strassman, M.; Ceci, L. N. Enzymatic formation of α-ketoadipic acid from homoisocitric acid. *J. Biol. Chem.* **1965**, *240*, 4357-4361.

25. Matsuda, M.; Ogur, M. Enzymatic and physiological properties of yeast glutamate-α-ketoadipate transaminase. *J. Biol. Chem* **1969**, *244*, 5153-5158.

Reproduced with permission of the copyright owner. Further reproduction prohibited without permission.

26. Ehmann, D. E.; Gehring, A. M.; Walsh, C. T. Lysine biosynthesis in *Saccharomyces cerevisiae*: Mechanism of α-aminoadipate reductase (*Lys*2) involves posttranslational phosphpantetheinylation by *Lys*5. *Biochemistry* **1999**, *38*, 6171-6177.

27. Ramos, F.; Dubois, E.; Pierard, A. Control of enzyme-synthesis in the lysine biosynthetic pathway of *Saccharomyces cerevisiae*: Evidence for a regulatory role of gene *Lys*14. *Eur. J. Biochem.* **1988**, *171*, 171-176.

28. Ogawa, H.; Fujioka, M. The reaction of pyridoxal 5'-phosphate with an essential lysine residue of saccharopine dehydrogenase. *J. Biol. Chem.* **1980**, *255*, 7420-7425.

29. Vogel, H. J. On biochemical evolution: Lysine formation in higher plants. *Proc. Natl. Acad. Sci. USA* **1959**, *45*, 1717-1721.

30. Mazelis, M.; Whatley, F. R.; Whatley, J. Enzymology of lysine biosynthesis in higher plants: Occurrence, characterization, and some regulatory properties of dehydrodipicolinate synthase. *FEBS Lett.* **1977**, *84*, 236-240.

31. Galili, G. New insights into the regulation and functional significance of lysine metabolism in plants. *Annu. Rev. Plant. Biol.* **2002**, *53*, 27-43.

32. Hudsona, A.; Blessa, C.; Macedoa, P.; Chatterjeeb, S.; Singhc, B. K.; C., G.; Leustek, T. Biosynthesis of lysine in plants: Evidence for a variant of the known bacterial pathways. *Biochimica et Biophysica Acta* **2005**, *1721*, 27-36.

Reproduced with permission of the copyright owner. Further reproduction prohibited without permission.

33. Chatterjee, S. P.; Singh, B. K.; Gilvarg, C. Biosynthesis of lysine in plants: The putative role of *meso*-diaminopimelate dehydrogenase. *Plant Mol. Biol.* **1994**, *26*, 285-290.

34. Tyagi, V. V. S.; Henke, R. R.; Farkas, W. R. Partial purification and characterization of dihydrodipicolonic acid reductase from maize. *Plant Physiol.* **1983**, *73*, 687-691.

35. Hudson, A. O.; Singh, B. K.; Leustek, T.; Gilvarg, C. An LL-diaminopimelate aminotransferase defines a novel variant of the lysine biosynthesis pathway in plants. *Plant Physiol.* **2006**, *140*, 292-301.

36. Wiseman, J. S.; Nichols, J. S. Purification and proerties of diaminopimelic acid epimerase from *Escherichia coli*. *J. Biol. Chem.* **1984**, *259*, 8907-8914.

37. Cox, R. J.; Sutherland, A.; Vederas, J. C. Bacterial diaminopimelate metabolism as a target for antiobiotic design. *Bioorg. Med. Chem.* **2000**, *8*, 843-871.

38. Albery, W. J.; Knowles, J. R. Energetics and mechanism of proline racemase. *Biochemistry* **1986**, *25*, 2572-2577.

39. Glavas, S.; Tanner, M. E. Active site residues of glutamate racemase. *Biochemistry* **2001**, *40*, 6199-6204.

40. Mobitz, H.; Bruice, T. C. Multiple substrate binding states and chiral recognition in cofactor-independant glutamate racemase: A molecular dynamics study. *Biochemistry* **2004**, *43*, 9685-9694.

41. Liu, L.; Iwata, K.; Kita, A.; Kawarabayasi, Y.; Yohda, M.; Miki, K. Crystal structure of aspartate racemase from *Pyrococcus horikoshii* OT3 and its

Reproduced with permission of the copyright owner. Further reproduction prohibited without permission.

implications for molecular mechanism of PLP-independant racemization. *J. Mol. Biol.* **2002**, *319*, 479-489.

42. Koo, C. W.; Blanchard, J. S. Chemical mechanism of *Haemophilus influenzae* diaminopimelate epimerase. *Biochemistry* **1999**, *38*, 4416-4422.

43. Gelb, M. H.; Lin, Y.; Pickard, M. A.; Song, Y.; Vederas, J. C. Synthesis of 3-fluorodiaminopimelic acid isomers as inhibitors of diaminopimelate epimerase: Stereocontrolled enzymatic elimination of hydrogen fluoride. *J. Am. Chem. Soc.* **1990**, *112*, 4932-4942.

44. Koo, C. W.; Sutherland, A.; Vederas, J. C.; Blanchard, J. S. Identification of active site cysteine residues that function as general bases: Diaminopimelate epimerase. *J. Am. Chem. Soc.* **2000**, *122*, 6122-6123.

45. Cirilli, M.; Zheng, R.; Scapin, G.; Blanchard, J. S. Structural symmetry: The three dimensional structure of *Haemophilus influenzae* diaminopimelate epimerase. *Biochemistry* **1998**, *37*, 16452-16458.

46. Lloyd, A. J.; Huyton, T.; Turkenburg, J.; Roper, D. I. Refinement of *Haemophilus influenzae* diaminopimelic acid epimerase (*DapF*) at 1.75 angstrom resolution suggests a mechanism for stereocontrol during catalysis. *Acta Crystallogr. Sect. D* **2004**, *60*, 397-400.

47. Diaper, C. M.; Sutherland, A.; Pillai, B.; James, M. N. G.; Semchuk, P.; Vederas, J. C. The stereoselective synthesis of aziridine analogues of diaminopimelic acid (DAP) and their interaction with DAP epimerase. *Org. Biomol. Chem.* **2005**, *3*, 4402-4411.

Reproduced with permission of the copyright owner. Further reproduction prohibited without permission.

48. Gerhart, F.; Higgins, W.; Tardif, C.; Ducep, J. 2-(4-Amino-4-carboxybutyl)aziridine-2-carboxylic acid: A potent irreversible inhibitor of diaminopimelic acid epimerase. *J. Med. Chem.* **1990**, *33*, 2157-2162.

49. Eliot, A. C.; Kirsch, J. F. Pyridoxal phosphate enzymes: Mechanistic, structural, and evolutionary considerations. *Annu. Rev. Biochem.* **2004**, *73*, 383-415.

50. Kochhar, S.; Christen, P. Mechanism of racemization of amino acids by aspartate aminotransferase. *Eur. J. Bio. Chem.* **1992**, *203*, 563-569.

51. Rios, A.; Amyes, T. L.; Richard, J. P. Formation and stability of organic zwitterions in aqueous solution: Enolates of the amino acid glycine and its derivatives. *J. Am. Chem. Soc.* **2000**, *122*, 9373-9385.

52. Chatelus, G. La decarboxylation thermique des acides α-amines. *Bull. Soc. Chim. Fr.* **1964**, *10*, 2523-2533.

53. Hashimoto, M.; Eda, Y.; Osanai, Y.; Iwai, T.; Aoki, S. Amino acid decarboxylation catalyzed by 2-cyclohexen-1-one. *Chem. Lett.* **1986**, *6*, 893-896.

54. Wallbaum, S.; Mehler, T.; Martens, J. Decarboxylation of α-amino acids containing 2 and 3 stereogenic centers: A simple one-step procedure to prepare 2 optically active β-amino alcohols and bicyclic pyrrolidine derivative. *Synth. Commun.* **1994**, *24*, 1381-1387.

55. Nakai, H.; Sato, Y.; Mizoguchi, T.; Kanaoka, Y. Preparation of *N*-benzoylamines by photodecarboxylation of *N*-benzoyl-α-amino acids. *Synthesis* **1982**, 141-143.

Reproduced with permission of the copyright owner. Further reproduction prohibited without permission.

56. Kametani, T.; Takano, S.; Takeshita, M.; Hibino, S. Studies on the synthesis of heterocyclic compounds: Simple preparation of tryptamine. *Synthesis* **1972**, 475-479.

57. Rossen, K.; Simpson, P. M.; Wells, K. A practical synthesis of both enantiomers of 1-amino-2-propanol and propylene oxide. *Synth. Commun.* **1993**, *23*, 1071-1074.

58. Bommarius, A. S.; Schwarm, M.; Drauz, K. Biocatalysis to amino acid-based chiral pharmaceuticals: Examples and perspectives. *J. Mol. Cat. B* **1998**, *5*, 1-11.

59. Cho, B. K.; Cho, H. J.; Park, S. H.; Yun, H.; Kim, B. G. Simultaneous synthesis of enantiomerically pure (*S*)-amino acids and (*R*)-amines using coupled transaminase reactions. *Biotechnol. Bioeng.* **2003**, *81*, 783-789.

60. Breuer, M.; Ditrich, K.; Habicher, T.; Hauer, B.; KeBeler, M.; Sturmer, R.; Zelinski, T. Enantiomerically pure intermediates. *Angew. Chem. Int. Ed.* **2004**, *43*, 788-824.

61. Griesbeck, A. G.; Kramer, W.; Oelgemoller, M. Synthetic applications of photoinduced electron transfer decarboxylation reactions. *Synlett* **1999**, 1169-1178.

62. Okada, K.; Okubo, K.; Oda, M. A simple and covenient photodecarboxylation method of intact carboxylic acids in the presence of aza aromatic compounds. *J. Photochem. Photobiol. A: Chem.* **1991**, *57*, 265-277.

Reproduced with permission of the copyright owner. Further reproduction prohibited without permission.

63. Koshima, H.; Matsuura, T. Solid state photoreactions occurring at the interface between crystallites of two different organic compounds. *J. Photochem. Photobiol. A: Chem.* **1996**, *100*, 85-91.

64. Koshima, H.; Wang, Y.; Matsuura, T.; Miyahara, I.; Mizutani, H.; Hirotsu, K.; Ashi, T.; Masuhara, T. Photoreactivities to two kinds of bimolecular crystals formed from acridine and phenothiazine. *J. Chem. Soc., Perkin Trans. 2* **1997**, 2033-2038.

65. Koshima, H.; Ding, K.; Chisaka, Y.; Matsuura, T.; Miyahara, I.; Hirotsu, K. Stoichiometrically sensitized decarboxylation occurring in the two-component molecular crystals of aza aromatic compounds and alkyl carboxylic acids. *J. Am. Chem. Soc.* **1997**, *119*, 10317-10324.

66. Koshima, H.; Matsushige, D.; Miyauchi, M.; Fujita, J. Solid-state photoreaction in two-component molecular crystals of thienylacetic acids and aza aromatic compounds. *Tetrahedron* **2000**, *56*, 6945-6952.

67. Stuk, T. L.; Haight, A. R.; Scarpetti, D.; Allen, M. S.; Menzia, J. A.; Robbins, T. A.; Parekh, S. I.; Langridge, D. C.; Tien, J. J.; Pariza, R. J.; Kerdesky, F. A. J. An efficient stereocontrolled strategy for the synthesis of hydroxyethylene dipeptide isoteres. *J. Org. Chem.* **1994**, *59*, 4040-4041.

68. Verardo, G.; Geatti, E.; Pol, E.; Giumanini, A. G. Sodium borohydride: A versatile reagent in the reductive *N*-monoalkylations of α-amino acids and α-amino methyl esters. *Can. J. Chem.* **2002**, *80*, 779-788.

Reproduced with permission of the copyright owner. Further reproduction prohibited without permission.

69. Parker, D. NMR determination of enantiomeric purity. *Chem. Rev.* **1991**, *91*, 1441-1457.

70. Dale, J. A.; Dull, D. L.; Mosher, H. S. α-Methoxy-α-trifluoromethylphenylacetic acid: A versatile reagent for determination of enantiomeric composition of alcohols and amines. *J. Org. Chem.* **1969**, *34*, 2543-2549.

71. Kusumi, T.; Fukushima, T.; Ohtani, I.; Kakisawa, H. Elucidation of the absolute configurations of amino acids and amines by the modified Mosher method. *Tetrahedron Lett.* **1991**, *32*, 2939-2942.

72. Nordlander, J. E.; Njoroge, F. G.; Payne, M. J.; Warman, D. *N*-(Trifluoroacetyl)-α-amino acid chlorides as chiral shift reagents for Friedel-Crafts synthesis. *J. Org. Chem.* **1985**, *50*, 3481-3484.

73. Ohtani, I.; Kusumi, T.; Kashman, Y.; Kakisawa, H. High-field FT NMR application of Mosher's method. The absolute configurations of marine terpenoids. *J. Am. Chem. Soc.* **1991**, *113*, 4092-4096.

74. Sullivan, G. R.; Dale, J. A.; Mosher, H. S. Correlation of configuration and F-19 chemical shifts of α-methoxy-α-trifluoromethylphenylacetate derivatives. *J. Org. Chem.* **1973**, *38*, 2143-2147.

75. Snyder, H. R.; Freier, H. E. Some substituted 1,10-phenanthrolines. *J. Am. Chem. Soc.* **1946**, *68*, 1320-1322.

76. Graf, G. I.; Hastreiter, D.; da Silva, L. E.; Rebelo, R. A.; Montalban, A. G.; McKillop, A. The synthesis of aromatic diazatricycles for

Reproduced with permission of the copyright owner. Further reproduction prohibited without permission.

phenylenediaminebis(methylene Meldrum's acid) derivatives. *Tetrahedron* **2002**, *58*, 9095-9100.

77. Wehman, P.; Kaasjager, V. E.; de Lange, W. G. J.; Hartl, F.; Kamer, P. C. J.; van Leeuwen, P. W. N. M. Subtle balance between various phenanthroline ligands and anions in the palladium-catalyzed reductive carbonylation of nitrobenzene. *Organometallics* **1995**, *14*, 3751-3761.

78. Cheng, C. C.; Yan, S. The Friedlander synthesis of quinolines. *J. Org. React.* **1982**, *28*, 37-200.

79. Wu, F.; Thummel, R. P. Ru(II) complexes of crowded delocalized diimine ligands. *Inorg. Chem. Acta.* **2002**, *327*, 26-30.

80. Roubelakis, M. M.; Vougioukalakis, G. C.; Angelis, Y. S.; Orfanopoulos, M. Solvent dependant changes in the ene reaction of RTAD with alkenes: The cyclopropyl group as a mechanistic probe. *Org. Lett* **2006**, *8*, 39-42.

81. Shimizu, N.; Nishida, S. Reactions of carbene with 1,1-dicyclopropylethylene: A new tool to investigate radical cycloadditions. *J. Chem. Soc. Chem. Commun.* **1972**, 389-390.

82. Padron, J. M.; Kokotos, T.; Martin, T.; Markidis, T.; Gibbons, W. A.; Martin, V. S. Enantiospecific synthesis of α-amino acid semialdehydes: A key step for the synthesis of unnatural unsaturated and saturated α-amino acids. *Tetrahedron Asymm.* **1998**, *9*, 3381-3394.

Reproduced with permission of the copyright owner. Further reproduction prohibited without permission.

83. Bycroft, B. W.; Chhabra, S. R.; Kellam, B.; Smith, P. Convient synthese of (3*S*,5*S*)-carbapenam-3-carboxylates and their biosynthetic relevance. *Tetrahedron Lett.* **2003**, *44*, 973-976.

84. Bayston, D. J.; Griffin, J. L. W.; Gruman, A.; Polywka, M. E. C.; Scott, R. M. Process for the preparation of cyclopropylglycne. US 6,090,982, **2000**.

85. Huang, S.; Kruger, D. E.; Frizzi, A.; D'Ordine, R. L.; Florida, C. A.; Adams, W. R.; Brown, W. E.; Luethy, M. H. High-lysine corn produced by the combination of enhanced lysine biosynthesis and reduced zein accumulation. *Plant Biotech.* **2005**, *3*, 555-569.

86. Bouchaudon, J.; Dutruc-Rosset, G.; Frage, D.; James, C. Synthesis of RP-56142: A new immunoactive peptide. *J. Chem. Soc., Perkin Trans 1* **1989**, 695-701.

87. Hiebl, J.; Blanka, M.; Guttman, A.; Kollmann, H.; Leitner, K.; Mayrhofer, G.; Rovenzsky, F.; Winkler, K. A detailed investigation of the preparation of 2,7-diaminosuberic acid and 2,5-diaminoadipic acid derivatives using Kolbe electrolysis. *Tetrahedron* **1998**, *54*, 2059-2074.

88. Arakawa, Y.; Goto, T.; Kawase, K.; Yoshifuji, S. Stereospecific synthesis of cyclic hydrazoacetic acids and *meso*-diaminodicarboxylic acids. *Chem. Pharm. Bull.* **1998**, *46*, 674-680.

89. Jackson, R. F.; Turner, D.; Block, M. H. Carbonylative coupling of organozinc reagents in the presence and absence of aryl iodides: Synthesis of unsymmetrical and symmetrical ketones. *J. Chem. Soc., Perkin Trans. 1* **1997**, 865-870.

Reproduced with permission of the copyright owner. Further reproduction prohibited without permission.

90. Cox, R. J.; Sherwin, W. A.; Lam, L.; Vederas, J. C. Synthesis and evaluation of novel substrates and inhibitors of *N*-succinyl-LL-diaminopimelate aminotransferase (DAP-AT) from *Escherichia coli*. *J. Am. Chem. Soc.* **1996**, *118*, 7449-7460.

91. Gao, Y.; Lane-Bell, P.; Vederas, J. C. Steroselective synthesis of *meso*-2,6-diaminopimelic acid and its selectively protected derivatives. *J. Org. Chem.* **1998**, *63*, 2133-2143.

92. Williams, R. M.; Fegley, G. J.; Gallegos, R.; Schaefer, F.; Pruess, D. L. Asymmetric synthesis of (2*S*,3*S*,6*S*)-, (2*S*,3*S*,6*R*)-, and (2*R*,3*R*,6*S*)-2,3-methano-2,6-diaminopimelic acids. Studies directed towards the design of novel substrate-based inhibitors of LL-diaminopimelate epimerase. *Tetrahedron* **1996**, *52*, 1149-1164.

93. Jurgens, A. R. Asymmetric synthesis of differentially protected *meso*-2,6-diaminopimelic acid. *Tetrahedron Lett.* **1992**, *33*, 4727-4730.

94. Bold, G.; Allmendinger, T.; Herold, P.; Moesch, L.; Scar, H.; Duthaler, R. O. Stereospecific synthesis of (2*S*,6*S*)-2,6-diaminoheptanedioic acid and of unsymmetrical derivatives of *meso*-2,6-diaminoheptanedioic acid. *Helv. Chim. Acta* **1992**, *75*, 865-882.

95. Paradisi, F.; Porzi, G.; Rinaldi, S.; Sandri, S. A simple asymmetric synthesis of (+)- and (-)-2,6-diaminopimelic acids. *Tetrahedron Asym.* **2000**, *11*, 1259-1262.

96. Feldhues, M.; Schafer, H. Selective mixed coupling of carboxylic acids. *Tetrahedron* **1985**, *41*, 4195-4212.

Reproduced with permission of the copyright owner. Further reproduction prohibited without permission.

97. Linhardt, R. J.; Murr, B. L.; Montgomery, E.; Osby, J.; Sherbine, J. Mechanism of diacyl peroxide decomposition. *J. Org. Chem.* **1982**, *47*, 2242-2251.

98. Spantulescu, M. D.; Jain, R. P.; Derksen, D. J.; Vederas, J. C. Photolysis of diacyl peroxides: A radical based approach for the synthesis of functionalized amino acids. *Org. Lett.* **2003**, *5*, 2963-2965.

99. Jain, R. P.; Vederas, J. C. Synthesis of β-cyclopropylalinines by photolysis of diacyl peroxides. *Org. Lett.* **2003**, *5*, 4669-4672.

100. Dussault, P.; Sahli, A. 2-Methoxyprop-2-yl hydroperoxide: A convenient reagent for the synthesis of hydroperoxides and peracids. *J. Org. Chem.* **1992**, *57*, 1009-1012.

101. Rhuland, L. E.; Work, E.; Denman, R. F.; Hoare, D. S. The behavior of isomers of α,ε-diaminopimelic acid on paper chromatograms *J. Am. Chem. Soc.* **1955**, *77*, 4844-4846.

102. Staneck, J. L.; Roberts, G. D. Simplified approach to identification of aerobic actinomycetes by thin-layer chromatography. *App. Microbiol.* **1974**, *28*, 226-231.

103. ElWaziry, A. M.; Tomita, Y.; Ling, J. R.; Onodera, R. Measurement of total and separate stereoisomers of diaminopimelic acid in rumen bacteria by high-performance liquid chromatography. *J. Chromatogr. B* **1996**, *677*, 53-59.

104. Medvedovici, A.; Sandra, P.; Kot, A.; Kolodziejczyk, A. Study on the separation of D,L- and *meso-N,N'*-di(carbobenzyloxy)-2,6-diaminopimelic acid by SFC. *J. High Res. Chromatogr.* **1996**, *19*, 227-228.

Reproduced with permission of the copyright owner. Further reproduction prohibited without permission.

105. Nagasawa, T.; Ling, J. R.; Onodera, R. Chiral high performance liquid chromatographic separation of the 3 stereoisomers of 2,6-diaminopimelic acid without derivatization. *J. Chromatogr. A* **1993**, *653*, 336-340.

106. McKerrow, J.; Vagg, S.; McKinney, T.; Seviour, E. M.; Maszenan, A. M.; Brokks, P.; Seviour, R. J. A simple HPLC method for analysing diaminopimelic acid diastereomers in cell walls of Gram-positive bacteria. *Lett. Appl. Microbiol.* **2000**, *30*, 178-182.

107. Abbott, S. D.; Lane-Bell, P.; Sidhu, K. P. S.; Vederas, J. C. Synthesis and testing of heterocyclic analogues of diaminopimelic acid (DAP) as inhibitors of DAP dehydrogenase and DAP epimerase. *J. Am. Chem. Soc.* **1994**, *116*, 6513-6520.

108. Qiagen Website: http://www1.qiagen.com/literature/handbooks/PDF/ProteinExpressionQXP_QIAexpressionist1024473_QXPHB_0603.pdf (October 2002)

109. Lamzin, V. S.; Dauter, Z.; Wilson, K. S. How nature deals with stereoisomers. *Curr. Opin. Struct. Biol.* **1995**, *5*, 830-836.

110. Prelog, V. Chirality in chemistry. *Science* **1976**, *193*, 17-24.

111. Corrigan, J. J. D-Amino acids in animals. *Science* **1969**, *164*, 142-149.

112. Jilek, A.; Mollay, C.; Tippelt, C.; Grassi, J.; Mignogna, G.; Mullegger, J.; Sander, V.; Fehrer, C.; Barra, D.; Kreil, G. Biosynthesis of a D-amino acid in peptide linkage by an enzyme from frog skin secretions. *Proc. Natl. Acad. Sci. USA* **2005**, *102*, 4235-4239.

Reproduced with permission of the copyright owner. Further reproduction prohibited without permission.

113. Bruckner, H.; Schieber, A. Determination of free D-amino acids in mammalia by chiral gas chromatography-mass spectrometry. *J. High. Resol. Chromatogr.* **2000**, *23*, 576-582.

114. Schieber, A.; Bruckner, H.; Ling, J. R. GC-MS analysis of diaminopimelic acid stereoisomers and amino acid enantiomers in rumen bacteria. *Biomed. Chromatogr.* **1999**, *13*, 46-50.

115. Schopf, C.; Steuer, H. Die synthese des rutaecarpins unter zellmöglichen bedingungen. *Just. Liebigs, Ann. Chem.* **1947**, *558*, 124-136.

116. Liepman, A. H.; Olsen, L. J. Genomic analysis of aminotransferases in *Arabidopsis thaliana*. *CRC Crit. Rev. Plant Sci.* **2004**, *23*, 73-89.

117. Braunstein, A. E.; Goryachenkova, E. V.; Tolosa, E. A.; Willhardt, I. H.; Yefremova, L. L. Specificity and some other properties of liver serine sulphhydrase: Evidence for its identity with cystathionine β-synthase. *Biochim. Biophys. Acta* **1971**, *242*, 247-260.

118. Kery, V.; Poneleit, L.; Meyer, J. D.; Manning, M. C.; Kraus, J. P. Binding of pyridoxal 5'-phosphate to the heme protein human cystathionine β-synthase. *Biochemistry* **1999**, *38*, 2716-2724.

119. Lee, W. M.; Elliott, J. E.; Brownsey, R. W. Inhibition of acetyl-CoA carboxylase isoforms by pyridoxal phosphate. *J. Biol. Chem.* **2005**, *280*, 41835-41843.

120. Maurs, M.; Trigalo, F.; Azerad, R. Resolution of α-substituted amino acid enantiomers by high performance liquid chromatography after derivatization with

Reproduced with permission of the copyright owner. Further reproduction prohibited without permission.

a chiral adduct of ortho-phthalaldehyde: Application to glutamic acid analogs. *J. Chromatogr.* **1988**, *440*, 209-215.

121. Tellier, F.; Acher, F.; Brabet, I.; Pin, J.; Bockaert, J.; Azerad, R. Synthesis of conformationally-constrained stereospecfic analogs of glutamic acid as antagonists of metabotropic receptors. *Bioorg. Med. Chem. Lett.* **1995**, *5*, 2627-2632.

122. Trigalo, F.; Acher, F.; Azerad, R. Synthesis and resolution of DHCGA, a new conformationally rigid 3,4-dehydroglutamic acid analogue. *Tetrahedron* **1990**, *46*, 5203-5212.

123. Greenfield, A. A.; Butera, J. A. Convenient synthesis and isolation of conformationally rigid glutamic acid analogues. *Synth. Commun.* **2004**, *34*, 3939-3947.

124. Curry, K.; Peet, M. J.; Magnuson, S. K.; McLennan, H. Synthesis, resolution, and absolute configuration of the isomers of the neuronal excitant 1-amino-1,3-cyclopentanedicarboxylic acid. *J. Med. Chem.* **1988**, *31*, 864-867.

125. Sekiyama, Y.; Palaniappan, N.; Reynolds, K. A.; Osada, H. Biosynthesis of phoslactomycins: Cyclohexanecarboxylic acid as the starter unit. *Tetrahedron* **2003**, *59*, 7465-7471.

126. Trigalo, F.; Buisson, D.; Azerad, R. Chemoenzymatic synthesis of conformationally rigid glutamic acid analogues. *Tetrahedron Lett.* **1988**, *29*, 6109-6112.

Reproduced with permission of the copyright owner. Further reproduction prohibited without permission.

127. Buisson, D.; Azerad, R. Diastereoselective and enantioselective microbial reduction of cyclic α-alkyl β-ketoesters. *Tetrahedron Lett.* **1986**, *27*, 2631-2634.

128. Konig, W. A.; Benecke, I.; Sievers, S. New procedure for gas chromatographic enantiomer separation: Application to chiral amines and hydroxy acids. *J. Chromatogr.* **1982**, *238*, 427-432.

129. Perrin, D. D.; Armarego, W. L. F.; Perrin, D. R. *Purification of Laboratory Chemicals*. 2nd ed.; Pergamon Press: New York, **1980**.

130. Vogel, A. *Vogel's Textbook of Practical Organic Chemistry*. 4th ed.; J. Wiley & Sons Inc.: New York, **1978**.

131. Still, W. C.; Kahn, M.; Mitra, A. Rapid chromatographic technique for preparative separations with moderate resolution. *J. Org. Chem* **1978**, *43*, 2923-2925.

132. Spantulescu, M. D. Synthetic methods for amino acids and hydroxyacids using photolysis of diacyl peroxides and peresters. University of Alberta, Edmonton, 2006.

133. Alexander, M. D.; Anderson, R. E.; Sisko, J.; Weinreb, S. M. A general method for the reductive carbamation and sulfonamidation of aldehydes. *J. Org. Chem.* **1990**, *55*, 2563-2564.

134. Westerman, P. W.; Roberts, J. D. Nitrogen-15 magnetic resonance spectroscopy. Natural abundance spectra of secondary amines. *J. Org. Chem.* **1978**, *43*, 1177-1179.

Reproduced with permission of the copyright owner. Further reproduction prohibited without permission.

135. Shao, H.; Wu, Y.; Li, R. A highly practical method for monobenzylation of amino acids. *Synth. Commun.* **2000**, *30*, 1911-1915.

136. Reetz, M. T.; Drewes, M. W.; Mattews, B. R.; Lennick, K. A simple synthetic route to statine and statine analogues. *J. Chem. Soc., Chem. Commun.* **1989**, 1474-1475.

137. Taguchi, T.; Mukaiyama, T. A convenient method for the syntheses of benxyl *N*-monoalkylcarbamates and *N*-benzyloxycarbonylamino acids. *Chem. Lett* **1973**, 1-2.

138. Kusumi, T.; Fukushima, T.; Ohtani, I.; Kakisawa, H. Elucidation of the absolute configurations of amino acids and amines by the modified Mosher's method. *Tetrahedron Lett.* **1991**, *32*, 2939-2942.

139. Handoo, K. L.; Cheng, J.; Parker, V. D. Hydrogen atom abstraction by radical cations. The reactions of 9-substituted acridine radical cations with cyclohexa-1,4-diene. *J. Chem. Soc., Perkin Trans. 2* **2001**, 1476-1480.

140. Shiosaki, K.; Nadzan, A. M.; Kopecka, H.; Shue, Y. K. Preparation of acyltetrapeptide derivatives as cholecystokinin (CCK) agonists. WO 9006937, **1990**.

141. Liu, H.; Tully, D.; Alper, P.; Epple, R.; Chatterjee, A.; Roberts, M. Preparation of benzoxazolyaminoalkylcarboxamides and related compounds as selective inhibitors of cathepsin S. WO 2004112709, **2004**.

142. Morelle, N.; Gharbi-Benarous, J.; Acher, F.; Valle, G.; Crisma, M.; Toniolo, C.; Azerad, R.; Girault, J. Conformational analysis of cyclohexane-derived analogues

Reproduced with permission of the copyright owner. Further reproduction prohibited without permission.

of glutamic acid by X-ray crystallography, NMR spectroscopy in solution, and molecular dynamics. *J. Chem. Soc., Perkin Trans. 2* **1993**, 525-533.

143. Acher, F.; Azerad, R. Synthesis of diastereomeric peptides incorporating cycloglutamic acids. *Int. J. Peptide Protein Res.* **1991**, *37*, 210-219.

144. Wright, J. L.; Caprathe, B. W.; Downing, D. M.; Glase, S. A.; Heffner, T. G.; Jaen, J. C.; Johnson, S. J.; Kesten, S. R.; MacKenzie, R. G.; Meltzer, L. T.; Pugsley, T. A.; Smith, S. J.; Wise, L. D.; Wustrow, D. J. The discovery and structure: Activity relationships of 1,2,3,6-tetrahydro-4-phenyl-1-[(arylcyclohexenyl)alkyl]pyridines. Dopamine autoreceptor agonists and potential antipsychotic agents. *J. Med. Chem.* **1994**, *37*, 3523-3533.

145. Fonteneau, L.; Rosa, S.; Buisson, D. Chemoenzymatic synthesis of enantiopure isopropyl (3*R*)-and (3*S*)-3-hydroxycyclohex-1-ene-1-carboxylates and their reduction to isomers of isopropyl 3-hydroxy-cyclohexane-1-carboxylate. *Tetrahedron Asymm.* **2002**, *13*, 579-585.

Reproduced with permission of the copyright owner. Further reproduction prohibited without permission.